Carbonation induced corrosion in integral and non-integral surface treated lightweight foam concrete

by

Marlin Mubatapasango

Thesis presented in fulfilment of the requirements for the degree of Master of Engineering in the Faculty of Engineering at Stellenbosch University

Supervisor:Mr Algurnon Steve van Rooyen

December 2017

Stellenbosch University https://scholar.sun.ac.za

DECLARATION

I, the undersigned, hereby declare the work contained in this thesis is my own original work except where specifically referenced in text, and that I have not previously in its entirety or in part submitted it at any university for a degree.

Date: December 2017

Copyright © 2017 Stellenbosch University
All rights reserved

Stellenbosch University https://scholar.sun.ac.za

UNIVERSITEIT·STELLENBOSCH·UNIVERSITY
jou kennisvennoot • your knowledge partner

Plagiaatverklaring / *Plagiarism Declaration*

1 Plagiaat is die oorneem en gebruik van die idees, materiaal en ander intellektuele eiendom van ander persone asof dit jou eie werk is.
Plagiarism is the use of ideas, material and other intellectual property of another's work and to present is as my own.

2 Ek erken dat die pleeg van plagiaat 'n strafbare oortreding is aangesien dit 'n vorm van diefstal is.
I agree that plagiarism is a punishable offence because it constitutes theft.

3 Ek verstaan ook dat direkte vertalings plagiaat is.
I also understand that direct translations are plagiarism.

4 Dienooreenkomstig is alle aanhalings en bydraes vanuit enige bron (ingesluit die internet) volledig verwys (erken). Ek erken dat die woordelikse aanhaal van teks sonder aanhalingstekens (selfs al word die bron volledig erken) plagiaat is.
Accordingly all quotations and contributions from any source whatsoever (including the internet) have been cited fully. I understand that the reproduction of text without quotation marks (even when the source is cited) is plagiarism.

5 Ek verklaar dat die werk in hierdie skryfstuk vervat, behalwe waar anders aangedui, my eie oorspronklike werk is en dat ek dit nie vantevore in die geheel of gedeeltelik ingehandig het vir bepunting in hierdie module/werkstuk of 'n ander module/werkstuk nie.
I declare that the work contained in this assignment, except where otherwise stated, is my original work and that I have not previously (in its entirety or in part) submitted it for grading in this module/assignment or another module/assignment.

16881753 **Studentenommer / *Student number***	**Handtekening / *Signature***
M.S MUBATAPASANGO **Voorletters en van / *Initials and surname***	2017/09/11 **Datum / *Date***

6

Stellenbosch University https://scholar.sun.ac.za

ABSTRACT

Carbonation induced corrosion is a concern in reinforced lightweight foam concrete (R/LWFC) as a result of air entrainment. Concerns arise from whether the air voids increase diffusivity of carbon dioxide (CO_2) into LWFC. The effect of carbonation is the destruction of the protective cover for the steel reinforcement.

LWFC is a low density concrete in which at least 20 per cent air by volume is entrained in a base mix comprising water, cement and a filler. The air entrainment is achieved by adding stable foam to the base mix. LWFC is a versatile construction material whose density can be altered by using various amounts of entrained air to suit the required function, structural or non-structural. The significant amount of air entrainment give LWFC its advantages of high strength to weight ratio and improved insulating properties. While progress in LWFC on mix designs and suitable compressive strengths for structural use has been made, other properties such as durability have not been adequately explored. In normal weight concrete, surface treatment has been used to improve durability, little research has been conducted on the efficacy of surface treatment agent on the durability of LWFC. Surface treatments are applied either during mixing (integral) or after curing (non-integral).

This study investigates the durability of R/LWFC with a particular focus on carbonation and whether surface treatment can be used to limit corrosion induced by carbonation. The influence of surface treatment on the lightweight foamed concrete is also characterised. In this investigation R/LWFC is used with a target casting density of 1400 kg/m^3 for testing changes in microstructure via CT scans, compressive strength, penetration depth (carbonation front and silane) and half-cell potential corrosion measurement. Application of integral and non-integral surface treatment is done and the effects on the R/LWFC and evaluated against results from control samples. CT scanning is used for investigating the effect of surface treatment on the lightweight foam concrete. An accelerated carbonation set-up is used to investigate carbonation resistance. Phenolphthalein indicator solution is used to determine the depth of carbonation.

Integral surface treatment affected the size and distribution of voids compared to non-integral treatment. Consequently, the compressive strengths observed for integral surface treatment were higher than for control and non-integral treatment. The shape of the voids in integral and non-integral surface treated concrete were similar. Integral surface treatment provided the highest resistance to carbonation followed by the non-integral surface treatment. High levels of carbonation and carbonation rates were observed for control samples.

Stellenbosch University https://scholar.sun.ac.za

The observed half-cell potentials showed that integral treatment resulted in high carbonation resistance. Little difference was observed between control samples and non-integral treatment.

This investigation concluded that surface treatment can be used in lightweight foamed concrete to improve its durability against carbonation. The use of integral surface treatment in lightweight foam concrete resulted in additional benefits in increased compressive strengths thereby increasing its strength to weight ratio.

Stellenbosch University https://scholar.sun.ac.za

OPSOMMING

Koolstof-geïnduseerde korrosie is 'n besorgdheid in gewapende ligte skuimbeton (G / LSB) as gevolg van luginrigting. Bekommernisse ontstaan uit of die lugruimtes diffusiwiteit van koolstofdioksied (CO2) in LSB verhoog. Die effek van karbonering is die vernietiging van die beskermende omhulsel vir die staalversterking.

LSB is 'n lae digtheid beton waarin minstens 20 persent lug per volume in 'n basismengsel bestaan wat water, sement en 'n vulstof bevat. Die lugverbindings word behaal deur stabiele skuim by die basismengsel te voeg. LSB is 'n veelsydige konstruksiemateriaal waarvan die digtheid verander kan word deur gebruik te maak van verskillende hoeveelhede ingehokte lug om die vereiste funksie, strukturele of nie-strukturele, te pas. Die aansienlike hoeveelheid luginvoeding gee LSB sy voordele van hoë sterkte tot gewigsverhouding en verbeterde isolerende eienskappe. Alhoewel vordering gemaak is in LSB op mengontwerpe en geskikte druksterkte vir strukturele gebruik, is ander eienskappe soos duursaamheid nog agter gelaat. In normale gewigsbeton is oppervlakbehandeling gebruik om duursaamheid te verbeter. Geen ondersoek is gedoen na die effektiwiteit van oppervlakbehandelingsmiddel op die duursaamheid van LWFC nie. Oppervlaktebehandelings word toegedien gedurende meng (integraal) of na genesing (nie-integraal).

Hierdie studie ondersoek die duursaamheid van R / LSB met 'n spesifieke fokus op karbonering en of oppervlakbehandeling gebruik kan word om die korrosie wat deur koolsuur veroorsaak word, te beperk. Die invloed van oppervlakbehandeling op die liggewig skuimbeton word ook gekenmerk. In hierdie ondersoek word R / LSB gebruik met 'n teikengietdigtheid van 1400 kg / m3 vir die toetsing van veranderinge in mikrostruktuur deur middel van RT-skanderings, druksterkte, penetrasie diepte (carbonation front en silaan) en half-sel potensiële korrosie meting. Toepassing van integrale en nie-integrale oppervlakbehandeling word gedoen en die effekte op die R / LSB en geëvalueer teen die resultate van kontrole monsters. RT-skanderings word gebruik om die effek van oppervlakbehandeling op die ligte skuimbeton te ondersoek. 'N Versnelde koolstofopstelling word gebruik om koolstofasiet weerstand te ondersoek. Fenolftaleïen-indikatoroplossing word gebruik om die diepte van karbonering te bepaal.

Integrale oppervlakbehandeling het die grootte en verspreiding van holtes beïnvloed in vergelyking met nie-integrale behandeling. Gevolglik was die druksterkte waargeneem vir integrale oppervlakbehandeling hoër as vir beheer en nie-integrale behandeling. Die vorm van die holtes in integrale en nie-integrale oppervlak behandelde beton was soortgelyk. Integrale oppervlakbehandeling het die hoogste weerstand teen koolsuurwerk gevolg, gevolg deur die nie-integrale oppervlakbehandeling. Hoë vlakke van karbonasie en koolstofasietempo's is waargeneem vir kontrole monsters. Die waargenome halfsellepotensiale het getoon dat integrale behandeling tot hoë koolsuurweerstand gelei het. Daar is min verskil tussen kontrole monsters en nie-integrale behandeling.

Stellenbosch University https://scholar.sun.ac.za

Hierdie ondersoek het tot die gevolgtrekking gekom dat oppervlakbehandeling gebruik kan word in ligte skuimbeton om sy duursaamheid teen koolsuur te verbeter. Die gebruik van integrale oppervlaktebehandeling in liggewigskuimbeton het bykomende voordele in verhoogde druksterkte tot gevolg gehad, waardeur die sterkte tot gewigsverhouding daarvan verhoog is.

Stellenbosch University https://scholar.sun.ac.za

ACKNOWLEDGEMENTS

I would like to express my gratitude to my supervisor, Mr A S van Rooyen for his consistent guidance, support and encouragement throughout the entirety of this study.

I would also like to express my heartfelt gratitude to:

The Institute of Structural Engineering, Stellenbosch University for funding my studies.

TRAC for the provision of the CO_2 measuring equipment which was vital for the study at no cost.

Sika for sponsoring their Sikagard® 706 Thixo product.

The structural engineering department staff at Stellenbosch University for their support, involvement and guidance.

Mr Johan van der Merwe, whose invaluable input in the workshop helped a great deal in the completion of this project.

Colleagues with whom we shared the burden and carried each other through in times good and bad.

I would also like to thank my entire family and friends for their unreserved support, proofreading this document, encouragement and prayers which I always counted on.

Above all, the Lord Almighty for the abundance of grace.

Stellenbosch University https://scholar.sun.ac.za

LIST OF TABLES

Stellenbosch University https://scholar.sun.ac.za

TABLE OF FIGURES

Stellenbosch University https://scholar.sun.ac.za

Stellenbosch University https://scholar.sun.ac.za

TABLE OF CONTENTS

Stellenbosch University https://scholar.sun.ac.za

Stellenbosch University https://scholar.sun.ac.za

Stellenbosch University https://scholar.sun.ac.za

NOMENCLATURE

Latin letters

A –area in m^2.

B –Stern-Geary constant.

a/c –ash to cement ratio.

c –cement content in kg/m^3.

C –amount of alkaline material in kg/m^3.

$[CO_2]$ –concentration of carbon dioxide in %

D –diffusion constant in m^2/s.

$D_{CO2,air}$ –diffusion coefficient of carbon dioxide in air m^2/s.

D_M –diffusion coefficient of carbon dioxide in the coating m^2/s.

$D_{e,CO2}$ –effective diffusion coefficient of carbon dioxide in m^2/s.

E –induced potential in mV

f_c –compressive strength in MPa.

I –perturbation current in mA.

i_{corr} –corrosion current density in $\mu A/cm^2$.

k –coefficient of carbonation in mm^2/s.

n –amount of carbon dioxide in kg.

n_t –potential at time t in mV.

n_o –initial potential in mV.

p. –porosity.

R_c –charge transfer resistance in Ohm.

R_s –concrete cover resistance in Ohm.

R_p-polarisation resistance in Ohm.

RH –relative humidity in %

RD_a –relative density of ash.

RD_c –relative density of cement.

RD_f –relative density of foam.

r –concentration of carbon dioxide at the surface in kg/m^3.

Stellenbosch University https://scholar.sun.ac.za

r_x –concentration of carbon dioxide at depth x in kg/m^3.

s_D –equivalent layer thickness in metres.

s –thickness of coating in metres.

t –time in weeks.

V_f –volume of foam in litres.

w –water content in kg/m^3.

w/a –water to ash ratio.

w/b –water to binder ratio.

w/c –water to cement ratio.

x –carbonation depth in mm

Greek letters

ρ_c –density of cement in kg/m^3.

ρ_m –target density in kg/m^3.

ρ_w –density of water in kg/m^3.

τ –time constant.

Stellenbosch University https://scholar.sun.ac.za

ABBREVIATIONS

2D –Two Dimensional.

3D –Three Dimensional.

C-H –Calcium Hydroxide.

C-S-H –Calcium Silicate Hydrate.

COV –Coefficient of Variation.

CSE –Copper Sulphate Electrode.

CT scan –X-ray Computed Tomography scan.

CO_2 –Carbon dioxide.

FA –Fly Ash.

FT-IR –Fourier Transform Infra-red spectroscopy.

HCP –Half-Cell Potential.

IST –Integral Surface Treatment.

LPR –linear Polarisation Resistance

LWFC –Lightweight Foam Concrete.

NIST –Non-integral Surface Treatment.

SCE –Saturated Calomel Electrode.

SCM –Supplementary Cementitious Materials.

STA –Surface Treatment Agents.

TGA –Thermal Gravimetric Analysis.

XRD –X-ray Diffraction.

Stellenbosch University https://scholar.sun.ac.za

CHAPTER 1 INTRODUCTION

Lightweight foamed concrete (LWFC) is an emerging, promising material that has the ability to reshape the construction industry. In a world where efficiency is increasingly taking centre stage, foamed concrete provides an alternative material, with a high strength to weight ratio and opportunities to incorporate high volumes of waste products as fillers. Foamed concrete is an attractive alternative construction material to normal concrete owing to its high strength to weight ratio, thermal and acoustic properties, good fire resistance and ease of use properties. These properties are a result of the air entrained in the mortar.

The level of air entrainment can be adjusted to produce concrete of varying densities ranging from as low as 300 kg/m^3 to 1680 kg/m^3 thereby giving it variety of functions. The durability concerns of LWFC arise from the vesicular material which makes it susceptible to ingress by corrosive agents. The protection of concrete against deleterious materials is important as concrete also plays a role as a protective cover of the steel reinforcement. If the barrier which concrete provides is breached, the reinforcement is vulnerable to corrosion resulting in the loss of bond strength and load carrying capacity.

While in normal concrete various solutions such as sacrificial plating, painted reinforcement bars and concrete surface protection systems have been developed to protect the concrete reinforcement, little has been done in LWFC. One of the solutions that have been developed for normal weight concrete are surface treatment agents (STA). While STA have been used extensively in normal weight concrete, little research has been done on whether they can be extended to LWFC in order to improve its durability. These durability concerns give result in a need for further study in LWFC durability, the application of STA to improve durability and the effect of the surface treatment on the LWFC.

1.1 Background

In 2012, the National Development Plan (2012), which is South Africa's vision for 2030, estimated that the housing backlog stood at 2.1 million units at a staggering cost of R300 billion (2012 figures). LWFC low-rise, precast residential units were identified as a potential solution. The need for low cost quality housing is further exacerbated by intermittent fires in slum settlements. By tapping into the advantageous insulating properties of LWFC, it positions LWFC as a worthy alternative. In addition, given the moderate seismicity of parts of South Africa, it provides the construction industry with a potential solution owing to its high strength to weight ratio. In order to reap the benefits of LWFC, further research is required on the durability of the material.

Stellenbosch University https://scholar.sun.ac.za

Given that air is entrained in LWFC, there are concerns whether the concrete still provides enough corrosion protection to the steel reinforcement. Some of the implications of rusting include loss of load carrying capacity, loss of bond at the concrete steel interface, and reduced ductility.

One of the processes that may increase the vulnerability of the steel reinforcement in LWFC is carbonation. Carbonation is a process in which CO_2 in the environment reacts with calcium hydroxide to form $CaCO_3$. This depletion of the calcium hydroxide during carbonation exposes the steel reinforcement to corrosion. The steel reinforcement derives its chemical protection from the high alkalinity provided by the calcium hydroxide.

One of the potential solutions in reducing or inhibiting ingress of CO_2 into LWFC is surface treatment. Surface treatment makes use of admixtures applied to concrete either during the mixing or stripping stages to improve durability. While there are various types of surface treatment available on the market that do provide carbonation resistance, they have been mainly tested on normal weight concrete or have been designed for use in normal weight concrete.

This study aims to determine the efficacy of surface treatment products currently available on the market in foam concrete to improve its durability against carbonation-induced corrosion. This is necessary as LWFC has entrained air voids which may increase the diffusivity of the CO_2 into the concrete. Since surface treated products currently available on the market are designed for a less porous concrete, their efficacy in LWFC thus needs to be tested. In addition, there is a need to determine the effects the surface treatment has on the voids, properties and corrosion of reinforcement in LWFC. This is important so that the benefits of LWFC are not lost whilst trying to improve durability.

1.2 Problem statement

The benefits of LWFC can be fully exploited if more information about the material is available, including allaying durability concerns. As a result, an attempt to test the efficacy of surface treatment products available on the market against carbonation-induced corrosion is one of the main focuses of this research. The other focus of this research is to determine the influence of surface treatment on the void properties in foamed concrete and the strength of LWFC.

Stellenbosch University https://scholar.sun.ac.za

CHAPTER 2 LITERATURE REVIEW

A review of lightweight foam concrete (LWFC), carbonation, surface treatment agents (STA) and corrosion measuring techniques is contained in Chapter 2. The literature review focuses on the mix constituents of LWFC and the role of the mix design process in improving the durability. Also included in the review is the process of carbonation, carbonation prediction models, mass transfer systems and surface treatment.

2.1 Foamed Concrete

According to Bindiganavile (2008), foamed concrete is defined as a cementitious construction material with a minimum of 20 % of entrained air by volume in the plastic mortar. The air entrainment is achieved by adding foam to the cement paste. The foam is generated using a foaming agent diluted in water while air is pumped through the mixture. The foam is mechanically entrained into the plastic cement paste which differentiates foamed concrete with gas concrete. Gas concrete which is also known as aerated concrete or autoclave concrete is produced using an aluminium based powder which is added into the cement paste to react with calcium hydroxide (C-H) from the hydration of cement.

The three minimum constituents of foamed concrete are water, cement and foam. However, the partial or full replacement of cement with supplementary cementitious materials (SCM) can be done. According to Hilal et al. (2015), the incorporation of SCM can lead to enhanced foamed concrete properties. The water content in foamed concrete is a critical variable as it has implications on the foam stability.

2.2 Mix constituents of foamed concrete

The mix design process of foamed concrete is different from that of normal concrete (NC). Whereas in NC the water/cement (w/c) ratio plays a distinct role in controlling the strength and workability, in foamed concrete, this is not the case. According to Kearsley (1999), the required water content lies in a narrow range and the implications of missing this range include foam degeneration and segregation. On the one hand, if too much water is used, segregation can occur because the slurry mix is not able to hold the bubbles and on the other hand, too little water in the mix can result in the degradation of foam as water is drawn from the foam to hydrate the cement.

SCM can also be incorporated into LWFC. This is done in order to enhance the properties of foamed concrete depending on the proposed use. One of the most widely used SCM is fly ash (FA). FA is a by-product of coal fired power stations and is widely accessible given the high prevalence of coal-fired power stations in South Africa.

Stellenbosch University https://scholar.sun.ac.za

A study by Kearsley (1999) showed increased long term strength when 75 % of the cement had been replaced with fly ash (FA). This could be attributed to the fact that FA is initially an inert filler and only begins to hydrate after the production of C-H. The study showed that partial replacement of cement with FA results in a cost effective mix designs.

In a different study, Kearsley and Mostert (2005) determined that FA had a lower water demand compared to cement. This determination came about from using flow table tests on the workability of foamed concrete. Also, according to Nambiar and Ramamurthy (2006), inclusion of FA resulted in a more uniform air void distribution owing to its fineness. The FA provided a uniform coating on the voids thereby reducing the coalescence and overlapping of the voids.

Another SCM that can be incorporated into foamed concrete is silica fume. Silica fume is a by-product from electric furnaces. According to Chen and Liu (2008), the addition of silica fume improves the early age strength but also reduces the workability. According to the Cement and Concrete Institute (2009), the improved early age strength gain can be attributed to a more compact and less permeable microstructure. The compact microstructure is a result of the fineness of the silica fume particles which act as nuclei for the formation of calcium silicate hydrate (C-S-H).

Foamed concrete is highly responsive to water demand. Water demand in foamed concrete used to be determined by increasing the water/binder ratio until no visual foam breakdown occurs. Research by Kearsley (2005) realised that the water demand of foamed concrete could also be determined using an adaptation of the flow table test on hydraulic cement as specified by ASTM C230 (2010). The adaption took into account the w/c ratio at which no foam degradation due to insufficient water for cement hydration took place and the workability of the foamed concrete. From this research together with the water demand from the visual foam breakdown, a range of flow circle diameters required for optimum w/c ratio for foamed concrete was determined which was between 220 mm and 250 mm. When SCM are taken into account, the total water demand for the foamed concrete was adapted to cater for the different water demand of the SCM. In the case of FA, it acted as a filler in the early stages of hydration and so its water demand was less than that of cement. The formation of the C-H then initiated the pozzolanic reaction of the FA.

Another critical component of foamed concrete is the foam. The amount of foam use has a direct effect on the density of LWFC. The purpose of the foam is to create enclosed bubbles of air that are stable. The foam is created from a foaming agent.

Stellenbosch University https://scholar.sun.ac.za

Foaming agents are either synthetic hydrophilic amphiprotic substances or organic protein hydrolysed substances. While both types of foaming agents have been successfully used across the world, research by Panesar (2013) has shown that protein based foaming agents produced smaller more isolated air bubbles than synthetic foaming agents.

According to Kearsley (1999), the 28 day strength of the protein based foaming agent foamed concrete was higher than that of synthetic foaming agent based foamed concrete. There are two methods in which the foam is produced namely pre-foaming and mixed foaming. According to Zulkarnain and Ramli (2011), the base mix and the foam are produced separately and then mixed later in the pre-foaming method while in the mixed foaming method the active surface agents are added to the base mix constituents. Despite the method used, the foam produced must be firm and stable so that the target density of the LWFC is attained.

2.3 Density of Foamed Concrete

One of the most important properties in LWFC is density. Other properties such compressive strength and thermal resistance are dependent on the density of the LWFC. As a result, LWFC is produced towards a specified target density. Research by Kearsley (1999) has shown that a minor difference in density can result in a big change in target strength. Consequently, a limited margin of error is necessary for LWFC. According to Jones and McCarthy (2005), the prime design criterion of foamed concrete is towards a specified target plastic density.

In order to design to a specified target casting density, the w/c ratio, ash to cement ratio (a/c) and the water to ash ratio (w/a) are chosen. Using these parameters and the relative densities of the mix constituents, the volume of the required foam is determined. The following set of equations developed by Kearsley (1999) are used in order to achieve a specified target density.

$$\rho_m = c + c \times \left(\frac{w}{c}\right) + c \times \left(\frac{a}{c}\right) + c \times \left(\frac{a}{c}\right)\left(\frac{w}{a}\right) + RD_f \times V_f$$

Equation 2-1: Target density equation

$$1000 = \frac{c}{RD_c} + c \times \left(\frac{w}{c}\right) + \frac{c \times (a/c)}{RD_a} + c \times \left(\frac{a}{c}\right)\left(\frac{w}{a}\right) + V_f$$

Equation 2-2: Volume of mix equation

Where:

ρ_m = target density (kg/m^3)

c = amount of cement (kg/m^3)

Stellenbosch University https://scholar.sun.ac.za

V_f = volume of foam (litres)

RD_f = relative density of foam

RD_a = relative density of FA.

RD_c = relative density of cement

An acceptance criterion based on the density is used in order to check if the mix is acceptable. According to Brady (2001), foamed concrete with a density less than 1600 kg/m^3 is acceptable if the plastic density falls within a tolerance of ±50 kg/m^3 while for densities greater than 1600 kg/m^3, the acceptable tolerance is ±100 kg/m^3. The hardened foamed concrete also has an acceptance criterion based on the deviation from the mean density of specimens from a particular mix. The tolerance of the acceptable deviation is ±100 kg/m^3. The acceptance criterion are also a useful tool to check if segregation occurred. According to Kearsley (1999), meeting the acceptance criterion is indicative of the consistency of the mix. A visit to a foam concrete prefabrication plant revealed that the acceptance criterion is dependent on context of practical conditions. For instance, at that plant, significant increase in density observed was attributed to the handling. Further investigations revealed that the increase in density was due to collapse of bubbles due to transportation and handling from the mixer to the curing area. As a result, there was an adjustment to the acceptance criterion to account for the collapse of bubbles.

Another acceptance criterion that can be used for LWFC is the characteristic compressive strength after 28 days of curing. The characteristic compressive strength is the value such that less than 5 % of the compressive strength measurements fall in. Given the link between strength and density in LWFC, the compressive strengths obtained can therefore be compared to the characteristic compressive strength of the LWFC at that density. This test is useful in checking the repeatability of LWFC. According to Brady(2001), the compressive strength of the cubes should be all be higher than the characteristic compressive strength. Furthermore, in cases where the strength requirements exceed 10 MPa, a 56 day characteristic strength is preferred.

2.4 Voids in foamed concrete

An important characteristic of foamed concrete is plastic density, which is controlled by the volume of the voids entrained in the concrete. There are different types of voids in foamed concrete. According to Nambiar and Ramamurthy (2006), there are three types of voids in concrete namely gel pores, capillary pores and macro pores. Gel pores are responsible for creep and shrinkage. Gel pores have diameters ranging from 1.5 nanometres to 2 nanometres. Capillary pores have a characteristic diameter range of 5 nanometres to 5000 nanometres and are responsible for elasticity and strength. The macro pores are a result of air entrained by the foam bubbles and irregular compaction.

Stellenbosch University https://scholar.sun.ac.za

Another source of macro pores would be entrapped air due to coarse aggregates. However, foamed concrete does not contain coarse aggregates and is a self-flowing and self-compacting which results in minimal air entrapment. According to Wee et al. (2006), the size of the macro pores are approximately 0.1 to 1 mm in diameter. It is important to note that the size may increase due to coalescence of bubbles as a result of mixing, handling, and transportation.

The relationship between the foam volume in the mix design and amount of voids in foamed concrete is important. While the role of the foam is to provide air entrainment, it is not the only source of voids but rather the major source of macro voids. According to Mindess (2008), the voids volume is a function of the amount of foam in the concrete as it is the source of the entrained air in the foamed concrete. A study by Nambiar and Ramamurthy (2006) revealed that an increase in the foam volume resulted in the increase in percentage of voids in two test mix designs, one containing cement and sand and the other containing cement and FA.

Voids in foamed concrete play multiple roles ranging from being some sort of aggregate to a means by which the density in foamed concrete is controlled. As an aggregate, the entrained air does not lead to interfacial effects as it is more consistent in terms of the size. According to Kearsley and Wainwright (2001), the inclusion of entrained air voids as an aggregate is unlikely to cause interfacial effects due to their small size. The replacement of coarse aggregate in foamed concrete with bubbles of entrained air provide foam concrete with some desirable properties such as being self-compacting, self-flowing as well as having improved thermal and acoustic properties. The latter are due to the trapped air that is a poor conductor and emitter of both heat and sound. According to Jones and McCarthy (2005), foamed concrete has performed well in terms of fire resistance. The good fire properties are attributed to the thermal properties of foamed concrete which in turn are attributed to the presence of air pockets in the matrix.

The entrainment of air in concrete has also raised concerns about durability. A study by Nambiar and Ramamurthy (2009) showed that water absorption of foamed concrete increased with increasing density. This behaviour is attributed to a decreased paste volume phase and hence low capillary pore volume. The water absorption is controlled by capillary pores in the paste and not by the entrained air. This is because the entrained air pockets are not entirely connected and hence do not form channels which allow for the transportation of water.

Furthermore, oxygen and water vapour permeability also increased with increasing voids volume. This is in contrast to water absorption and according to Kearsley (1999), this disparity might be indicative of the part played by all voids in mass transfer of water vapour.

Stellenbosch University https://scholar.sun.ac.za

Also, according to Jones and McCarthy (2005), foam concrete specimens exhibited higher carbonation depths in comparison to normal weight concrete. This outcome can be argued to corroborate the conclusions by Kearsley on the involvement of all voids in the diffusion process as opposed to the capillary action in water absorption. It is important to note that water vapour permeability and water absorption are important indicators of durability as most deleterious substances penetrate concrete either by diffusion for gasses or in aqueous solution for salts and liquids.

2.4.1 Assessment of porosity, pore connectivity, pore size and pore distribution

According to Kearsley (1999), the durability of concrete is influenced by, among other influences, the availability of transport properties. The voids in concrete can coalesce together to form channels in which deleterious materials can ingress through. In porous materials, the interconnectivity of voids increase the permeability of the material. Focusing on foamed concrete, foamed concrete has a high porosity due to the entrainment of air voids. The entrainment of air increases the likelihood of interconnectivity of voids. As a result, the assessment of void connectivity has to be done in conjunction with size and distribution.

X-ray computed tomography scanning (CT scans) is a simple and quick method that can be used to assess porosity, connectivity and pore size distribution of pores in the concrete. One of the advantages of using CT scans is that there is no need for prior preparation (such as drying) of the samples. The CT scan is a flexible assessment method which can be done at different resolutions depending on the quality of results sought and the cost. According to du Plessis et al. (2014), high resolution scanning allowed detection of much smaller voids than low resolution scanning did. As a consequence, the porosity detected by the high resolution scanning was higher than that detected by low resolution scanning. However, the duration of the lower resolution scanning was 5 minutes while the higher quality scans took 1 hour.

The sample size used in CT scans is important. The smaller the sample size, the better the quality of the results obtained. For samples less than 10mm on the longest axis, nanoCT scan equipment is used. According to du Plessis et al.(2016), the reason for using nanoCT scan equipment on small samples is to achieve better sample stability and additionally, sharper images are acquired from the use of the lower power X-ray tube over long periods. For samples larger than 10mm, microCT scanning equipment is used. However, the scan times are long and therefore it is better to use medical CT scans for improved efficiency.

Stellenbosch University https://scholar.sun.ac.za

2.4.1.1 Background of CT scan

According to the central analytics facility (CAF) at Stellenbosch (2016), the CT scanner is an x-ray machine that produces 2D and 3D x-ray scans of materials allowing the investigation and analysis of the interior at high resolution and high contrast. Collimated x-ray beams are directed to samples and the absorbed radiation is measured by a sensor placed on the opposite side of the sample. The process is repeated on a range of different angles thereby creating a 3D reconstruction. All this is done non-destructively. Afterwards, the images are analysed using specialised software and the internal structure of the samples is determined. Figure 2-1 illustrates the set-up of the CT scan.

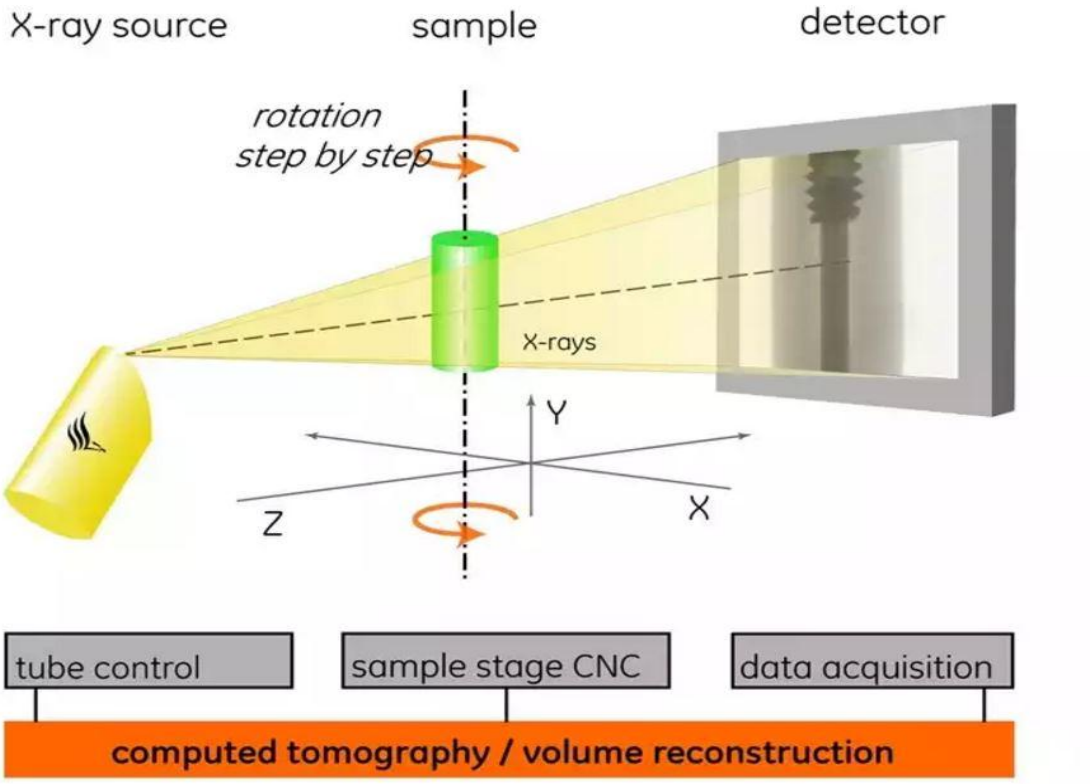

Figure 2-1: Illustration of the CT scan process (2016)

2.5 Durability of reinforced foamed concrete

As for any material, the resistance of foamed concrete to the influences of the environment is a significant consideration. According to Al-Neshawy and Sistonen (2015), in the case of concrete, the negative influences of the environment can be broadly classified into two categories namely mechanical and chemical. The mechanical influences include abrasion, weathering and cracking and the chemical include seepage of aqueous chemical solutions and diffusion of gases. Some of the aqueous chemical solutions include chlorides and sulphates while carbon dioxide is an example of a gas that threatens the durability of reinforced concrete.

Stellenbosch University https://scholar.sun.ac.za

According to Roy et al. (1999), reinforcement corrosion is the most critical factor in the durability of reinforced concrete. The reinforcement corrosion is a result of exposure to deleterious substances either by mechanical or chemical means. In terms of physical means, abrasion delaminates the concrete that protects the reinforcing while cracking results in direct transport channels to the reinforcement. Chemically, deleterious substances enter the concrete matrix by capillary action and seepage. The influence of carbonation will be examined in great detail as it is the main focus of this research.

2.5.1 Influence of carbonation on durability

Carbonation is a chemical process which occurs at pore level in concrete. While carbonation is not a problem in unreinforced concrete, it is a source of concern in reinforced concrete. According to Saetta et al. (1993), carbonation is the process in which a reaction between calcium hydroxide (C-H) and carbon dioxide (CO_2) results in the formation of calcium carbonate ($CaCO_3$). The main consequence of this reaction is lowering the pore solution pH from a range of 13.5-12.5 to about 8.3. The effect of this acidification reaction is the destruction of a passivation layer protecting the reinforcing steel. The destruction of the passivation layer leaves the reinforcing steel vulnerable to rusting.

According to Borges et al. (2009), the CO_2 initially dissolves in the pore solution producing CO_3^{2-} ions and HCO_3^- ions. These ions then react with Ca^{2+} ions from the C-H or the calcium silicate hydrates (C-S-H) in the cement paste to form $CaCO_3$. The C-H is depleted first and then the C-S-H is used in the carbonation reactions. Furthermore, according to Houst (1997), the C-H exists in crystalline form while C-S-H is in an amorphous state.

The $CaCO_3$ formed exists in either one of three states namely: calcite, aragonite and vaterite. The type of $CaCO_3$ formed is dependent upon temperature and pressure. The $CaCO_3$ formed has a larger molecular volume than the C-H and the C-S-H and the percentage increase is dependent on the type of $CaCO_3$ formed. Where calcite is formed, a 12 % molecular volume increase is observed, where aragonite is formed, a molecular volume increase of 3 % is observed and lastly where vaterite is formed, the molecular volume increase is 19 %. Of the 3 types of carbonates formed, calcite is the most stable variety and is formed under room temperature and pressure conditions. The molecular volume increase observed has the effect of reducing the porosity of the concrete.

In the case of foamed concrete, a study by Jones and McCarthy(2005) revealed that foam concrete specimens exhibited higher rates of carbonation and subsequently deep carbonation depths. This was attributed to the high vapour permeability of foamed concrete.

Stellenbosch University https://scholar.sun.ac.za

This is corroborated by the hypothesis by Kearsley(1999) that foamed concrete exhibited high water vapour permeability as both volume paste voids and entrained pores took part in water vapour permeability.

The high rates of carbonation in foamed concrete can therefore be thought of as a risk to the reinforcement given that the passivation layer is destroyed by the acidification reactions occurring during the carbonation process.

2.5.2 Influence of transport properties on carbonation

The process of carbonation is dependent on the CO_2 and the rate at which the gas can penetrate the concrete. Given that CO_2 is in gaseous state, the mass transport system facilitating CO_2 penetration into concrete is diffusion. According to Richardson (2004d), the permeability of the CO_2 is dependent on the pore structure, extent of interconnectivity of voids and the moisture content of the pores in the concrete. Regarding the pore structure, the size of the pores is larger than the molecules and ions. This guarantees a certain level of permeability. The interconnectivity of pores controls the ease with which transportation occurs. If a high degree of interconnectivity exists, there is an increased ease of movement of mass and vice versa. The moisture content is also important as it governs the extent to which the pores can be used for instance in diffusion. Where the pores are water-filled, little diffusion takes place but may facilitate ionic diffusion where ions in solution are involved.

According to Broomfield (2013), the rate of penetration is approximated to Fick's 1st law of diffusion where the penetration depth is proportional to the rate of movement. The inaccuracy of this approximation is borne from the fact that the structure of concrete changes with the progression of carbonation. Also, other influences on the rate of movement such as crack development, moisture level and concrete composition are not accounted for, although they do have an effect on the rate of mass movement.

2.5.3 Carbonation shrinkage

The carbonation process results in the occurrence of carbonation shrinkage. While the exact cause of carbonation shrinkage is unknown, there are two hypotheses that have been accepted. The first hypothesis suggested that carbonation shrinkage is similar to drying shrinkage. According to Swenson and Sereda (1968), carbonation shrinkage is caused by a moisture gradient due to the carbonation reaction. The moisture trapped within the passivated layer remains trapped while the moisture outside will be lost to the atmosphere as a result of drying. Consequently, an internal moisture gradient is created which ultimately results in cracking.

Stellenbosch University https://scholar.sun.ac.za

The second hypothesis suggested that carbonation shrinkage was linked to carbonation of C-S-H. According to Chen et al. (2006), carbonation shrinkage is a type of decalcification shrinkage. Where carbonation of the C-S-H occurred, it was accompanied by a reduction in the ratio of Ca/Si ratio. The extent of C-S-H carbonation is dependent on the initial ratio of Ca/Si. As the C-S-H carbonates, the Ca/Si ratio decreases and the carbonation rate increases.

As Ca^{2+} ions are removed from the C-S-H layers and precipitated as $CaCO_3$, an amorphous silica gel is formed. The process then leads to a realignment of atoms resulting in a sheet-like structure from a fractal structure. This polymerisation of chains to sheet-like structures is the cause of the shrinkage. The cracking is then caused by the differential decalcification. The consequence of the cracking from carbonation shrinkage is to aid ingress of deleterious substances in the manner highlighted in Section 2.5.2.

2.6 Application of Surface Treatment Agents

Surface treatment agents (STA) have been adopted in improving the durability of reinforced concrete structures. According to EN1504-2 (2004), the STA are classified into three groups namely hydrophobic impregnations, impregnations and coatings. The STA function in relation to specific mass transport mechanisms which include gas diffusion, capillary suction and diffusion due to a concentration gradient.

The hydrophobic impregnations form a thin microscopic water repelling film on the surface of the concrete. According to Christodoulou et al. (2013), hydrophobic impregnations are used to prevent the ingress of water and ions in solution into the concrete. Also, according to Sandin (n.d.), deleterious ions like chloride ingress into the concrete in solution form. Also, the ingress of water into LWFC has an effect on the heat conductivity of the material. If the moisture content in LWFC is increased by between 4 to 17 %, the increase in the heat conductivity is 50 %. This results in the loss of a key advantage of LWFC of being an insulating material. In LWFC, moisture content of up to 30 % has been reported in practice.

The types of mass transfer that the hydrophobic impregnation target are capillary suction due to surface tension and diffusion due to a concentration gradient. There are two major types of hydrophobic impregnations namely silanes and siloxanes. Silanes contain a single silicon atom in the molecule while siloxanes contain multiple silicon chains. According to Freitag and Bruce (2010), both silanes and siloxanes react with C-H and the C-S-H in the hydrated cement to form silicon polymers. Since the silanes are smaller molecules (owing to the single silicon atom), they are able to penetrate deeper than siloxanes. However, they are more volatile than the siloxanes which result in loss due to vaporisation when being applied.

Stellenbosch University https://scholar.sun.ac.za

According to Hager (1998), silicone based products are advantageous as a result of their inertness and resistance to physical, chemical and microbial attack. According to Broomfield (2013), the hydrophobic impregnations form a hydrophobic film by reacting with pore water. This film however allows water vapour in and out and so the concrete can still breathe. The film formed is within the concrete and thus it is protected from physical degradation and damage from ultraviolet exposure. Figure 2-2 shows a pictorial representation of the hydrophobic impregnation.

The application procedure and form of hydrophobic impregnations is an important aspect in the penetration depth of the surface treatment agent. Typically, the hydrophobic impregnation products exist in liquid, gel or cream form. The liquid phase products are usually accompanied with solvents and have to be applied in multiple stages. This is in contrast with products in gel or cream form which can be applied in one step and do not require additional solvents. A review of the application procedures by Hager (1998), showed that STA in gel form had improved penetration depths when applied on vertical walls and overhead surfaces. This was due to the high viscosity of the STA which eliminated run-off or washing away of the product. Furthermore, hydrophobic impregnation treatment in gel or cream form was found to be less volatile, thereby reducing loss to the environment. Other advantages of using hydrophobic treatment in gel or cream form include:

- high content of active ingredients,
- improved resistance against the alkaline materials in concrete,
- increased capillary water reduction,
- better adhesion to the concrete and
- elimination of use of solvents which makes it environmentally friendly.

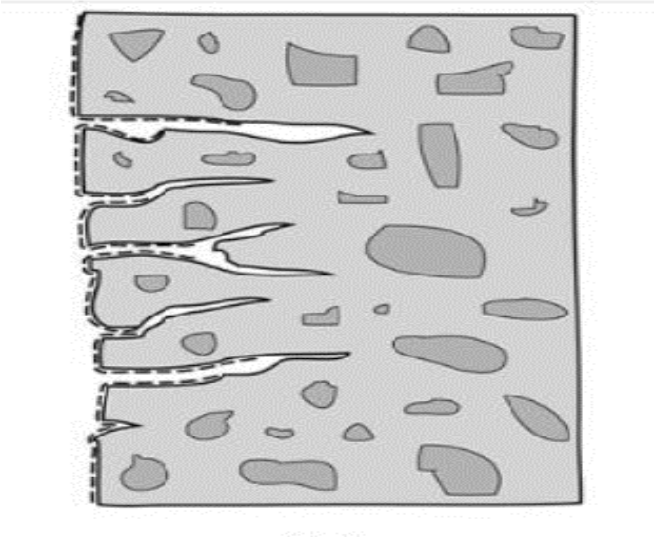

Figure 2-2:Hydrophobic impregnation ,EN1504-2 (2004)

Stellenbosch University https://scholar.sun.ac.za

The second group of STA are impregnations which are also known as pore-blockers. The EN1504-2 standard defines the impregnation treatment as a reduction of surface porosity and strengthening of a surface. Pores and capillaries are partially or completely filled with the pore-blockers. According to Janz et al. (2001), the pore-blockers reduce the ingress of fluids by increasing the resistance under a pressure gradient. Prominent pore-blockers are water glass (sodium and potassium silicate) and fluoride-based compounds. According to Thompson et al. (1997), sodium silicate reacts with the C-H forming C-S-H increasing strength and overall durability as shown in Equation 2-3. This reaction results in the denser outer layer which results in reduced ingress, lower diffusion and increased strength. Figure 2-3 illustrates impregnation treatment.

$$Na_2SiO_3 + xCa(OH)_2 \rightarrow xCaOSiO_2yH_2O + 2NaOH$$

Equation 2-3:Sodium silicate reaction with C-H, Thompson et al. (1997)

According to research by Ibrahim et al. (1999), the use of impregnation treatment did not effectively reduce concrete deterioration due to chemicals in solution such as chloride and sulphate ions. However, for carbonation, impregnation treatment resulted in a decrease in carbonation depth of almost 55 %. This difference in the results can be explained by the fact that impregnation treatment results in a denser cement matrix which reduces the rate of CO_2 diffusion. In the case of ions in solution, impregnation treatment was ineffective as it lacked any water-repelling properties. This difference in performance also highlighted the mass transfer properties which are affected by applying either surface treatment. Based on these outcomes, it can be inferred that the solution to this was the combination of water repellent pore-blocking products which are now available on the market.

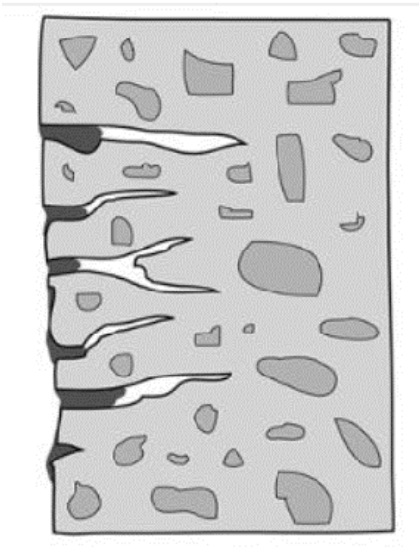

Figure 2-3:Impregnation treatment schematic diagram, EN1504-2 (2004)

Stellenbosch University https://scholar.sun.ac.za

The last group of STA are the coatings. The EN 1504-2 defined coating treatment as a continuous barrier on the surface of concrete with a typical thickness ranging from 0.1 mm to 5 mm. According to Janz et al. (2001), given that coatings are an external barrier as shown in Figure 2-4, they are susceptible to damage from chemical and physical attacks including but not limited to abrasion and acid attack. Some of the prominent coatings include epoxies and acryl compounds.

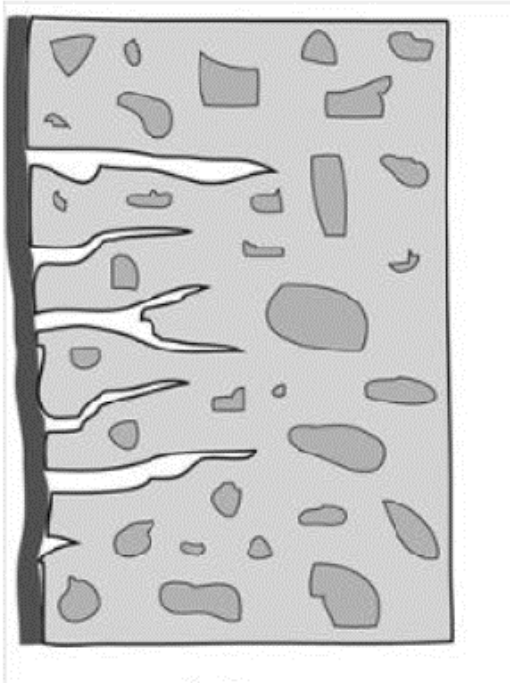

Figure 2-4: Coating schematic diagram, EN1504-2 (2004)

The choice of surface treatment must be informed by the degradation process that must be prevented. This is because various degradation processes are enabled by specific mass transfer properties. There are 3 types of mass transport mechanisms which are permeation under a pressure gradient, diffusion and absorption and capillary flow. Diffusion is split into 2 which are ionic diffusion for substances in solution and gaseous diffusion for substances in vapour phase. Ionic diffusion is associated with ingress of chlorides and sulphates while carbonation is associated with vapour diffusion. Permeation under pressure gradient is associated with groundwater and freeze/thaw action. The surface treatment chosen is therefore dependant on its ability to work against the mass transfer mechanism of the deleterious substance. According to Janz et al. (2001), the application of STA must also be informed by the durability of the STA group chosen and its susceptibility to damage, for instance, the application of coatings where there is high exposure of ultraviolet radiation is ill-advised given that coatings are damaged by ultraviolet radiation.

Stellenbosch University https://scholar.sun.ac.za

2.6.1 Influence of STA on carbonation

A study by Ibrahim, al-Gahtani et al. (1999) revealed that surface treated concrete has lower carbonation depths than untreated concrete (control specimen). Looking at the 3 groups of STA, coatings provided the best protection with no carbon dioxide penetration registered. Sodium silicate, a pore-blocker resulted in a reduction of the carbonation depth by almost 50 %. Hydrophobic impregnations performed the worst with a slight reduction in the carbonation depth when compared to the control sample. Figure 2-5 summarises the findings of that study. It should be noted that no information with regard to the RH and CO_2 concentration were available which makes it difficult to fully understand the results.

The elimination of carbon dioxide penetration after coatings had been applied confirms the ability of coatings to protect the concrete from the environment. Even though coatings were desirable in the case of carbonation, it prevents the concrete from "breathing". The good performance of the pore-blocker could be attributed to the densification of the treated concrete which had a significant effect on the diffusion rate. The reduced efficacy of hydrophobic impregnation treatment could also be attributed to the type of mass transport which is affected by hydrophobic impregnation. Carbonation being a diffusion orientated process could not have been affected significantly by application of the hydrophobic agents.

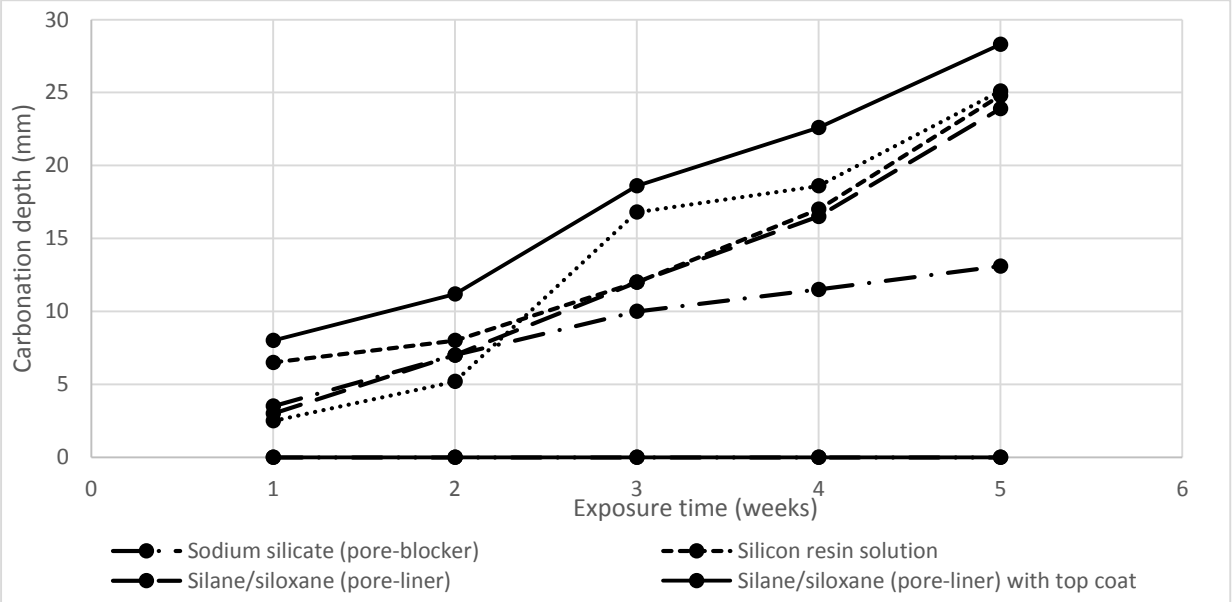

Figure 2-5: Carbonation depth in surface treated concrete samples, Ibrahim et al. (1999)

Stellenbosch University https://scholar.sun.ac.za

Another study by Ho and Ritchie (1992) in which two unidentified coatings were compared observed that in the one coating with a penetration depth of 1 mm. The observed carbonation depth was significantly lower than the other whose penetration depth was 5 mm. This reinforces the idea that surface treatments which restrict moisture ingress but not necessarily vapour ingress may increase the rates of carbonation by giving pores more capacity for CO_2 diffusion.

According to Freitag and Bruce (2010), application of silane/siloxane-based surface treatment on carbonated concrete may not be efficient as polymerisation took longer as a result of vaporisation of the surface treatment. In that regard, use of STA in the form of gel or cream was recommended.

2.7 Carbonation models

Various models of carbonation have been developed over the years. However, most of the models have been for normal concrete and little has been done with regard to foamed concrete. Carbonation models have been used to predict the durability of reinforced concrete. An approximate general relationship shown in Equation 2-4 has been widely accepted.

$$x = k \times \sqrt{t}$$

Equation 2-4: The general carbonation model

Where,

x is the depth of carbonation,

k is a factor dependent on concentration of CO_2, environmental conditions, diffusion coefficient and chemical composition of the concrete and

t is the time of exposure.

According to Kari et al. (2014), the relationship in Equation 2-4 is based on Fick's 1st law of diffusion (mass transport) which assumes steady state diffusion. The constant *k* lumps up all the properties influencing concrete carbonation into one variable. According to Lagerblad (2005) ,where there is greater scrutiny on the other properties influencing diffusion and where there is a non-steady state nature of diffusion ,that is, change of concentration with time and space, Fick's 2nd law of diffusion is used to model carbonation. While carbonation based on Fick's 2nd law is more realistic, it requires taking into account factors such as inward diffusion of CO_2 and CO_3^{2-} ions, outward diffusion of Ca^{2+} ions, solubility, precipitation and porosity change with time among other factors which make the equation computationally expensive and difficult. Consequently, limited information was available on models based on the Fick's 2nd law. As a result, models based on Fick's 1st law were considered in this review.

Stellenbosch University https://scholar.sun.ac.za

2.7.1 Mathematical model of carbonation

A theoretical mathematical model of the carbonation model supporting the square root model in Equation 2-4 has been developed. This mathematical model takes into account two processes: CO_2 diffusion and the chemical reaction between CO_2 and C-H. According to Richardson (2004), the model is developed on the basis of Fick's 1st law of diffusion. Figure 2-6 illustrates the parameters involved.

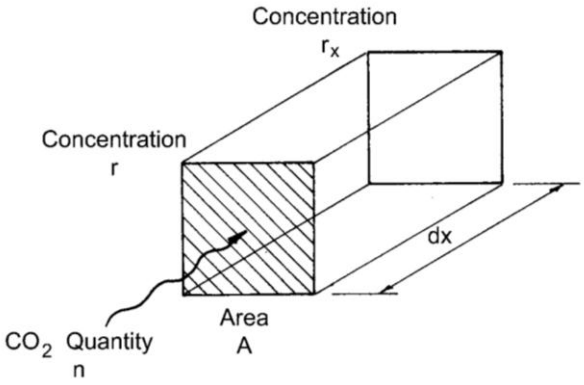

Figure 2-6: Illustration of parameters involved in the theoretical model of rate of carbonation, Richardson (2004)

Where,

n is amount of CO_2 diffusing through an area into the element (kg),

D is the diffusion constant (m/s^2),

A is the area (m^2),

r is CO_2 concentration at the surface (kg/m^3),

r_x is CO_2 concentration at depth x (kg/m^3),

C is the amount of alkaline material in a unit volume (kg/m^3) and

t is time (s).

The diffusion of CO_2 illustrated in Figure 2-6 is described by the mathematical model in Equation 2-5. This mathematical relationship assumes that all the CO_2 that diffuses into the concrete is used in carbonation and that beyond the carbonation front, there are negligible CO_2 quantities. The carbonation front is the boundary between the carbonated and non-carbonated sections in the concrete.

$$dn = -D \times A \times \frac{r - r_x}{x} \times dt$$

Equation 2-5: Mathematical relationship of Fickian diffusion, Richardson (2004)

Stellenbosch University https://scholar.sun.ac.za

The mathematical relation of the chemical reaction between C-H and CO_2 is described by Equation 2-6 . This model relates the amount of CO_2 to the amount of C-H in a unit volume. The amount of C-H is calculated from the amount of calcium oxide (CaO) in the cement.

$$dn = C \times A \times dx$$

Equation 2-6: Mathematical relationship of the chemical reaction of C-H and CO2, Richardson (2004)

By equating the amount of CO_2 in Equation 2-5 and Equation *2-6*, a new relationship between the CO_2 concentration and the amount of alkaline material is derived.

$$C \times A \times dx = D \times A \times \frac{r - r_x}{x} \times dt$$

Equation 2-7: Relationship between CO_2 concentration and amount of alkaline material, (2004)

Equation 2-7 is simplified by cancelling out like terms on both sides of the equation. Assuming that the concentration of CO_2 beyond the carbonation front is negligible, r_x is taken as zero. Integrating with respect to time, a carbonation depth model as shown in Equation 2-8 is developed.

$$x = \sqrt{\frac{2 \times D \times r \times t}{C}}$$

Equation 2-8: Derived carbonation depth model, Richardson (2004)

The parameters c and r can be reasonably estimated. Parameter c, which is the amount of alkaline material, is calculated as a constituent of cement. In Portland cement, the fraction of CaO is about 65 % and hence an amount in kg/m^3 can be calculated. Taking into account the molecular masses of CO_2 (44) and CaO (56), it was calculated that a unit mass of CO_2 required 0.786 of alkaline material. From this, the amount of alkaline material, c is determined by multiplying cement density, 3140 kg/m^3 by mass fraction, 0.786 and by percentage of CaO, 65 % to get 1604 kg/m^3. The concentration of CO_2 was calculated using the fraction of CO_2 in air. According to CO2.Earth (2016), the fraction of CO_2 in the atmosphere is 403.51 ppm which equates to about 8.3 x10^{-4} kg/m^3. For accelerated carbonation where CO_2 levels of up to 5 % are used, the fraction is 50 000 ppm. This results in the CO_2 amount being 0.1 kg/m^3.The only unknown parameter is the diffusivity constant, D. Owing to the scarcity of research on foam concrete carbonation, a model for the diffusivity of foam concrete could not be established.

Stellenbosch University https://scholar.sun.ac.za

The mathematical model is not perfect. It does not take into account the influences of porosity, RH and the change in microstructure due to carbonation. The carbonation process results in a denser microstructure due to the formation of $CaCO_3$. Given the important role of moisture, the RH cannot be ignored in carbonation. The CO_2 gas reacts with the pore water to form an aqueous solution before reacting with the alkaline material in the concrete. However, saturated pores hinder the rate of diffusion of CO_2. If the moisture content is too low, the rate of diffusion of CO_2 is high but there is not enough pore water for the dissolution process to occur optimally. Based on this, a function of relative humidity is necessary in order to account for its effect on carbonation.

2.7.2 Reaction rate model

The rate of reaction carbonation model was developed on the basis of the rates of reaction and conservation of mass of CO_2, C-H and C-S-H. According to Papadakis (2000) ,the reactions include diffusion of CO_2, dissolution of CO_2 and the reaction of aqueous CO_2 with C-S-H, C-H and unhydrated cement phases. This model took into account the reduction of porosity due to formation of $CaCO_3$, the SCM where applicable and the moisture content as can be seen in Equation 2-9.

$$x_c = 350 \times \left(\frac{\rho_c}{\rho_w}\right) \times \left\{\frac{\frac{w}{c} - 0.3}{\left(1 + \frac{\rho_c}{\rho_w} \times \frac{w}{c}\right)}\right\} \times \left(1 - \frac{RH}{100}\right) \times \sqrt{\left(1 + \frac{w}{c} \times \frac{\rho_c}{\rho_w}\right) \times [CO2] \times t}$$

Equation 2-9: Simplified carbonation model based on rate of reaction, Richardson (2004)

Where,

$[CO_2]$ is the CO_2 concentration (%),

$D_{e,\,CO2}$ is the effective diffusivity of CO_2 in carbonated concrete (m^2/s),

c is the cement content (kg/m^3),

w is the water content (kg/m^3),

ρ_w is the water density (kg/m^3),

ρ_c is the cement density (kg/m^3) and

RH is the relative humidity (%).

Stellenbosch University https://scholar.sun.ac.za

The amount of C-H and C-S-H consumed during the carbonation process are calculated on the assumption that full hydration has taken place. The calculations were based on equations that took into account the amount of SCM in the mix design. Equation 2-9 was derived from regression analyses done on experimental work which was based on a w/c ratio within a range of 0.5 to 0.8.

The model was compared to carbonation depth data from Jones and McCarthy (2005). While Equation 2-10 has cement-based variables, total binder content was used as this research made use of FA. The model predicted lower carbonation depths as can be seen in Figure 2-7. This is consistent with the expectations because the model was developed for normal weight concrete which is denser and less porous than foamed concrete.

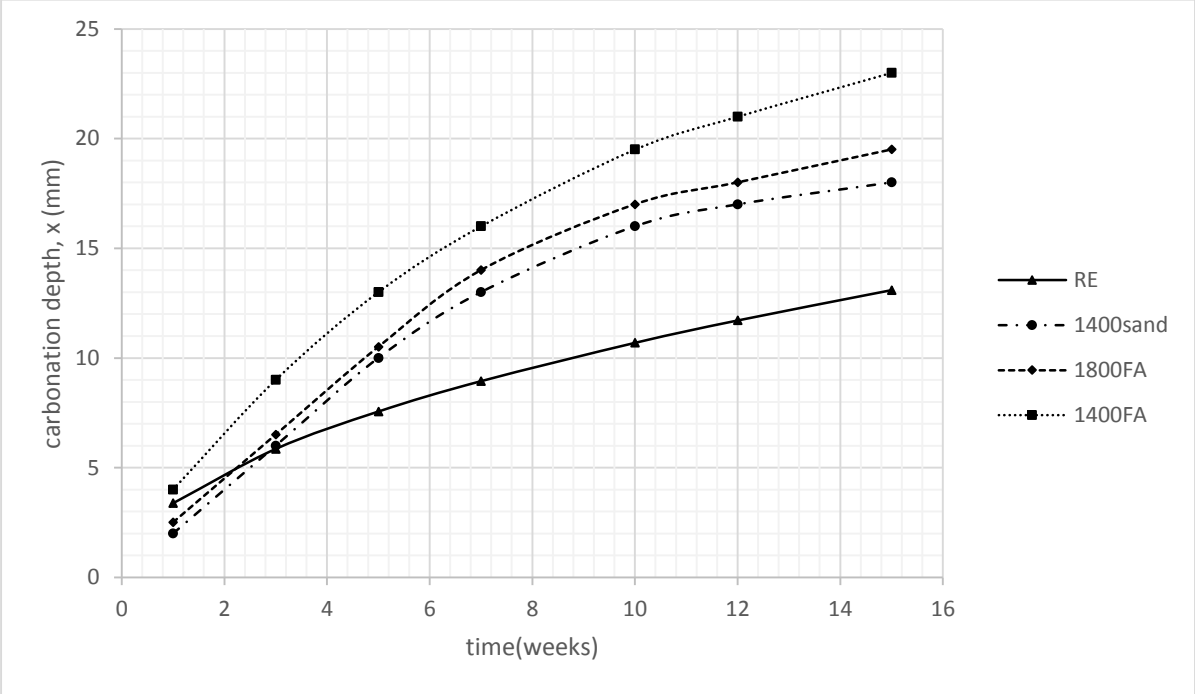

Figure 2-7: Reaction rate model vs experimental data from Jones and McCarthy (2005)

In order to account for the porosity of foamed concrete, the model was adjusted by using the model by Kearsley (2002) illustrated in Equation 2-10. The model estimates porosity based on the compressive strength of foamed concrete. The compressive strength was measured on 7 samples of foamed concrete with a target density of 1400 kg/m^3.

$$f_c = 39.6 \times (\ln(t))^{1.174} \times (1 - p)^{3.6}$$

Equation 2-10: Relationship between porosity and strength in foamed concrete, Kearsley (2002)

Where,

Stellenbosch University https://scholar.sun.ac.za

p is the mature porosity after 365 days,

f_c is the compressive strength of foamed concrete (MPa) and

t is the time since casting in days.

The carbonation prediction for the porosity-adjusted model gave a final depth of 120 mm after 15 weeks which was 9 times higher than the original model as seen in Figure 2-8. However, the original model understated carbonation depths by almost 45 %. It must be noted that the porosity adjusted model was used and that the samples that had 50 % partial cement replacement with fine FA while the samples used by Jones and McCarthy (2005) contained coarse FA in place of sand.

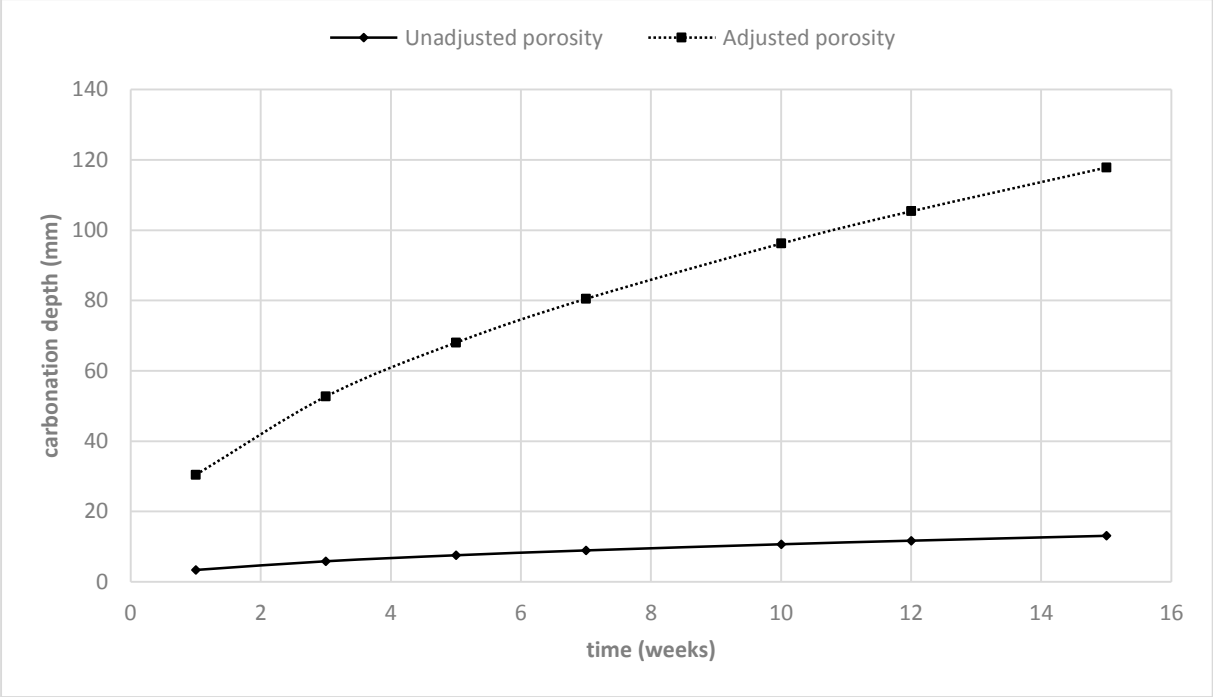

Figure 2-8: comparison of Rate of reaction model with porosity adjusted for foamed concrete and the original model

2.7.3 Carbonation model by Parrott

The carbonation model developed by Parrott (1994) had a different approach to the determination of the diffusion constant. The diffusion constant was estimated based on the oxygen (O_2) permeability tests. This is different from the diffusion constants referred to in Sections 2.7.1 and 2.7.2 which were estimated from the diffusion constant of $CaCO_3$. The diffusion constants measured on the basis of O_2permeability are not accurate because the O_2 molecule is smaller than that of CO_2. Furthermore, O_2 is neutral in concrete while CO_2 reacts with pore water and alkaline materials.

The Parrott model may also be reduced to the simplified carbonation equation in Equation 2-4 as illustrated in Equation 2-11.

Stellenbosch University https://scholar.sun.ac.za

$$x = \frac{64 \times K^{0.4} \times t^{0.5}}{c^{0.5}}$$

Equation 2-11: Carbonation model by Parrott, Richardson (2004)

Where,

K is the O_2 permeability in the order of 10^{-16} (m^2/s) and

C is the CaO content in the hydrated cement matrix (kg/m^3).

The coefficient in Equation 2-11 was used to magnify the depth of carbonation as the model estimated the minimum carbonation depth. The power on is estimated to 0.5 for indoor exposure but can then decrease with increasing RH beyond 70 %. The presence of the constant relating to CaO acknowledged the fact that durability of concrete is also dependent on the mix design of the concrete itself and not solely dependent on the environment. The O_2 permeability constant was determined at a RH of 60 % and an adjustment factor was developed to account for the change in permeability with RH. Where the RH is not 60 %, O_2 permeability is adjusted by multiplying the O_2 permeability at an RH of 60 % with the factor m from Figure 2-9 .

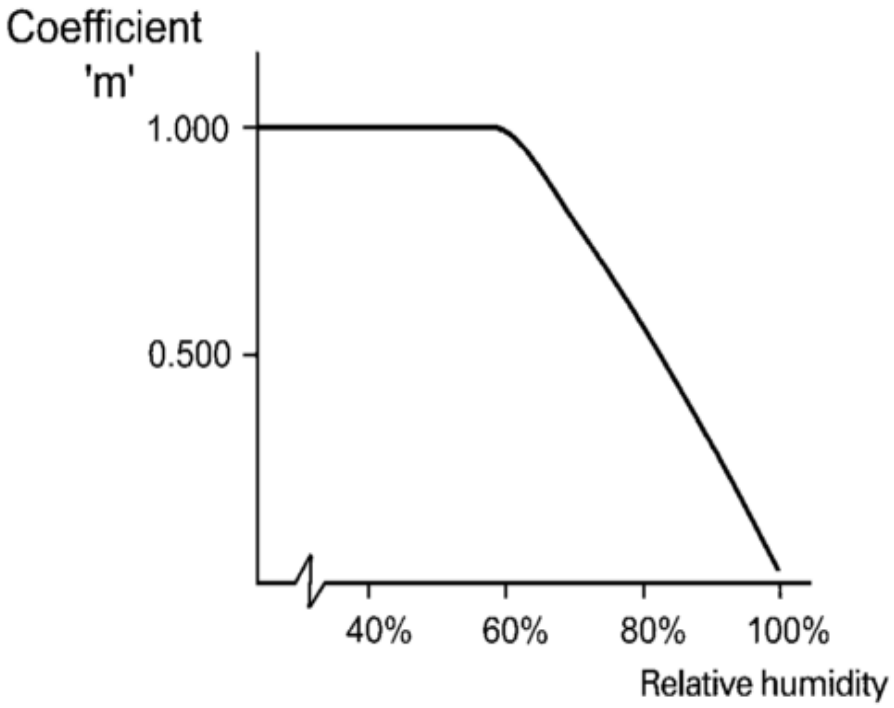

Figure 2-9: The coefficient m adjusting the permeability with respect to RH, (2004)

Stellenbosch University https://scholar.sun.ac.za

In order to test this model for its performance when foamed concrete was used, O_2 permeability had to be determined. Given the absence of a prediction model for permeability, a value of O_2 permeability from foamed concrete specimens by Kearsley (2001) with a density of 1500 kg/m^3 was used. Referring to Figure 2-10, the Parrott model predictions were lower than the actual carbonation depths of denser foamed concrete mixes. This result is expected as the O_2 molecule is smaller than the CO_2 molecule which might result in higher levels of permeability of O_2 than of CO_2. Also, the model was developed for normal weight concrete which is less permeable when compared to foamed concrete.

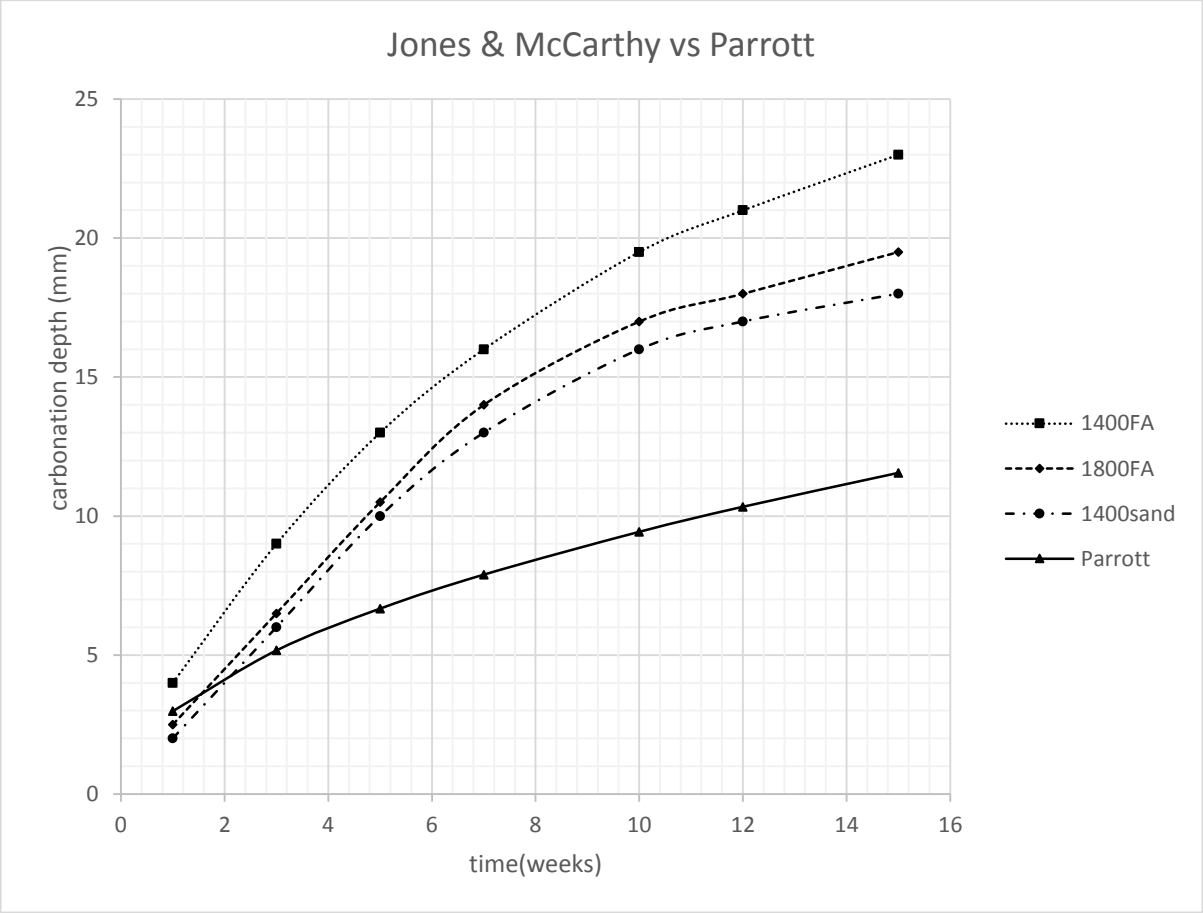

Figure 2-10: Parrott model vs the Jones & McCarthy carbonation experiments

The 3 carbonation models that were examined in this survey were derived for natural carbonation. This is also one of the reasons why the results did not compare reasonably to the accelerated carbonation results. A comparison of natural carbonation and accelerated carbonation by Sanjuan and Cheyrezy (2003) revealed that the models mentioned in 2.7 needed to be verified using short term testing methods in which adjustments could be made to parameters so that they can be adapted to suit various types of concretes. Also, the research failed to establish a scaling model which could be used to relate natural carbonation to accelerated carbonation.

Stellenbosch University https://scholar.sun.ac.za

2.8 Monitoring carbonation progression

Various methods have been used to track the progression of carbonation. The most popular method is the phenolphthalein test. Depending on the composition of the phenolphthalein solution, the indicator solution is sprayed on a freshly cut surface and the uncarbonated areas become pink, purple or red. Research by Sanjuan and del Olmo (2001) made use of phenolphthalein indicator solution made up of 1% phenolphthalein in ethanol. Even though its use is widespread, research has shown that phenolphthalein indicator solution has been linked to cancer and genetic defects prompting research to find safe alternatives. Research by Chinchon-Paya et al. (2016) has provided an alternative indicator solution using 0.5 % curcumin in ethanol which becomes yellowish-orange when sprayed on carbonated concrete and red when sprayed on non-carbonated areas.

Another method that can be used to determine the extent of carbonation is the Fourier-transform infra-red spectroscopy method (FT-IR). A beam of infra-red light is focused on a concrete sample and each function group that builds up the molecules resonates at its characteristic absorption frequency which lies in the infra-red region of the electromagnetic spectrum. The intensity of the infra-red beam focused on the sample reduces with the absorption of the functional group. The absorption is then calculated as a ratio of the infra-red light beam before and after being shone through the sample. The absorption is then plotted against each wavelength to obtain the infra-red spectrum of the sample. The plot is then used to identify the chemical compounds and functional groups that make up the molecules of the sample. According to research by Lo and Lee (2002), the use of FT-IR spectroscopy gave more consistent results as well as identifying regions where partial carbonation had occurred unlike using the phenolphthalein indicator test. Consequently, the carbonation depth determined by the FT-IR method was on average 24 % higher than that determined by using the phenolphthalein test. An illustration of the differences in the carbonation depth between the phenolphthalein indicator test and the FT-IR is shown in Figure 2-11.

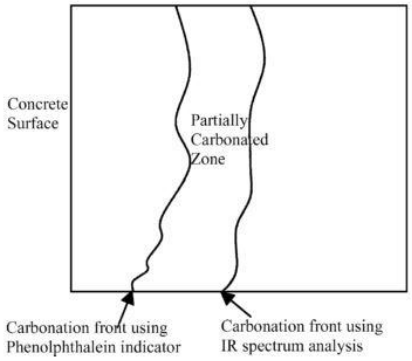

Figure 2-11: Illustration of the difference between the FT-IR and phenolphthalein indicator solution Lo and Lee (2002)

Stellenbosch University https://scholar.sun.ac.za

2.9 Fundamentals of reinforcement corrosion

According to Markeset and Myrdal (2008), reinforcing steel is thermodynamically unstable and hence will act in a manner so as to make itself stable. The thermodynamically stable states are the oxide states. In order to form the stable oxides, water and O_2 act as chemical drivers of the process. The process is described in terms of a thermochemical reaction in which electron transfer occurs. The kind of oxide formed is dependent on the exposure conditions. An example of a rusting process is illustrated in Equation 2-12. This rusting process is a combination of two electrode equations. A visual representation of the rusting process is shown in Figure 2-12. The anode reaction, which occurs at the reinforcement, is an electron donating process (oxidation) while the reaction at the cathode is electron consuming. The reaction at the cathode is where the O_2 and the moisture which are the driving forces are the inputs. This shows that for rusting process to proceed, the two driving forces have to have access to the steel reinforcement.

$$4Fe + 2H_2O + 3O_2 \rightarrow 4FeOOH$$

Equation 2-12: Rusting of iron

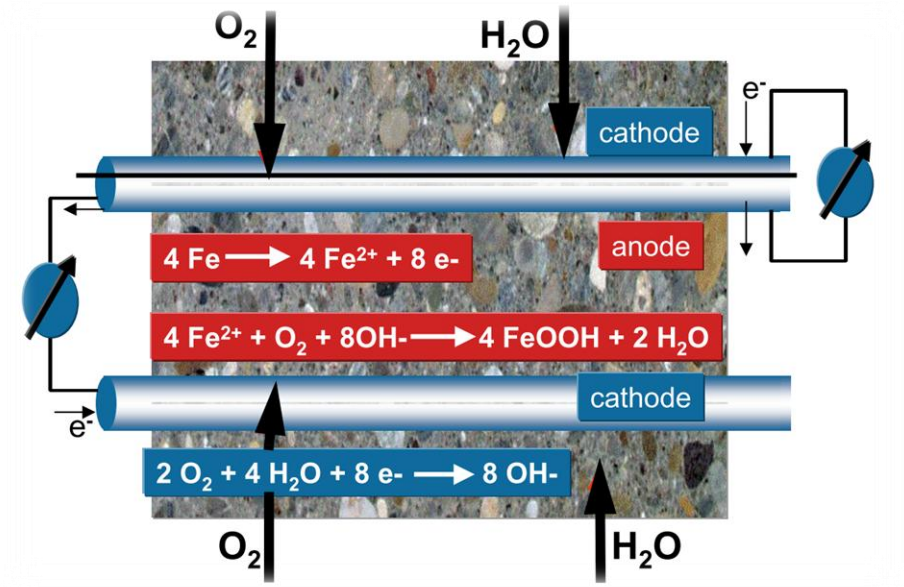

Figure 2-12: Schematic diagram of rusting process in reinforcement corrosion, Giessler et al. (2005)

In reinforced concrete, the concrete provides a cover to the steel. According to Giessler, Standke and Buchler (2005), the high pH of the concrete protects the reinforcing steel. This protective layer is called the passivation layer. The passivation layer is damaged by the ingress of chloride ions and depleted by carbonation. This results in the reduction of the pH and subsequently corrosion of the steel reinforcement.

Stellenbosch University https://scholar.sun.ac.za

Given that steel reinforcement corrosion commences when O_2 and moisture reach the steel reinforcement, corrosion probability is reduced by inhibiting them to access the steel reinforcement. While the steel reinforcement is protected by a passivation layer, the destruction of the passivation layer exposes the steel reinforcement. In the case of carbonation prone environments, ingress of CO_2 which reacts with the C-H and C-S-H in the concrete thereby destroying the passivation layer. Therefore, if surface treatment is applied, it must therefore retard or inhibit CO_2 diffusion. According to Janz et al. (2001), the surface treatment against carbonation ingress is achieved by increasing the density to a point where the rate of diffusion is decreased. For coatings, this property is evaluated according to EN1062-6 where CO_2 diffusion is analogous to an equivalent air layer thickness, s_D greater than 50 metres such that:

$$s_D = \frac{D_{air}}{D_m} \times s > 50m$$

Where,

D_{air} is diffusion coefficient of CO_2 in air (m^2/s),

D_M is the diffusion coefficient of CO_2 in the coating (m^2/s) and

s is the thickness of the coating.

2.10 Conclusion

Corrosion of the steel reinforcement in concrete is mainly induced by two major processes which are carbonation and chloride-induced corrosion. These two processes are influenced by mass transport mechanisms. This chapter reviewed the carbonation-induced corrosion and what influences it as it is the key theme of this study.

Carbonation-induced corrosion impacts on the durability of reinforced concrete as destroys the protection layer around the steel reinforcement. Carbonation occurs when CO_2 gas dissolves in the pore solution and then reacts with the alkaline products of cement hydration forming $CaCO_3$. The reaction results in the lowering of the pH in the concrete layer protecting the steel reinforcement thereby making it vulnerable to corrosion. The carbonation process has also been linked to carbonation shrinkage.

Carbonation-induced corrosion has been controlled in normal weight concrete using surface treatment. Surface treatment is available for use in two types which are integral and non-integral surface treatment. Integral surface treatment is applied during the mixing phase of the concrete while non-integral surface treatment is applied after hardening. There are 3 types of surface treatment which are pore-liners, pore-blockers and coatings. Pore-liners form a thin film on the pore surface which is hydrophobic and prevents water and ions in solution from ingress into the concrete. Pore-blockers partially or wholly fill the pores. This increases the resistance under a pressure gradient. Coatings form a layer on the surface of the concrete thereby making a physical barrier

Stellenbosch University https://scholar.sun.ac.za

around it. The surface treatments generally work by restricting particular mass transport mechanisms.

Prediction models for carbonation-induced corrosion have been developed for estimating the durability of concrete. The models are based on Fickian diffusion laws and take into account the mix design and thickness of the concrete protection layer. While no prediction model exists for foam concrete, fundamentals of prediction models are discussed.

The next chapter discusses corrosion assessment and measurement techniques.

Stellenbosch University https://scholar.sun.ac.za

CHAPTER 3 ASSESSMENT OF CORROSION

Various forms of corrosion assessment methods are reviewed in this chapter. Given that this study involves periodic corrosion measuring, non-destructive methods are selected. An in depth review of two of the most common method is covered. Factors influencing the methods and the experiment set-ups were also explored.

3.1 Background

Corrosion assessment is important in concrete structures. It is a helpful tool when determining the integrity of a structure. According to Song and Saraswathy (2007), there is no consensus regarding the most accurate method of corrosion assessment. Therefore, it is important to use multiple methods to ascertain levels of corrosion in the reinforcement.

Assessment of corrosion in steel reinforcement is dependent on how much information is required from the exercise. Corrosion assessment ranges from a visual assessment to an in-depth corrosion rate determination. The determination of rate of corrosion is done by means of electrochemical methods. The methods are classified into two groups namely destructive and non-destructive techniques. Non-destructive techniques are more suited to standing structures and can therefore be used to monitor the progression of steel reinforcement corrosion. A number of non-destructive techniques exist but only two are discussed. These are the half-cell potential (HCP) and the linear polarisation resistance (LPR) method. The LPR method was not used in this study.

The basis of corrosion assessment by means of electrochemical methods is on the rate of flow of electrons. According to Richardson (2004), cathodic and anodic processes culminate in positive and negative charges. When the two processes are combined, electrical neutralisation is achieved with no excess charge. This means that the rates of oxidation and reduction are equal and the rate of corrosion can be deduced from the rate of electron transfer. This rate of electron flow is computed as a corrosion current density which is the amount of electrons flowing per unit area.

3.2 Half-Cell Potential

The fundamentals of the HCP lie in the chemistry of metallic corrosion. According to Babaei (1986), metallic corrosion involves the flow of current of one metal to the other. Where two dissimilar metals are immersed in an aqueous solution, the one metal will have an affinity for electrons while the other releases electrons depending on their natural electromotive force. This type of cell is called a galvanic cell. Galvanic corrosion is not limited to dissimilar metals. It can also occur on the same metal as most of the metals are not homogenous and contain impurities.

Stellenbosch University https://scholar.sun.ac.za

The impurities in metals can also establish the cathodic and anodic electrodes. In reinforced concrete, iron is in a passive state in alkaline environments provided by the concrete cover. In dry conditions, the concrete does not provide an environment in which ion transfer occurs. However, as the moisture levels increase, the concrete acts as an electrolyte as its resistivity decreases. This reduced resistivity of concrete results in electron transfer or flow of current between the anodic and cathodic electrodes on the steel reinforcement, resulting in metallic corrosion which in this case is rusting. It is this current flow that is measured and used to deduce the likelihood of corrosion in reinforcement steel.

The HCP test is an estimation of the corrosion potential of uncoated steel reinforcement in field and laboratory concrete as defined by ASTM C876 (2009). Furthermore, given that the test method is limited by electric circuitry, it is important that the resistivity, which is the electrical resistance of the concrete, is low enough to enable the taking of measurements. Given that low moisture content in the concrete increases resistivity, high impedance circuitry is required in environments such as deserts and building interiors where concretes lose sufficient moisture. Moreover, where STA are applied, the resistivity of the concrete is also increased. In the case of coatings, it is highly unlikely to achieve a direct connection with the concrete which makes it nearly impossible for use in corrosion measurement.

According to Song and Saraswathy (2007), the concrete acts as an electrolyte while the steel bar develops a potential based on its environment. The potential may differ from place to place. The steel reinforcement potential is then measured relative to a reference standard electrode such as a saturated calomel electrode (SCE), copper/copper sulphate electrode (CSE) or silver/silver chloride electrode. Figure 3-1 illustrated the test setup of the HCP.

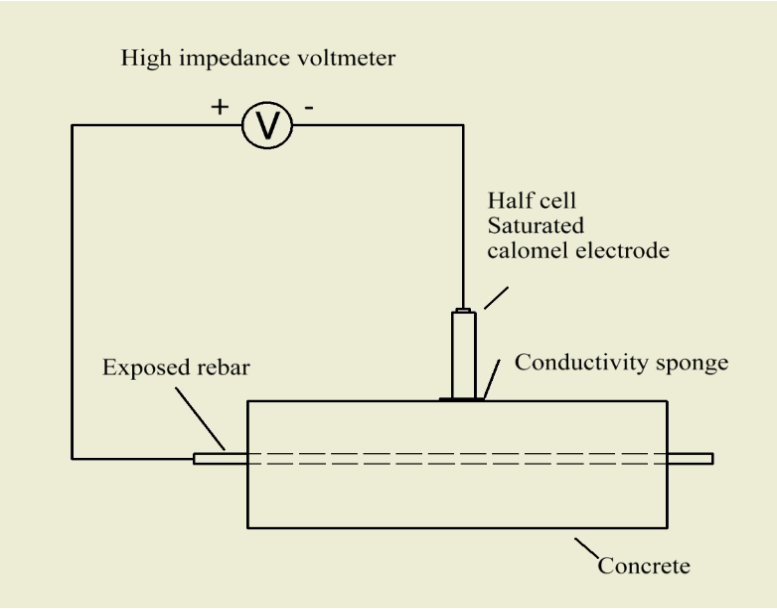

Figure 3-1: HCP test setup, Song and Saraswathy (2007)

Stellenbosch University https://scholar.sun.ac.za

The readings obtained from the high impedance voltmeter are used to estimate the probability of corrosion. The measured potential is compared to the threshold levels in Table 3-1. The values in the first column in Table 3-1 are for a SCE electrode and the second column values are for a CSE electrode. The corrosion condition is not an absolute truth but an indication of the likelihood of corrosion occurring. If certainty is sought, the HCP must be used in conjunction with other corrosion assessment methods.

Table 3-1 Corrosion potential measurement and the associated corrosion risk, Song and Saraswathy (2007)

Open circuit potential (OCP) values		
mV vs. SCE	mV vs. SCE	Corrosion condition
<-426	<-500	severe corrosion
<-276	<-350	High(,90% risk of corrosion)
-126 to -275	-350 to -200	intermediate corrosion risk
>-125	>-200	Low(10% risk of corrosion)

The potential readings obtained from the HCP test cannot be interpreted in isolation given that they are affected by a variety of factors which include but are not limited to concrete moisture, concrete porosity, O_2 concentration and carbonation.

3.2.1 Factors influencing half-cell potential readings

3.2.1.1 Concrete resistivity

According to Gulikers et al. (2003), the moisture on the surface of the concrete has a major influence on the potential readings. Where the surface of the concrete is wet, the resistivity of the concrete reduces. A reduction in the resistivity of concrete results in a shift towards more negative potential values even though the corroding spots do not change. Inconsistency in the moisture distribution of concrete surfaces enhances potential differences between the actively corroding areas and the passive areas.

Given that corrosion is an electrochemical process, an inverse relationship exists between the corrosion potential and resistivity. Therefore, any process that increases the resistivity of concrete results in a reduction of corrosion potential and ultimately a reduction in corrosion rate.

3.2.1.2 Oxygen diffusion

The concentration of O_2 at the concrete and steel reinforcement interface has an influence on the HCP readings. According to Ping and Beaudoin (1998), a low concentration of O_2 at the surface of the steel reinforcement shifts HCP towards the negative.

Stellenbosch University https://scholar.sun.ac.za

A more negative HCP reading may give the impression that there is a high likelihood of corrosion, which may not be the case. A low concentration of O_2 at the steel bar and at the concrete surface actually reduces the corrosion rate given that O_2 is a necessary ingredient for corrosion to occur.

The interpretation of the HCP readings with respect to O_2 concentration at the surface of the steel bar must be carefully considered. Research undertaken by Qian and Cusson (2004) showed that the negative shift in corrosion potentials reflected corrosion initiation due to cracking of the concrete cover while in certain areas, it reflected the O_2 depletion because high density concrete was used in that study. These observations were corroborated by another research by Assouli et al. (2008) were O_2 depletion at steel reinforcement level resulted in a negative potential shift in the HCP reading by 100 mV and in some severe cases 200 mV. In those cases, it is recommended that the threshold values be adjusted by a value equal to the potential shift.

3.2.1.3 Carbonation

Carbonation of concrete has two main effects on HCP readings. According to Elsener et al. (2003),due to the loss of the alkaline pore solution, the resistivity of concrete increases which results in increased difficulty in locating localised corrosion. As a result, more positive HCP readings are observed which suggests a low corrosion risk while corrosion may actually be happening. Also, according to Ping and Beaudoin (1998), the reduction of the pH due to the consumption of the alkaline material as a result of carbonation leaves the reinforcement vulnerable to corrosion. This results in a shift towards the negative of the HCP. This is consistent with expectations as loss of the passivation layer by the acidification exposes the steel reinforcement to oxidation.

3.2.1.4 Cover depth

The depth of the protective concrete to the steel reinforcement plays a role in the preventing or limiting of reinforcement corrosion. A comparison of two cover depths of 10 mm and 50 mm in a research by Polder and Peelen (2002) revealed that the resistivity of the reinforced concrete increased with increasing cover depth. Other research by Qian and Chagnon (2001) concluded that a thick concrete cover resulted in depressed O_2 concentration at the steel reinforcement -concrete interface resulting in a negative shift of the corrosion potential due to reduced O_2 diffusion.

According to ASTM C876 (2009), the HCP test can be used for any cover depth. However, the corrosion potentials obtained for cover depths in excess of 75 mm may be an average of adjacent corrosion potentials. This phenomenon makes it difficult to determine the variation of corrosion activity.

Stellenbosch University https://scholar.sun.ac.za

3.2.1.5 Surface treatment products

As outlined in the ASTM C876 (2009) standard, the HCP test method is limited by electrical circuitry. The use of coatings makes it difficult to have a direct electrical connection with the concrete. This makes it impossible to accurately measure the corrosion potentials.

The application of hydrophobic agents or pore-liners results in the reduction of moisture in the concrete. The low moisture content results in the increase in resistivity of concrete which may necessitate the use of high impedance circuitry in order to accurately measure the corrosion potentials. Furthermore, the use of pore-blockers results in the densification of the concrete matrix. The densification of concrete results in higher electrical resistivity of the concrete. Lastly, where the surface treatment agents have been applied irregularly, the HCP readings measured may not accurately reflect the state of corrosion of the steel reinforcement. According to Ping and Beaudoin (1998), where the concrete has been damaged and the STA have been compromised, measurements taken for the HCP may be affected due to loss of homogeneity.

3.3 Linear polarisation resistance

Linear polarisation resistance (LPR) is based on the relationship between the HCP of the steel reinforcement and an external impressed current. According to Sadowski (2010), the LPR is a rapid and portable testing method that can be used for both laboratory and field tests. The main theory behind the LPR is the perturbation current that is impressed on the steel reinforcement resulting in the disturbance of the corrosion equilibrium. The response of the system to the perturbation is monitored and measured with respect to the HCP on the concrete surface. The potential induced by the perturbation current is used to calculate the polarisation resistance R_P as in Equation 3-1.

$$R_p = \frac{\Delta E}{\Delta I}$$

Equation 3-1: Polarisation resistance calculated from the perturbation current and the induced potential, Sadowski (2010)

Where,

ΔE is the potential induced by the perturbation current and

ΔI is the perturbation current.

Stellenbosch University https://scholar.sun.ac.za

The corrosion interface is best described by an equivalent electrical circuit called Randle's circuit. Randle's circuit is comprised of a capacitor C_{dl} in parallel to a resistive interface R_{ct}. The parallel circuit is in series with the resistive concrete cover R_s. Randle's equivalent circuit is illustrated in Figure 3-2. The corrosion rate is proportional to the charge transfer resistance R_{ct}. The R_{ct} is calculated as the difference of the R_p and the concrete cover resistance R_p as shown in Equation 3-2

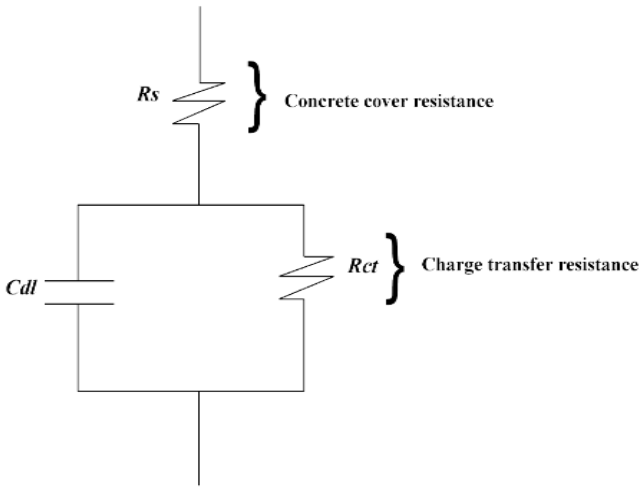

Figure 3-2: Randle's equivalent circuit, Sadowski (2010)

$$R_{ct} = R_p - R_s$$

Equation 3-2: Relationship between charge transfer resistance and concrete cover resistance, Sadowski (2010)

The corrosion current density is calculated from the charge transfer resistance and is also proportional to area of the steel under assessment as seen in Equation 3-3.

$$i_{corr} = \frac{B}{R_{ct} \times A}$$

Equation 3-3: Corrosion current density, Sadowski (2010)

Where,

B is the Stern-Geary constant and

A is the area of steel being assessed.

The value of the Stern-Geary constant is determined from Tafel slopes. According to Moreno et al (2004), the value of the constant has been estimated as 26 mV for passive corrosion of the steel reinforcement and 52 mV for active corrosion of the steel reinforcement

Stellenbosch University https://scholar.sun.ac.za

According to Otieno (2008), one of the drawbacks of the linear polarisation resistance method is determining the actual surface area of the steel reinforcement that would have been polarised or are undergoing active corrosion. In order to get around this drawback, a uniform polarised area is assumed and used to estimate the corrosion rate. Another drawback is that the corrosion rate determined by the Stern-Geary equation does not reflect how long the corrosion has been happening. It then means that it is difficult to ascertain the state of the corrosion.

In spite of the shortcomings of the linear polarisation resistance method, it provides a method of corrosion measuring which is non-destructive, simple to apply and gives definitive corrosion rate timeously.

Once the rate of corrosion has been determined, the corrosion state is determined. As shown in Table 3-2, there four corrosion states. From these corrosion states, the corrosion penetration rate can be estimated. Based on these penetration rates, appropriate interventions can be made.

Table 3-2: Corrosion states and penetration rates from the Linear Polarisation resistance, Sadowski (2010)

Corrosion classification	**Corrosion current density, $i_{corr}(\mu A/cm^2)$**	**Corrosion penetration rate *(µm/year)***
Passive/very low	Up to 0.2	up to 2
Low/moderate	0.2 to 0.5	2 to 6
Moderate/high	0.5 to 1.0	6 to 12
Very high	>1.0	>12

The LPR method is broadly classified into two methods. According to Hassanein et al. (1998), either a current is impressed on the reinforcement or a potential is induced. When a constant current is impressed, the technique is referred to as galvanostatic while if variable currents are impressed, it is referred to as galvanodynamic. In both cases, the potential due to impressed current(s) is examined and used to calculate the R_p. When small constant potential perturbation is applied, it is referred to as potentiostatic while if variable potential perturbations are applied, it is referred to as potentiodynamic. The response of the current is examined and used to calculate the R_p.

3.3.1 Coulostatic method

The Coulostatic method is a potentiostatic LPR method that determines the potential drop after a small current is impressed on to the reinforcing steel. According to Otieno (2008), the pulse impressed is for a known duration and is in the order of milliseconds.

Stellenbosch University https://scholar.sun.ac.za

The corrosion rates are then determined from the decay in potential after the pulse has been applied. The corrosion rates relate to a time constant that describes the exponential decay in the potential. Also, according to Glass (1995), high corrosion rates lead to rapid drop in potential while low corrosion rates result in more gradual potential drops. Equation 3-4 describes the potential transient state at any time after the pulse has been impressed on the reinforcing steel.

$$n_t = n_o \times e^{\frac{-t}{\tau}}$$

Equation 3-4: Potential transient equation, Glass (1995)

Where,

n_t is the potential shift at time t,

n_o is the initial potential shift and

τ is the time constant.

The value of the time constant is calculated using the capacitance C and the polarising resistance as shown in Equation 3-5.

$$\tau = C \times R_P$$

Equation 3-5: Time constant equation, Glass (1995)

Where C is the capacitance which is calculated from the charge divided by the initial potential shift. The potential shifts are measured about 0.1 seconds after the termination of the pulse. The measurements within the initial 30 seconds can be used for determining the potential shifts.

According to Glass (1995), the duration of the pulse has an impact on the shape of the potential transient state. Where pulses have been impressed on the reinforcing steel for longer periods, the flatter curves of potential relaxation while corollary is true for pulses of a lesser duration.

The coulostatic method has its own advantages and disadvantages. The advantages include:

- duration of pulse so small that it does not affect the diffusion process.
- the effects of the electrolyte need not be compensated.
- it is suitable for low frequency work unlike impedance measurements.
- the time constant is not dependent on the steel surface area.

The disadvantages of the coulostatic method include:

- long periods of time required in order to determine the transient potential.
- no indication of how long corrosion has been going on.

Stellenbosch University https://scholar.sun.ac.za

The experimental set up of the coulostatic method is illustrated in Figure 3-3.

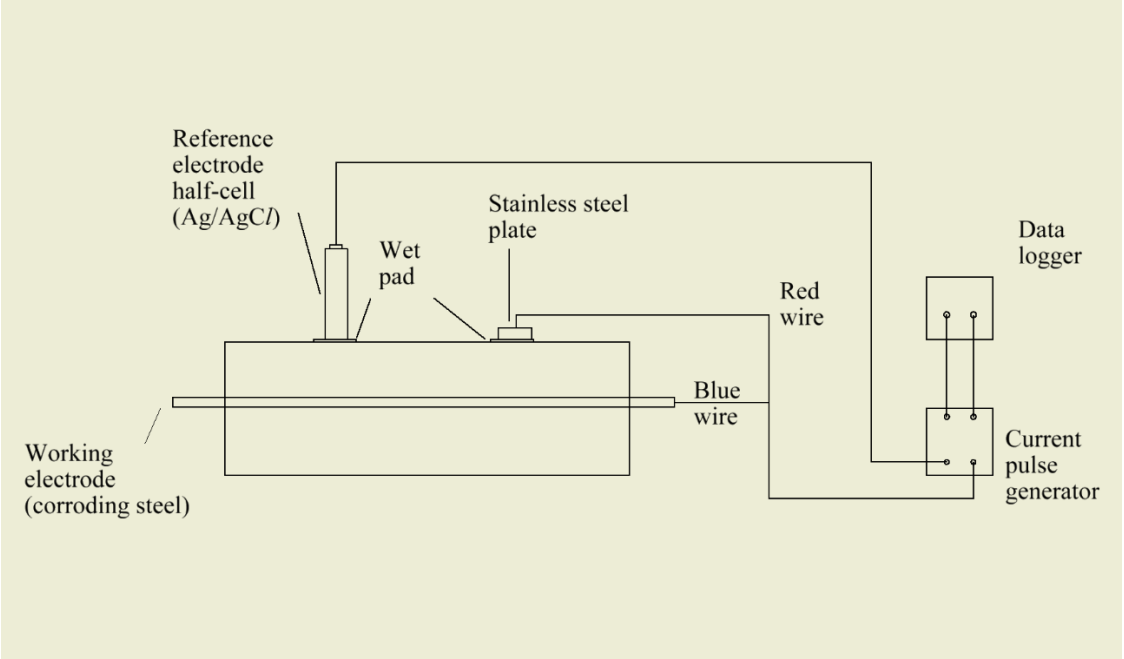

Figure 3-3: Illustration of the setup of the Coulostatic method, Paul (2015)

3.4 Conclusion

Assessment of corrosion is a function of how much information must be derived from the exercise. It ranges from visual assessment to an in-depth determination of the corrosion rate and state. A discussion of 2 methods of corrosion measurement is in this chapter. These are the HCP and the polarisation resistance methods. A more detailed discussion of the HCP is done as it is the method used in this research.

The next chapter discusses the experimental design and testing procedures used in this research.

Stellenbosch University https://scholar.sun.ac.za

CHAPTER 4 EXPERIMENTAL DESIGN

This chapter details the experiments performed during the period of study. These details include the mix design of the prepared samples, the equipment used in the preparation of the sample, the tests apparatus and test setups. Given that the influence of surface treatment agents (STA) was sought, a control set of specimens was used as baseline. Two types of STA were used namely integral and non-integral systems. The tests conducted were compressive strength, void distribution and size, carbonation depth, penetration of STA and corrosion monitoring on reinforced LWFC beams.

4.1 Introduction

The density of foam concrete is an important factor in early age and engineering properties of concrete. As a consequence, the attainment of the correct density was an important objective. Trial mixes were made in order to achieve the right density and consistency. An accelerated carbonation chamber was built and used to create a CO_2 rich environment. Compressive tests were done as a quality control measure and as an input for carbonation models. Corrosion measuring tests were then undertaken in accordance with standard test methods.

4.2 Mix design constituents

Sephaku CEM I 52.5 N ordinary Portland cement with a relative density of 3.14 was used. The cement is compliant with SANS 50197-1 (2013) and is compatible with cement extenders namely fly ash (FA), silica fume and ground granulated blast furnace slag. FA used in this study is compliant with the chemical and physical requirements of SAN 50450-1 (2014), category S. and has a relative density of 2.2.

4.3 Mix design procedure.

The mix design process was focused on attaining a specific target density. This was achieved by making use of Equation 2-1 and Equation 2-2. From Equation 2-1, the mass of the constituents should be equal to the target density. In order to calculate the volume of entrained air, Equation 2-2 was used. The equation is structured such that the total volume of all constituents is 1000 litres.

The mix design of foamed concrete is very sensitive to the water demand of the constituents. According to Kearsley (1999), if too little is used, foam breakdown occurs as the cement withdraws water from the bubbles for hydration. When too much water is used, segregation occurs. The simultaneous use of Equation 2-1 and Equation 2-2 allows for a mix design that ensures a stable mix. The quantities of the mix constituents used are shown in Table 4-1.

Stellenbosch University https://scholar.sun.ac.za

Table 4-1: Mix design constituents' quantities

Item	Quantity
Cement (kg)	511.7
Water (kg)	358.2
Fly-ash (kg)	511.7
Foam (l)	18.5
Target density, ρ_t (kg/m^3)	1400

The foam was produced in a foam generator in which the foaming agent, ferrous sulphate and water were used in combination. The ferrous sulphate was used to stabilise the foam. The resulting foam had a target relative density of 0.075.

Table 4-2: Constituents required for foam production and their quantities

Item	Quantity
water (l)	40
Foamtech (l)	1
Ferrous sulphate (g)	50

The constituent quantities for foam production as seen in Table 4-2 were derived from the specifications from the foaming agent manufacturer. It is important to note that the water requirement of the foam is independent of that required for hydration processes. Failure to ensure sufficient water for hydration results in foam breakdown.

4.4 Equipment

A drum mixer was used for mixing the constituents including the foam. A separate foam generator was used for foam production. A fixed mixing routine is required in order to get consistent mixes and accurate densities.

4.4.1 Foam concrete mixer

A 70 l drum mixer with a motor-powered rotating horizontal axle with fixed blades was used in this study. The mixer had a fixed rate of rotation. To maintain uniformity, the time taken to mix was standardised. An illustration of the mixer is shown in Figure 4-1.

Stellenbosch University https://scholar.sun.ac.za

Figure 4-1: Drum mixer for foam concrete

4.4.2 Foam generator

A standalone foam generator was used for producing foam. The foam generator, as seen in Figure 4-2, was connected to an external compressed air source of 6 bar. The foaming agent, sulphate and water were put in the tank of the generator. The foam generator also provided for a flexible flow rate with a flow rate regulator.

Figure 4-2: Foam generator

Stellenbosch University https://scholar.sun.ac.za

4.5 Mixing Method

The sequence of mixing the constituents of the mix design is important in the attainment of a consistent density of foamed concrete. This is critical since the capacity of the mixer is restricted resulting in a number of batches being required.

According to Kearsley (1999), it is recommended to first pour water into the mixer followed by the cement, FA and then the foam. From the trial mixes performed for this study, water leakages made it impossible to start the mixing regime by pouring water in the mix. A different sequence was adopted for this study. Firstly, half of the amounts of FA and cement were poured into the mixture. This was done to ensure that an even mix was achieved.

The first constituent to be thrown into the mixer was FA. The reason for that was that the clog of the dry FA at the drainage hole at base of the drum was easier to remove than a compacted cement clog. Also, the cement was the main binder while FA acted dually as a co-binder and fine filler. After the dry mix had been thrown into the mixer, the mixer was turned on for a minute. This ensured a uniform mix. After the dry mix was evenly mixed, about 80 % of the total water required was poured into the mixer. Following the addition of water, the mixer was allowed to run for three minutes. The dry material clogging the drainage hole was then extracted and put back into the mixer. The remaining water was then added and the mixer ran for a further two minutes.

Lastly, the pre-formed foam was added to the slurry paste. The pumping of foam was timed and the duration was calculated from the flow-rate of the foam generator. This final phase of mixing took three minutes with periodic checks for even and thorough mixing.

4.6 Sample Preparation and curing

After measuring the density of the concrete, the fresh concrete was then placed in wooden moulds in preparation for hardening. Figure 4-3 shows a dimensions of the moulds used. Two wooden stoppers were used on both ends of the mould in order to leave sufficient steel reinforcement overhang for corrosion measuring and handling.

The period of hardening was 24±3 hrs. During the 24 hours of setting, the concrete was in a climate room to eliminate the effect of variable environmental conditions. The reinforced beams had a concrete cover depth of 35 mm. While the nominal cover in SANS 10100-1 (2000) is at least the diameter of the reinforcing bar which was 12 mm, 35 mm was used for handling purposes as the concrete had not gained sufficient strength for proper handling.

Stellenbosch University https://scholar.sun.ac.za

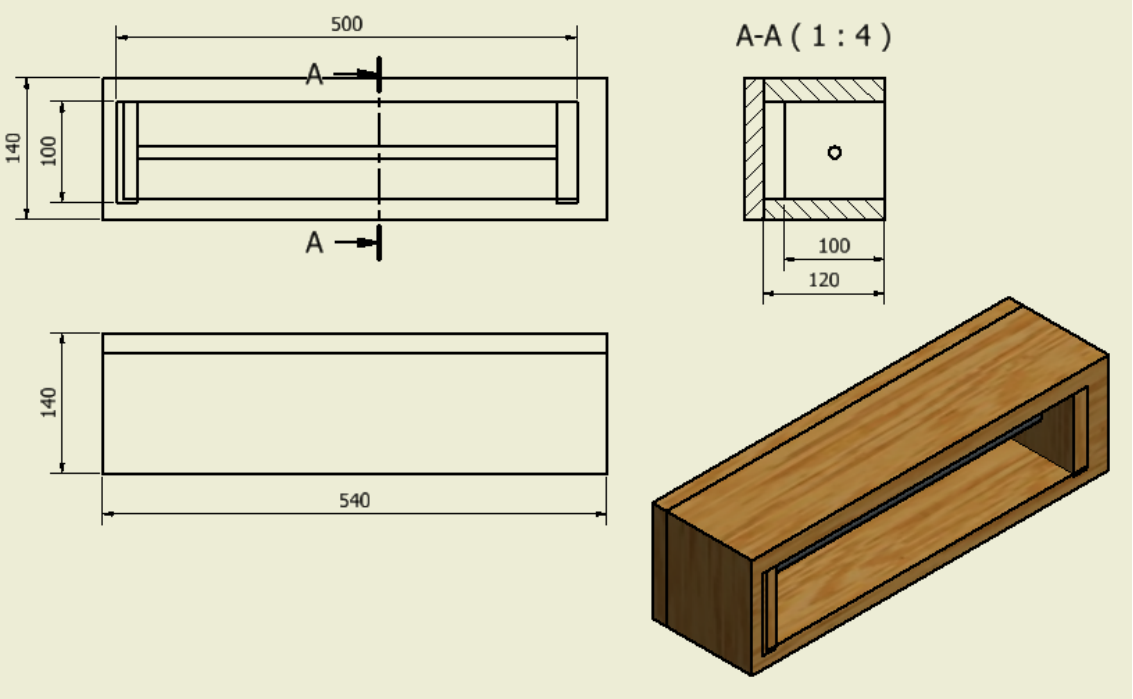

Figure 4-3: Schematics of the beam mould with the reinforcement steel

The concrete samples were removed from the moulds after 24±3 hours. A sample of the beams after hardening as shown in Figure 4-4. After the removal of the moulds, the samples were weighed before curing. The samples were then cured in a climate controlled room. The concrete was cured for 28 days. The climate room conditions were kept constant at 23±2 °C and 65 % RH respectively.

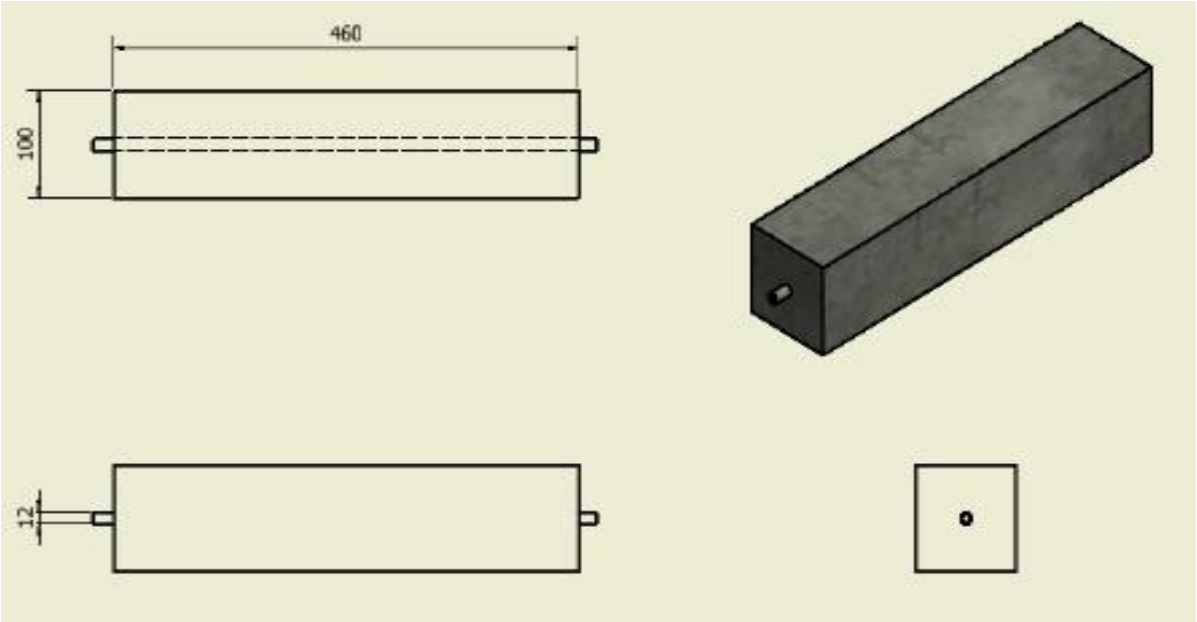

Figure 4-4: Schematic diagram of the reinforced LWFC concrete beam and its dimensions after hardening.

Stellenbosch University https://scholar.sun.ac.za

4.7 Application of STA

4.7.1 Non-integral STA

The non-integral STA used was Sikagard®-706 Thixo (2012) which is a silane based poreliner classified as a type two hydrophobic impregnation system in terms of penetration depth according to EN1504-2 (2004). The product has a density of 900 kg/m^3 and pH of 8. The product was in gel form. The STA had to be applied after 28 days of curing as per specifications of the manufacturer and was applied using a brush. According to the product brochure Sikagard®-706 Thixo (2012), the appropriate dosage of 200-300 g/m^2 was applied in a single coating from top to bottom on a clean dust free surface. This was achieved by using compressed air to remove loose debris. After application, the samples were stored in the climate room for drying. The minimum prescribed drying time was five hours.

4.7.2 Integral STA

The integral STA used for this research was Chryso® Fuge B (2012). Given that the product is completely miscible in water, it was added to the mixing water and stirred well (ensure proper mixing) before the water was added to the dry materials. The dosage specified by the manufacturer was either 0.3-0.5 kg per 100 kg of cement or 1.5 % of the cement weight. The latter was used given that it is a definitive dosage unlike the former which is a range. The addition of the STA had no influence on the water-demand of the concrete. Also, the product did not react with the foam chemically. In order to check that, water mixed with the STA was added to a container with the foam and indicator solution was used to determine if a chemical reaction occurred. According to the manufacturer Chryso® Fuge B (2012), the product conformed to EN480-5 standards on the capillary absorption test.

4.8 Penetration depth of non-integral STA

The penetration depths of the specimens were examined in accordance with EN1504-2 (2004). This involved splitting the specimens and spraying water on the cut surface. The hydrophobic part of the specimen did not absorb water while the rest of the specimen did as illustrated in Figure 4-5. The depth of the hydrophobic part is then measured from the surface on three points per side and a mean depth calculated.

Stellenbosch University https://scholar.sun.ac.za

Figure 4-5: Penetration depth of concrete

4.9 Porosity and void distribution measurements

The porosity and void distribution were determined by means of computed tomography scans (CT scans).Surface treated cube samples of side length 30 mm were used in the scanning. Control specimens were not included because non-integral surface treatment does not change the macrostructure and therefore it avoided duplication. The samples were subjected to one hour long scanning each. The tube voltage was 120 kV and the tube current was 100 µA. The primary image processing was done using specialised software VGStudioMax 2.2 (2016) by experts at the scanner facility while secondary processing for this research was done using myVGL (2016) software. The results of the image processing included slice images showing the interconnectivity while porosity and void distribution were determined from spreadsheets of the internal voids.

Stellenbosch University https://scholar.sun.ac.za

4.10 Carbonation tank

The schematic diagram of the carbonation set-up is shown in Figure 4-6. The accelerated carbonation process was set up using four units. The first unit was a 31.5 kg CO_2 gas cylinder, a 150 litre drum, a carbonation chamber and a condensation chamber. The CO_2 gas cylinder provided a reserve of CO_2 which was used to increase the concentration of CO_2 in the chamber. The drum contained two containers of ammonium nitrate (NH_4NO_3) saturated solution to control the RH at 65±5 %. From the drum, the cured CO_2 was then pumped into the tank. An outlet pressure valve was also installed on the chamber to avoid a pressure build-up inside. Once the concentration reached the required level of 0.13 %, the valve on the CO_2 regulator was closed. The level of CO_2 was tracked using a CO_2 sensor permanently connected to the carbonation chamber.

A hygrometer in the carbonation chamber was used to monitor the RH. A temperature sensor was also permanently connected to the carbonation chamber. A fan was installed close to the CO_2 inlet into the carbonation chamber to ensure circulation in the chamber. The CO_2 and temperature sensors were connected to a data logger and collected readings at a frequency of 0.25 Hz. The last part of the carbonation set-up was the condensation chamber. The condensation chamber was used to trap excess moisture in the carbonation chamber. This was achieved by putting an extra loop connected to the carbonation chamber in which excess moisture was trapped and air pumped back into the carbonation chamber.

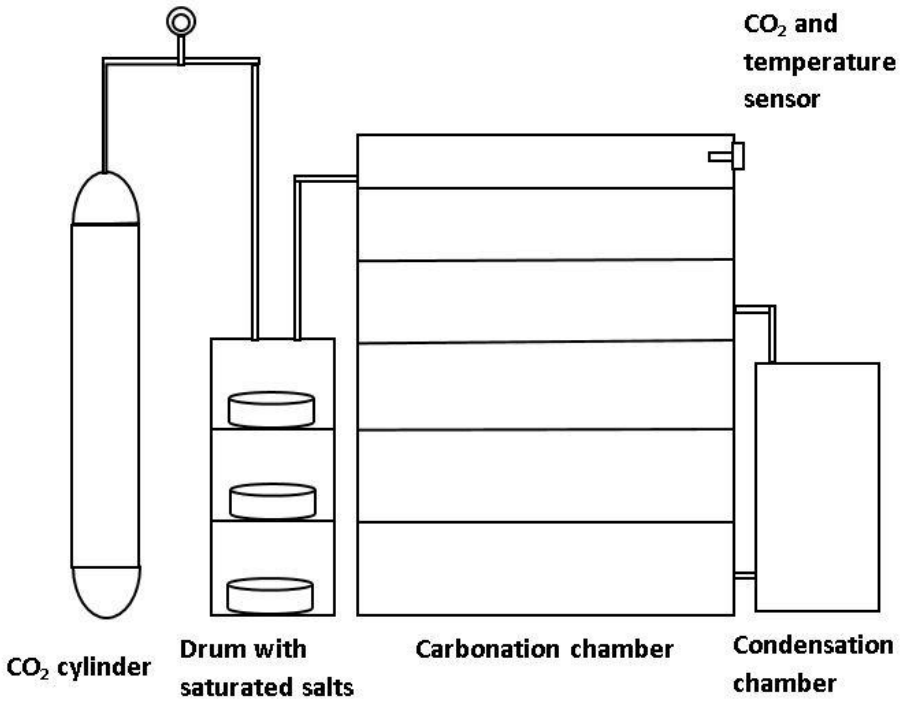

Figure 4-6: Schematic layout of the carbonation chamber.

Stellenbosch University https://scholar.sun.ac.za

4.11 Compressive strength tests

Compressive strength tests were done as a measure of the consistency of the of test specimens and to determine the effect of STA on the compressive strength of LWFC.

The compressive tests were done using an uniaxial compression Contest machine as illustrated in Figure 4-7. The test specimens were inspected for compliance with SANS 5860 (2006) before testing. The testing procedure was derived from SANS 5863 (2006) with the load application rate calibrated on the Contest machine being 180 kN/min. The compressive strength was calculated from the average failure load as in Equation 4-1.

Figure 4-7: The Contest machine for compressive strength determination.

Equation 4-1: Compressive failure stress of a cube, SANS (2014)

$$f_{cu} = \frac{F_{av}}{A}$$

Where,

f_{cu} is average cube failure stress (MPa),

F_{av} is the average failure load (kN) and

A is the area of contact (m^2).

Stellenbosch University https://scholar.sun.ac.za

4.12 Carbonation test

The depth of carbonation of the concrete specimens was measured on two specimens per mix at a time. This was done to track how the depth of penetration of CO_2 affected the rate of corrosion of the reinforcing steel. The depth of carbonation was measured by first cutting the cube specimens in half, then phenolphthalein indicator solution was sprayed on the freshly cut cube surface in compliance with the Rilem CPC-18 (1988). The freshly cut surface was cleared of dust and loose debris. The indicator solution turned pink when it came into contact with the uncarbonated concrete as illustrated in Figure 4-8. According to Roy et al. (1999), phenolphthalein turned purple when the pH was above a range of 8.4-9.8. This meant that in the areas where carbonation had occurred, no colour changes were witnessed. The recorded carbonation depths were then compared with the carbonation depths predicted using theoretical carbonation depth prediction models.

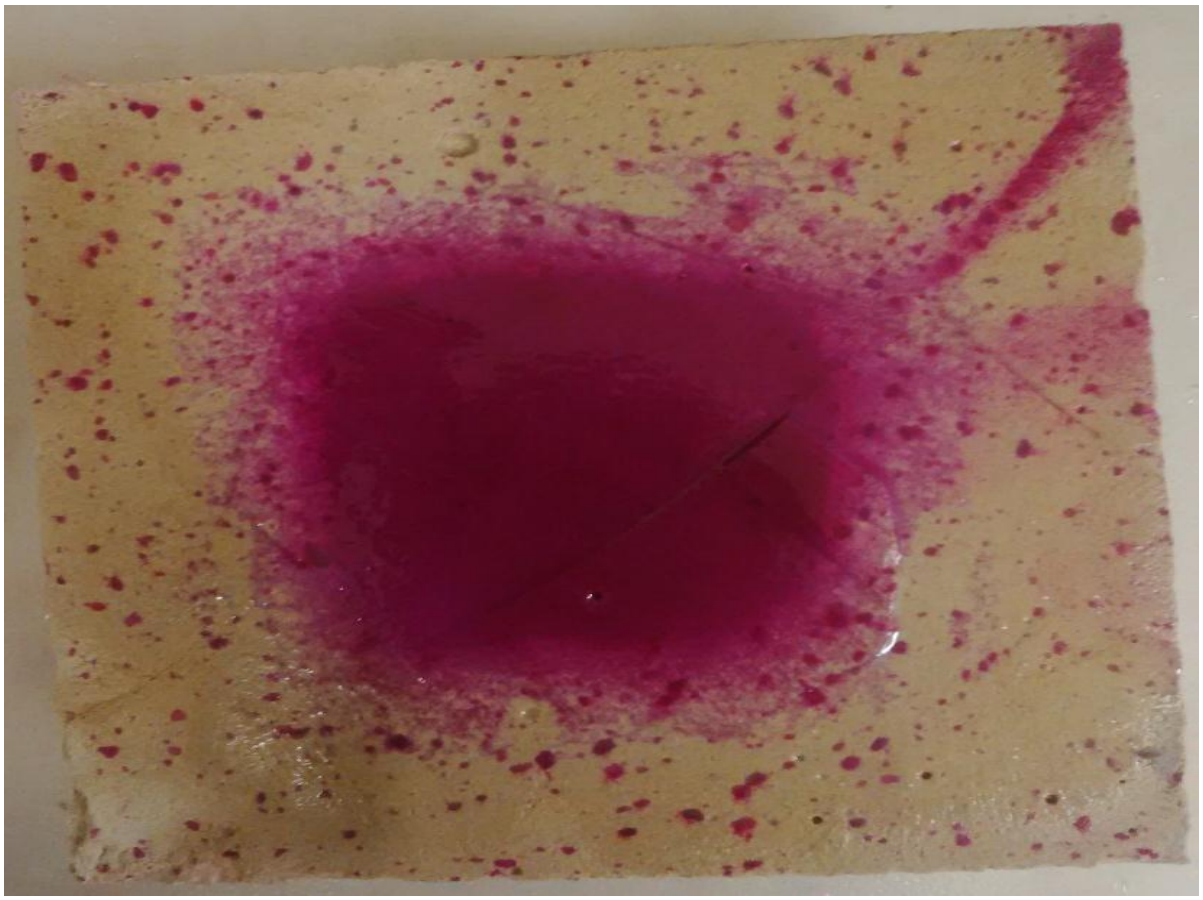

Figure 4-8: The phenolphthalein test

Stellenbosch University https://scholar.sun.ac.za

4.13 Corrosion measuring tests

The corrosion induced by the carbonation process was measured on the samples using the half-cell potential (HCP) method. These tests were performed on the same days as carbonation depth penetration tests to track the progression of the corrosion due to carbonation with time in 2 week intervals for 12 weeks after 28 days of curing. The influence of the STA was also compared to the control specimens. The HCP test was done in accordance with ASTM C876 (2009). An illustration of the test setup is shown in Figure 4-9. The cover depth of the concrete cover was kept constant at 35mm from the top and 40mm from the vertical edges.

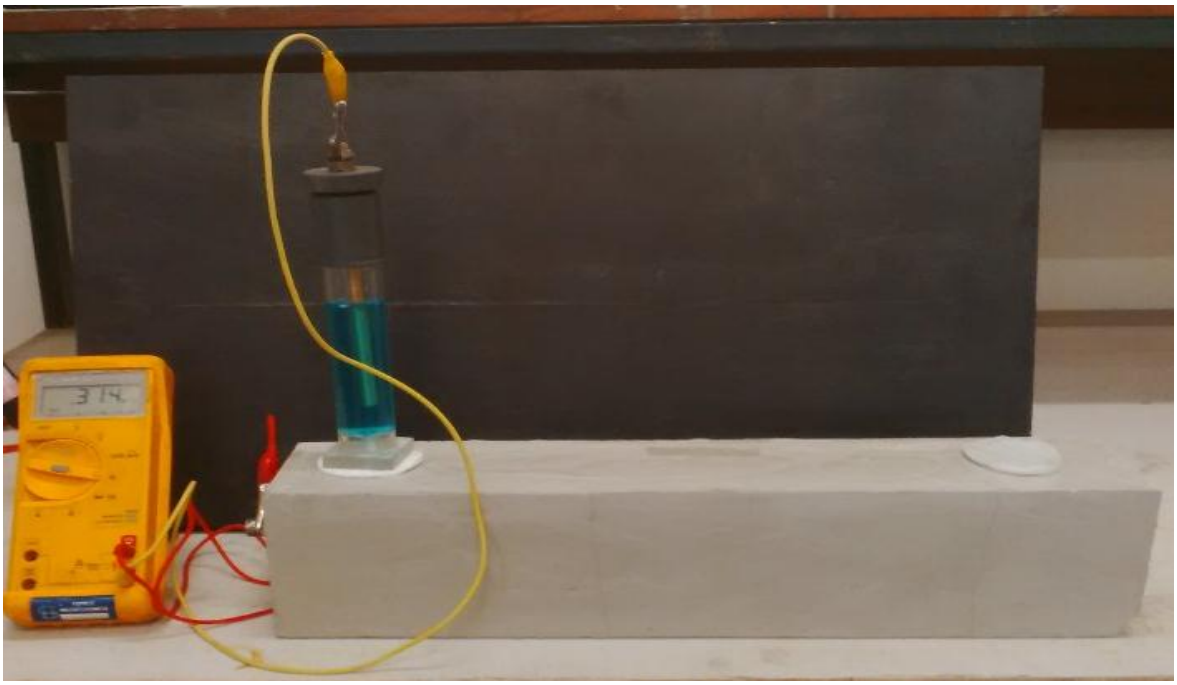

Figure 4-9: The setup of the HCP corrosion test

An electrical contact solution was prepared with household detergent as prescribed in ASTM C876 (2009). Cotton wool pads were used as conductivity sponges. A Cu-$CuSO_4$ electrode was used as the reference electrode. A small hole was drilled on the base of the electrode and plugged with cotton wool in order to make a porous plug. The corrosion potential was measured using a high impedance voltmeter which was connected to the half-cell and the steel reinforcement as shown in Figure 4-9. The probability of corrosion was then determined.

The experimental results and discussion of the results collected during the period of study are discussed in Chapter 5.

Stellenbosch University https://scholar.sun.ac.za

CHAPTER 5 RESULTS AND DISCUSSION

Presented in this chapter are the results from a series of tests performed to make sure that design specifications for lightweight foam concrete (LWFC) meet best practices. Some of the tests are code specified while some were best practices derived from past research. Some of the tests performed are acceptance criteria of LWFC batches, penetration depths of surface treatment agents, compressive strength tests, microstructure tests, carbonation depth tests and corrosion measurement tests. Discussions of test results and statistical analyses of the test results are also presented.

5.1 Mix design acceptance criterion

The mix design of the foamed concrete is done according to the procedure described in the Mix design procedure in 4.3. The target wet density in this study is 1400 kg/m^3. Given that most of the mechanical properties of foamed concrete are dependent on the density, a strict acceptance criterion and quality control was adopted.

According to Brady(2001), the acceptable deviation from the target plastic density is ±50 kg/m^3. For this study, the acceptable deviation is 25 kg/m^3. This strict acceptance criterion is informed on the strength of a study by de Villiers (2015) where a reduction in density by 50 kg/m^3 from a target density of 1400 kg/m^3 resulted in the loss of 2.46 MPa in strength. This is important in this study as effect of surface treatment agents (STA) on the compressive strength is also investigated. The density of concrete used in this research fell in the range of necessary for structural use which is 1000 kg/m^3 to 1700 kg/m^3. As a result, it was prudent to monitor the strength and its repeatability.

The concrete samples are made in batches owing to the size of the mixer as well to allow the application of the various STA. The plastic density and the demoulding density of each sample was then determined and the results are contained in Appendix A. The mean plastic densities and the standard deviations achieved are summarised in Table 5-1.

All the batches met the selection criterion with the largest deviation of the mean being 14 kg/m^3 realised for the cubes with integral surface treatment (IST) and the control beams. The IST beam batch recorded the largest standard deviation of 24 kg/m^3. The integral surface treated cubes had the least dispersion from the mean with a standard deviation of 9 kg/m^3. From Table 5-1, it can also be observed that beam samples had the highest standard deviations compared to the cube samples.

The stringent checks on the density of the samples were necessary given the cumbersome nature of the mixing process.

Stellenbosch University https://scholar.sun.ac.za

Table 5-1: Summary of statistics of the plastic densities of samples

Mix	Mean (kg/m^3)	Standard Deviation (kg/m^3)
control cubes	1394	13
IST cubes	1414	9
NIST cubes	1391	11
Control and NIST beams	1386	17
IST beams	1390	24

5.2 Practical considerations during mixing of foamed concrete

The attainment of foamed concrete specimens that met the acceptability criterion was due to a consistent mixing regime which took into account the inefficiencies of the available equipment. Firstly, a stringent control was used to determine the suitability of the foam density. Given that the target foam density was 75 kg/m^3, the acceptable deviation was taken as ±2 kg/m^3.The density of the foam was determined by measuring the mass of foam in a container of known volume. The density of the foam was then calculated accordingly.

Secondly, the mixing process itself was standardised for all the batches. This includes the size of the batch, the sequence involved and the batches of the mix constituents used. The use of mix constituents from the same batch was necessary to guard against chemical or physical changes by the manufacturers and suppliers.

Lastly, the pumping of foam into the base mix required special attention. Before pumping the foam, the consistency of the foam had to be verified. The consistency of the foam was dependent on the air pressure of the compressed air that was supplied to the lab. Where there were deviations in the air pressure of the supplied compressed air, an adjustment would have had to be done on the pressure system of the foam generator. This meant that the foam generator was allowed to run for about 10 seconds until the foam was consistent. Once the foam was consistent, it was then pumped into the base mix. The pumping of the foam into the base mix was a time dependent and hence the reaction time of the user had to be taken into account. This process was followed for all of the batches.

5.3 Penetration depth test results

The non-integral STA was applied after 28 days of sealed curing as recommended by the manufacturer. According to the product datasheet Sikagard®-706 Thixo (2012), the product was classified as a silane-based product complying with the highest requirements for hydrophobic pore-liners stipulated in BS EN1504-2 (2004). One of the compliance standards was the penetration depth. Being classified as a class 2 pore-liner, it meant that the expected penetration depth exceeded 10 mm.

Stellenbosch University https://scholar.sun.ac.za

While the compliance standards were determined using normal weight concrete with a water-cement ratio (w/c) of 0.7, the LWFC mix used in this research had an effective w/c ratio of 0.7. However, the water-binder ratio (w/b) was 0.35. When measured on 3 samples, mean depths of 4.53 mm, 4.42 mm and 4.48 mm were recorded as shown in Table 5-2. The penetration depths were measured on 8 points around a sawn cross section of cube samples. The rest of the measurements are shown in Appendix B.

Table 5-2: Penetration depth of non-integral surface treated concrete samples

	Sample 1	**Sample 2**	**Sample 3**
Mean (mm)	4.53	4.42	4.48
Median (mm)	4.52	4.40	4.49
Minimum (mm)	4.31	4.14	4.35
Maximum (mm)	4.74	4.90	4.69
COV (%)	3.42	5.49	2.50

The penetration depths achieved were about 50 % less than the specifications of the manufacturer. When compared to results from research by Bofeldt and Nyman (2002) in which a silane-based pore-liner was used on normal weight concrete with w/c ratio of 0.7, an average penetration depth of 7 mm was realised. However, the class of the pore-liner used in that research was not stated.

The penetration depths shown in Table 5-2 had coefficients of variance (COVs) of 3.42 %, 5.49 % and 2.50 % respectively which reflected a near uniformity in the measured penetration depths. Penetration depths at the corners of the cubes were higher than the rest as the coats of the STA intersected there. Consequently, those results were not considered. Given that LWFC has at least 20 % of voids in its make-up, it would be expected that greater penetration depths are achieved in LWFC as compared to normal concrete. The mix design used had 24.63 % by foam volume

5.4 Voids in foamed concrete

Computed Tomography (CT) scans were done on samples treated with STA to determine the void sizes, shape, porosity and interconnectedness of the LWFC. No control specimen were examined using this procedure.

5.4.1 Porosity

The pore volumes obtained from the CT scan results were used to calculate the porosity of the concrete specimens. The results showed the effect of the surface treatment on the porosity of the specimens. Control specimens were not sent for scanning because non-integral surface treatment has no effect on physical properties of concrete.

Stellenbosch University https://scholar.sun.ac.za

The integral surface treated concrete had a lower total void volume compared to the non-integral surface treated concrete as can be seen in Table 5-3.The integral surface treated concrete had a total air volume of 12.91 % of the total sample volume. In non-integral surface treated concrete samples, the total air volume was 16.07 % of the total sample volume. A similar study by Wei et al. (2013) where CT scanning was also used to examine porosity on LWFC with densities of 1300 kg/m^3 and 1500 kg/m^3, porosities of 21.39 % and 35.5 % were realised respectively. The differences may be attributed to the constituents of the mix design as they used a superplasticiser and a cement replacement of ash of 20 %. This observation was expected as non-integral surface treatment has no effect on the physical properties of concrete. According to BS EN1504-2 (2004), non-integral surface treatment adsorbs on the pore lining making a film. This is in contrast with integral surface treatment in which capillaries and pores are totally or partially filled.

The foam volume in the mix design used amounted to 24.63 % of the mix. While previous research by Nambiar and Ramamurthy (2006) showed that there was a relationship between foam volume in the mix design and the porosity of the LWFC, the porosities obtained in this research were not compatible with the foam volume. This could be attributed to the differences in the range of pore volumes examined.

Table 5-3: Porosity of integral and non-integral surface treated concrete samples

Sample Type	**Sample Volume [mm^3]**	**Void volume [mm^3]**	**Entrained air volume (%)**
Integral surface treated	27716.10	4109.62	12.91
Non-integral surface treated	26860.05	5141.67	16.07

The distribution of the voids in both surface treated samples was uniform as can be seen in the histogram in Figure 5-1. The only difference observed was that non-integral voids were larger than those seen in the integral surface treated concrete. The mean void volume of the non-integral surface treated concrete was 7.04×10^{-3} mm^3 in comparison to 4.36×10^{-3} mm^3 for the integral surface treated concrete. The largest void observed in the non-integral surface treated concrete was 21.96 mm^3 while for integral surface treated concrete it was 6.495 mm^3. The rest of the descriptive statistics are shown in Table 5-4.

Stellenbosch University https://scholar.sun.ac.za

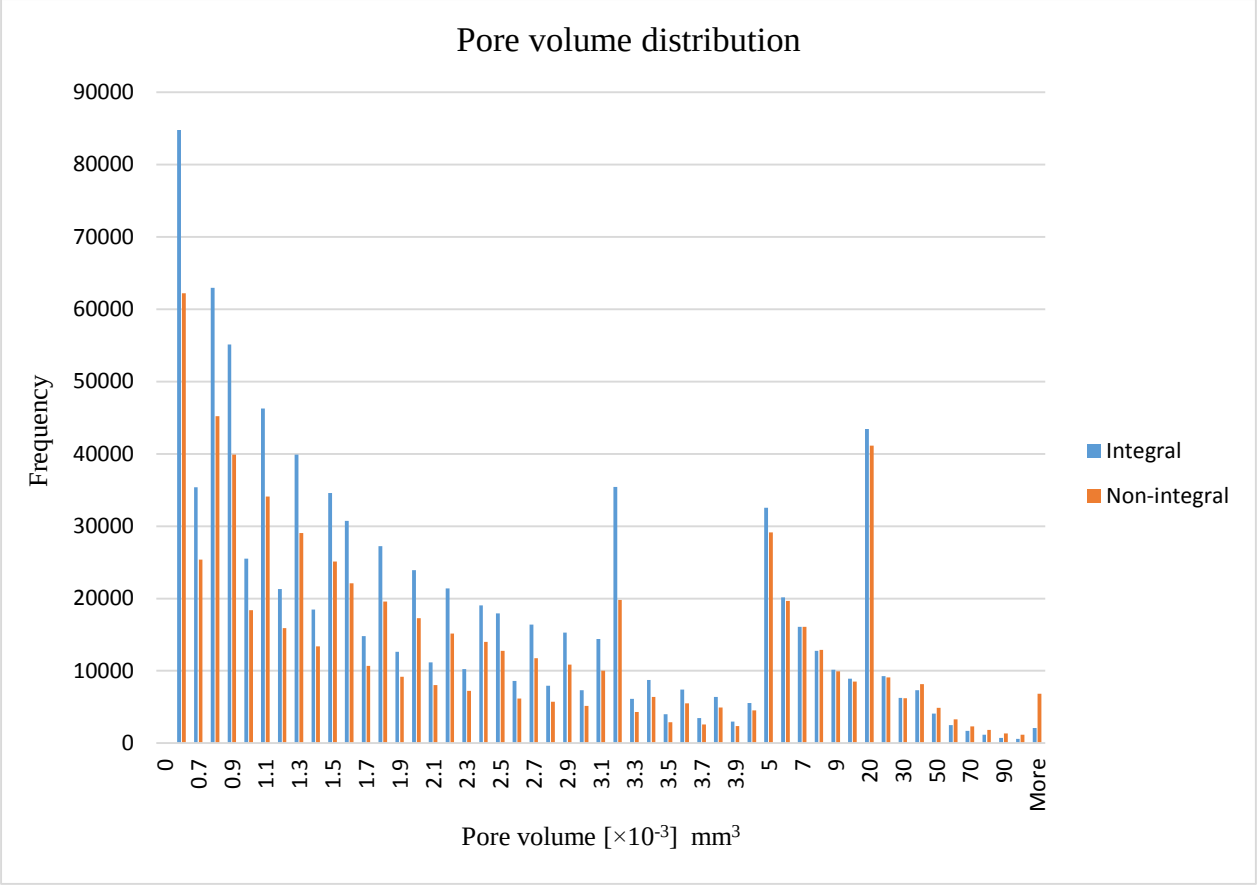

Figure 5-1: Pore volume size distribution comparison for integral and non-integral concrete specimens.

Table 5-4: Summary statistics for the pore volumes obtained for integral and non-integral surface treated concrete samples.

	Integral [×10^{-3} mm^3]	**Non-integral [×10^{-3} mm^3]**
Mean	4.36	7.04
Median	1.73	1.86
Mode	0.58	0.58
Minimum	0.51	0.51
Maximum	6495	21960

5.4.2 Void connectivity

The connectivity of voids was determined by means of the myVGL (2016) software which was used to analyse the results of the CT scan. The connectivity of voids has an impact on the ingress of deleterious substances as they provide transport channels into the concrete matrix. Using this software, a layer by layer analysis was used to highlight the areas which exhibited the large networks of voids that coalesced together.

Stellenbosch University https://scholar.sun.ac.za

In the non-integral surface treated concrete sample, the largest network of connected voids measured 21.96 mm^3 as can be seen in Figure 5-2. This was located at a depth of 3.52 mm from the top surface of the cube sample. In comparison to the integral surface treated concrete sample, the largest network of connected voids measured 6.49 mm^3. In the case of the integral surface treated concrete, this occurred at a layer 13.44 mm from the surface as illustrated in Figure 5-3. From the selected layers, it can be seen that the effect of bubbles coalescing was higher in non-integral surface treated concrete as compared to integral surface treated concrete. This can be explained by the larger entrained air voids that were observed in non-integral treated concrete as shown in Section 5.4.1 on porosity.

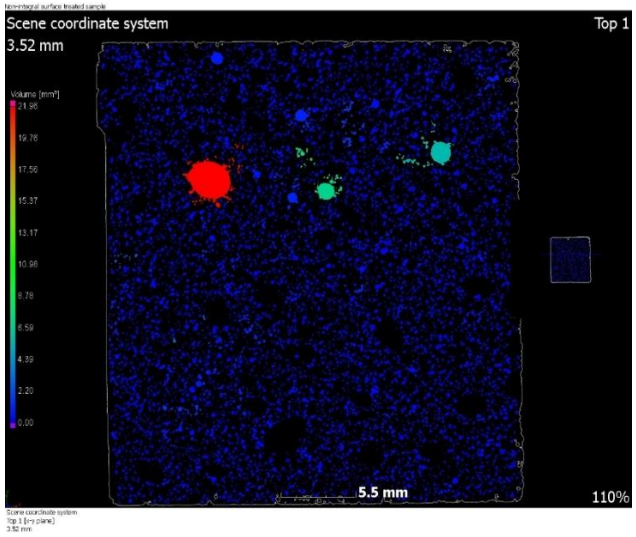

Figure 5-2: Illustration of void connectivity in non-integral surface treated concrete, myVGL (2016)

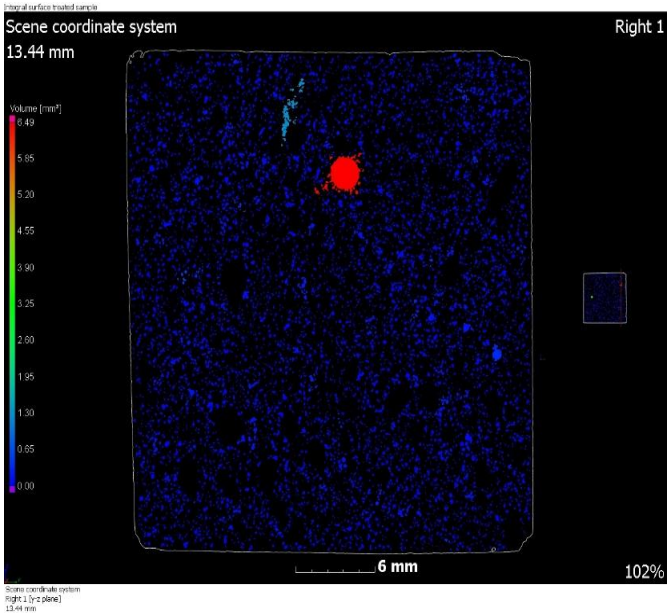

Figure 5-3: Illustration of void connectivity in integral surface treated concrete, myVGL(2016)

Stellenbosch University https://scholar.sun.ac.za

5.4.3 Void shape

The void shape is measured on a scale ranging from 0 to 1 with 1 being perfect sphericity while 0 is perfect irregularity. While there exists a formula to calculate void sphericity, the myVGL (2016) software used in the analysis of voids provided a direct output of results on the sphericity of voids. This data was used to check if a correlation existed between the voids diameter and the sphericity of the voids.

Examining the integral surface treated concrete samples, the correlation coefficient obtained was 0.839 as can be seen in Figure 5-4. A correlation coefficient of 0.839 is strong. The mean sphericity obtained was 0.5794 while the median was 0.5931. From these statistics, the overall level of sphericity of about 58 % is observed indicating that the voids were generally close to being round in the integral surface treated concrete samples.

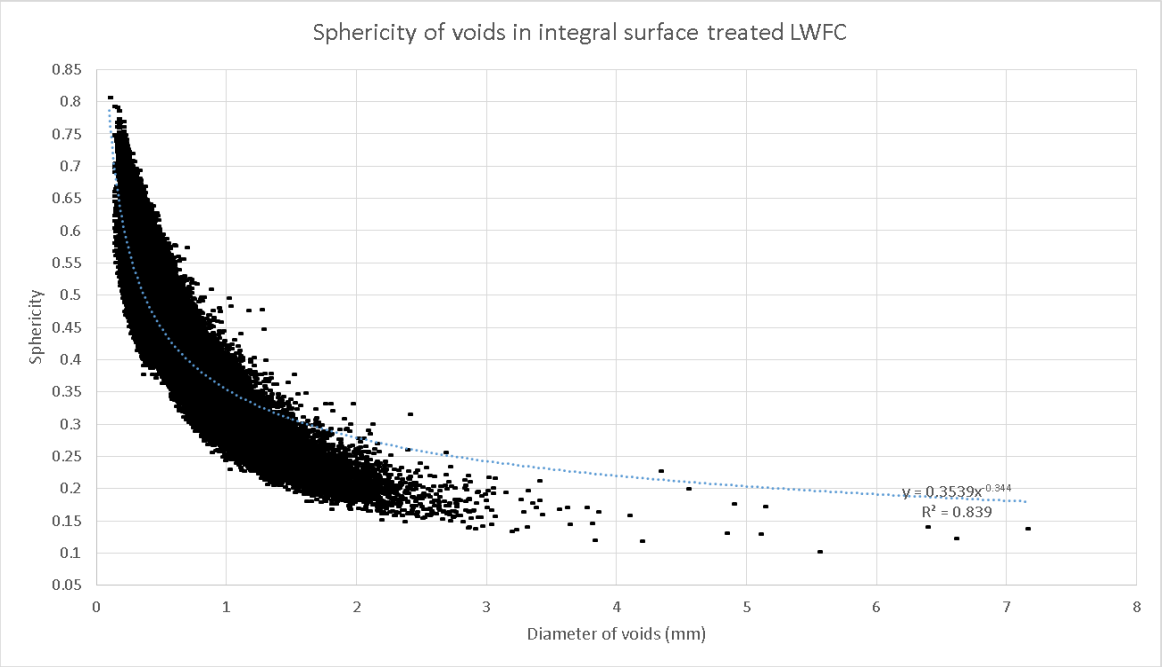

Figure 5-4: Correlation of the void diameter and sphericity of voids in integral surface treated concrete.

The correlation coefficient realised in the non-integral surface treated samples was a strong 0.859 which was marginally higher than the 0.839 obtained for integral surface treated concrete samples. The mean sphericity was 0.593 which was also marginally higher than that obtained for integral surface treated concrete. The overall sphericity level in the non-integral surface treated samples is 59%. Figure 5-5 illustrates the plot of the sphericity and the void diameter of the non-integral surface treated concrete.

Stellenbosch University https://scholar.sun.ac.za

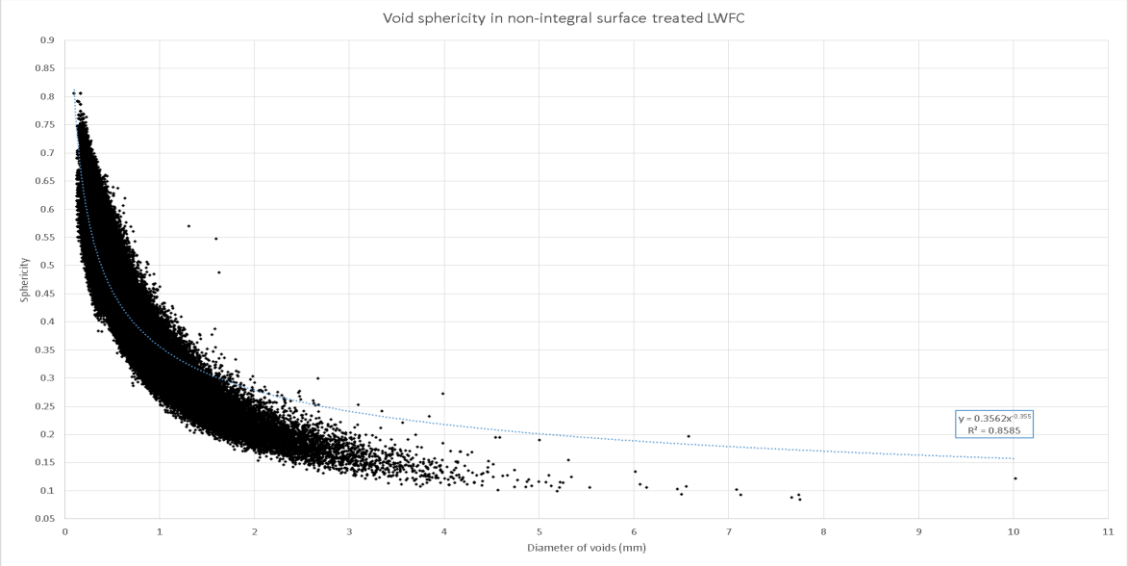

Figure 5-5: Correlation of the void diameter and sphericity of voids in non-integral surface treated concrete.

The higher correlation coefficient and the average sphericity of the non-integral surface treated concrete compared to the integral surface treated concrete is an anomaly given that there was greater incidence bubble coalescence in the non-integral surface treated concrete as seen in 5.4.2. Intuitively, the coalescence of bubbles, as evidenced in by the greater void connectivity in 5.4.2, should result in the formation of more irregular voids and hence where there is higher incidence of void coalescence, there should be a higher irregularity of void shape. Research by Hilal et al. (2015) also proved that where there was a greater degree of void merging, the irregularity of voids increased.

The small differences in average sphericity and correlation coefficient also indicate the small influence of additives such as surface treatment to the void shape unlike the size of the voids where significant differences can be seen. This finding is similar to research by Hilal et al. (2015), where the use of additives such as superplasticisers did not have an effect on the void shape but did influence the void size. Also, similar research on void properties by Visagie and Kearsley (2002) concluded that the shape of the void has no influence on the strength of LWFC. This is further corroborated by research by Nambiar and Ramamurthy (2006) which concluded that there was no correlation between void shape and strength and density of LWFC.

5.4.4 Void size

The void sizes determined from the scan results were also in tandem with the void volumes discussed in Section 5.4.1. The CT scan only detected pore diameters greater than 100µm. Non-integral surface treated concrete exhibited larger void diameters as compared to integral surface treated concrete. In non-integral surface treated concrete, the average void diameter obtained was 311 µm, while for integral surface treated concrete it was 286 µm.

Stellenbosch University https://scholar.sun.ac.za

Despite non-integral surface treated concrete having a higher mean void diameter, it exhibited a smaller median diameter of 220 µm compared to 230 µm for integral surface treated concrete. The modal diameter was similar for both types of surface treated concrete as can be seen in Table 5-5. The median values lay in the same range as those obtained in a similar study of the void structure by Hilalet al. (2015). The differences from the that study include the target density which was 1300 kg/m^3 and the mix constituents as it included silica fume.

Table 5-5: Summary statistics of void diameters of integral and non-integral surface treated concrete samples

	Integral (µm)	Non-integral (µm)
Mean	286	311
Median	230	220
Mode	140	140

Histograms were also plotted in order to show the distribution and frequencies of void diameters for both types of surface treatment as shown in Figure 5-6 and Figure 5-7. The shapes of the distributions were similar. The histograms were also similar to those obtained in a similar research by Hilal et al. (2015).

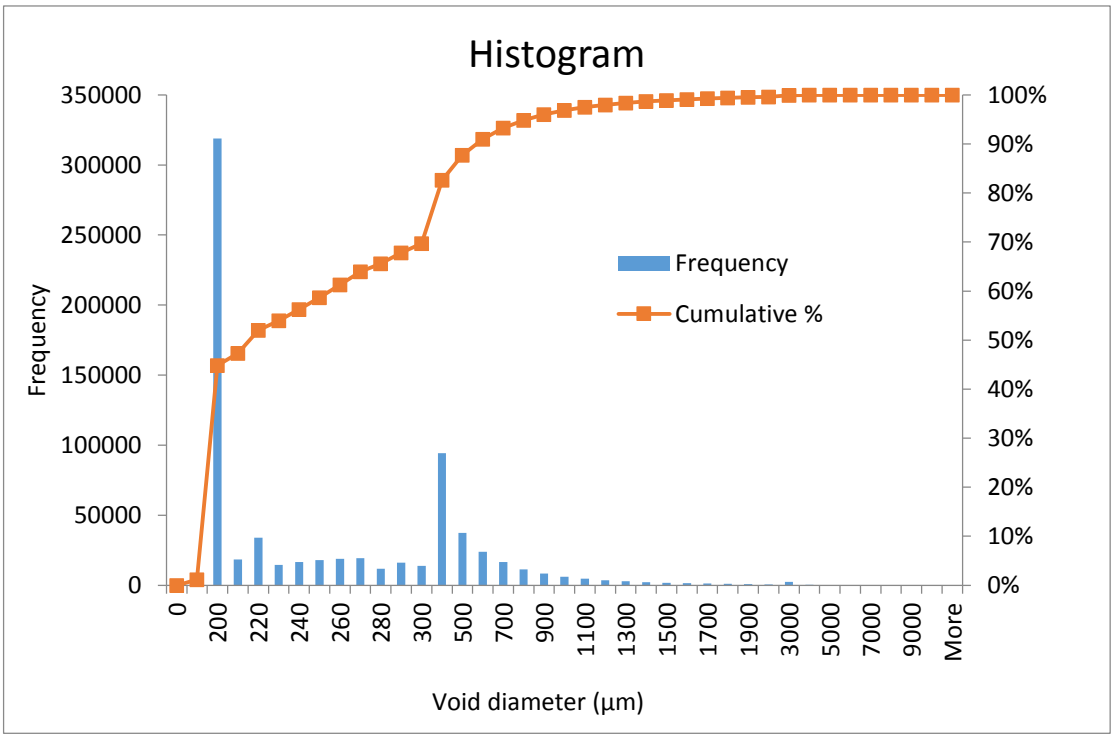

Figure 5-6: Histogram showing the range and frequency of void diameters in non-integral surface treated concrete

Stellenbosch University https://scholar.sun.ac.za

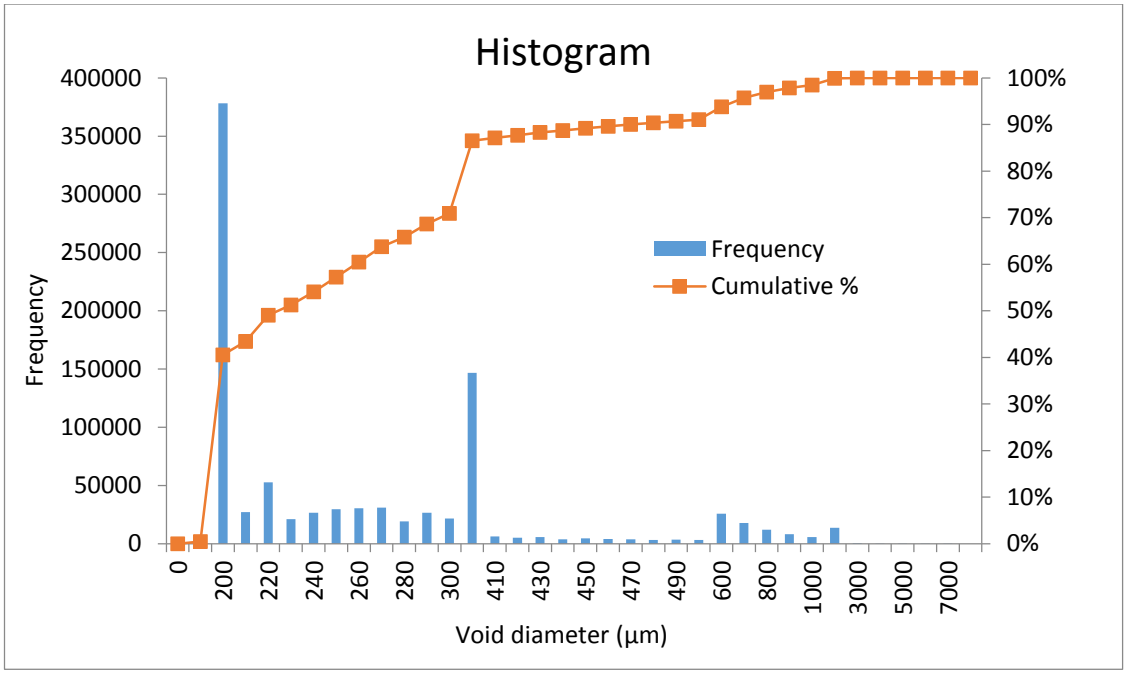

Figure 5-7: Histogram showing the range and frequencies of void diameters in integral surface treated concrete

5.5 Compressive strength test results

The compressive strength of the LWFC was tracked during the exposure to CO_2. Three cube samples were used for the compressive strength test for all three types of samples. As can be seen in Figure 5-8, the non-integral surface treatment had no effect on the strength of the concrete. Throughout the carbonation period, the non-integral treated concrete showed little difference in cube compressive strength when compared to the control specimens. Integral surface treated concrete exhibited compressive strengths which were between 30-35 % higher than the control and non-integral surface treated concrete.

Also, during the initial four weeks in the carbonation chamber, there was still some strength gain unlike in the control and non-integral surface treated concrete as shown in Figure 5-8. When compared with the compressive strength of a 1400 kg/m^3 plastic density mix with coarse fly ash, in a research study by Jones and McCarthy (2005) which attained a 28 days strength of 21 MPa, the results attained were in that range for the control and non-integral surface treated samples. Also, another research by Visagie (2000), 24.2 MPa on a mix with a target density of 1500 kg/m^3 with cement replacement of 50 % was observed.

The uniformity in the range of compressive strengths of the control and the non-integral surface treated concrete is further proof that the non-integral pore-liners have little effect on the microstructure of the concrete as they just chemically attach on the surface of the concrete.

Stellenbosch University https://scholar.sun.ac.za

Looking at integral surface treated concrete, after the strength gain measured during the first four weeks in the carbonation chamber, the compressive strength was at least 30 % higher than that of the control and non-integral surface treated concrete. This can be attributed to the lower porosity of the integral surface treated concrete as seen in Section 5.4.1.

Given that research on integral surface treatment is limited, comparisons were made using research on non-integral pore-blocking surface treatment. Research done by Song et al. (2016) on non-integral pore-blocking treatment revealed increased compactness as well as pores partially filled with the principal hydration product C-S-H formed from the surface treatment using x-ray diffraction (XRD) and thermal gravimetric analysis (TGA). While there are three theories on how the C-S-H is formed, the presence of the C-S-H in the pores accounts for the reduction of the porosity and strength increase. While the reduction in porosity was just under 4 % as seen in 5.4.1, it can be postulated that integral surface treatment resulted in the partial filling of pores across the whole cross-section of concrete in turn resulting in the significant strength gain compared to the control and the non-integral treatment.

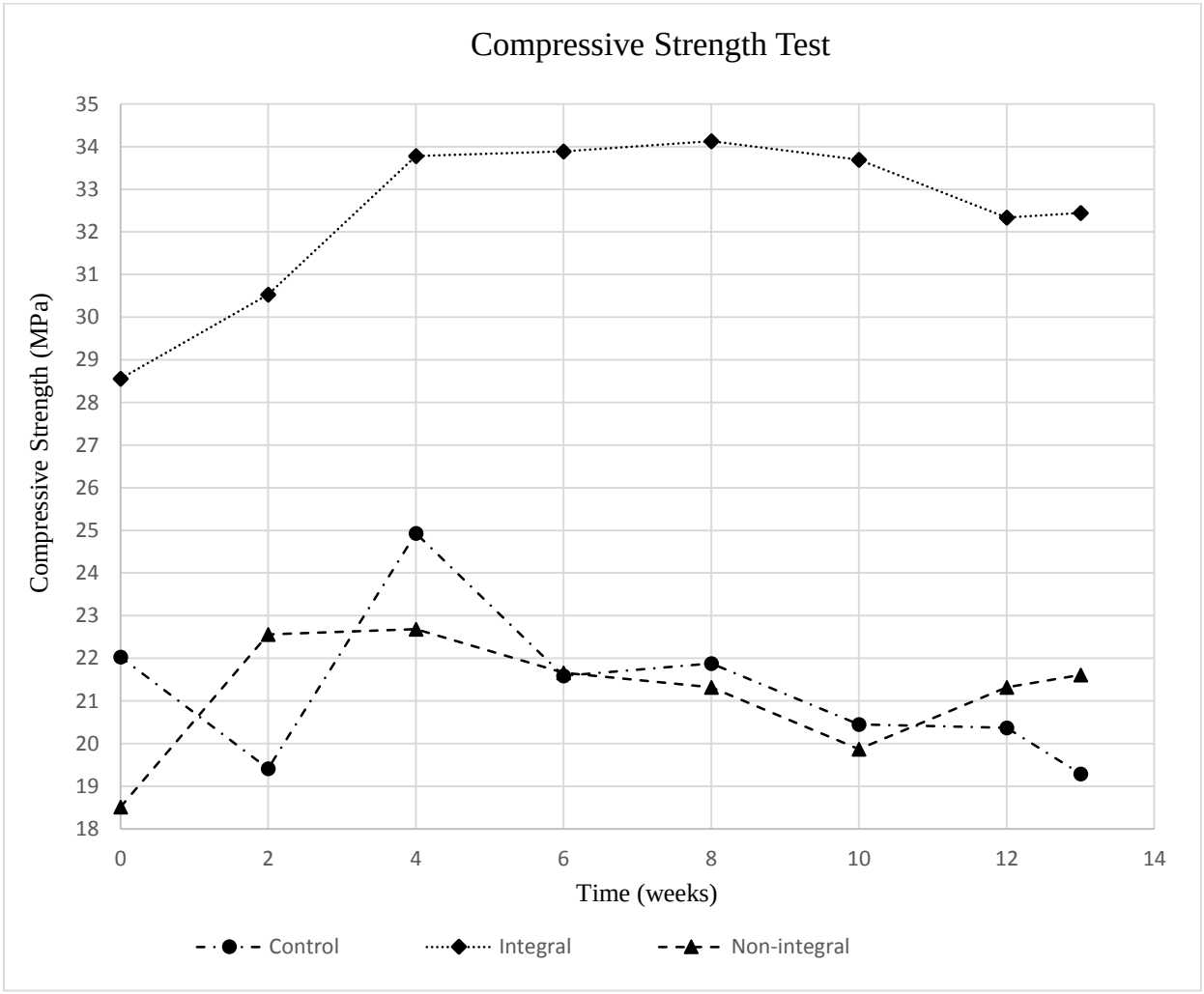

Figure 5-8: Compressive strength of samples during the carbonation period

Stellenbosch University https://scholar.sun.ac.za

Also, the increase in strength in the integral surface treated concrete could not be attributed to the shape of the voids. As seen in Section 5.4.3, there were marginal differences in void shape between the two types of surface treatment which could have warranted for the 30 % strength disparity in compressive strength. Furthermore, research by Nambiar and Ramamurthy (2006) showed that the void shape had no influence on the properties of foam concrete.

The air void distribution has been shown to have an effect on the strength of LWFC. According to Nambiar and Ramamurthy (2006), concrete mixes producing a narrow air-void size distribution has been proven to have higher compressive strengths compared to those with a wider air-void distributions. The observation was attributed to greater incidence of void merging witnessed in mixes with a wider air void distribution. This was also observed in this research as integral surface treated concrete had a narrower air-void distribution than non-integral surface treated concrete samples. This is highlighted in Figure 5-6 and Figure 5-7 where the range of diameters are shown in histograms.

5.6 Carbonation depth

The penetration of CO_2 was tracked by measuring the carbonation depth. During the first two weeks, the carbonation depth was measured weekly and thereafter it was measured fortnightly. The results are shown in Figure 5-9. During the first 2 weeks, little or no carbonation took place due to high RH. However, after the RH was controlled at 65±5 %, the carbonation accelerated. The control specimens exhibited the highest carbonation depths and carbonation rates.

At 4 weeks in the carbonation chamber, there was little difference between the treated samples. After the 4 weeks, the carbonation rate of the non-integral surface treated concrete grew moderately higher than the integral surface treated samples and was starting to stabilise at the end of the exposure period. CO_2 penetration of the integral surface treated samples increase over time at rate lower than that of the non-integral surface treated samples. At the end of the exposure period, the measured carbonation depth of integral surface treated concrete was just under 13.72 mm which was almost half that of the untreated concrete which was 24.63 mm. Non-integral surface treated concrete registered an average carbonation depth of 17.48 mm. Based on these results it can be seen that any form of treatment has a significant impact on reducing the carbonation depths.

Stellenbosch University https://scholar.sun.ac.za

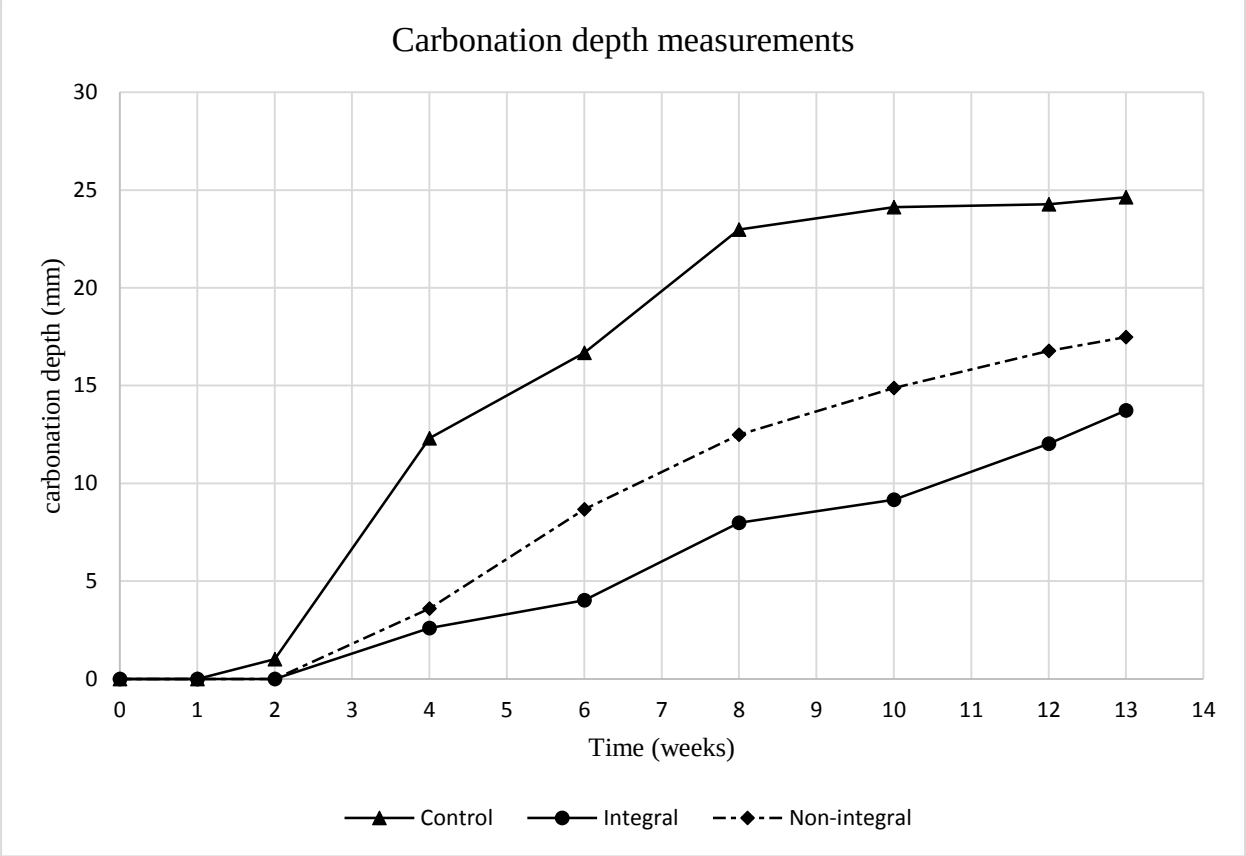

Figure 5-9: Carbonation depth measurements using the phenolphthalein test

An examination of the measurements taken for each of the samples types was done. Generally, a consistent distribution carbonation depth measurements about the average is noted. However, the measurements taken at weeks 8 and 10 show a much wider distribution about the average as seen in Figure 5-10 where the average depth and standard deviation from the mean are plotted.

Looking at the distribution of measurements taken for integral surface treated samples, the observed trend was different from control samples. The distributions of the readings was small for weeks 4, 6 and 10 and then widening from week 8 to the end of the testing period as can be seen in Figure 5-11.

Lastly, the distribution of measured depths for the non-integral surface treated samples was also examined. Similar to control samples, it can be seen that in Figure 5-12 that there is an even spread of the readings on carbonation depth with a wider distribution weeks 8 and 10. The exception of weeks 8 and 10 is similar to that of the control samples.

Stellenbosch University https://scholar.sun.ac.za

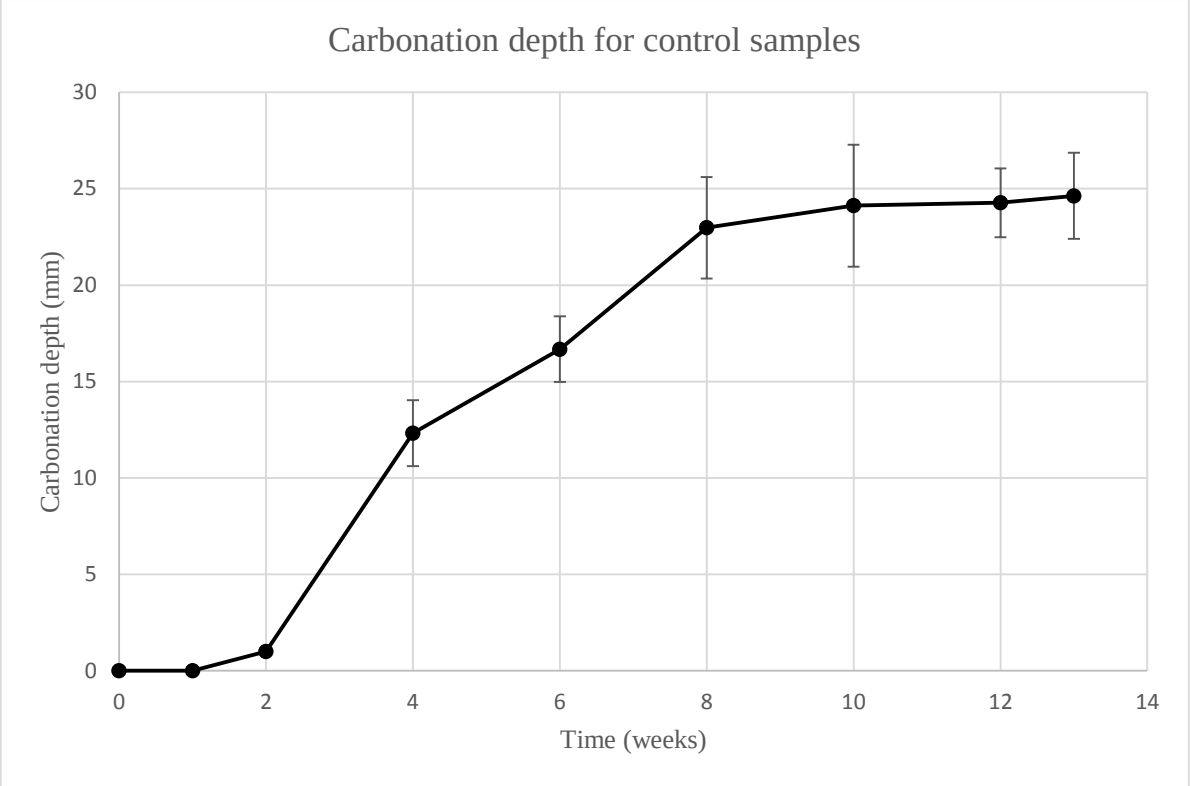

Figure 5-10: Carbonation depth for control concrete samples with the standard deviation.

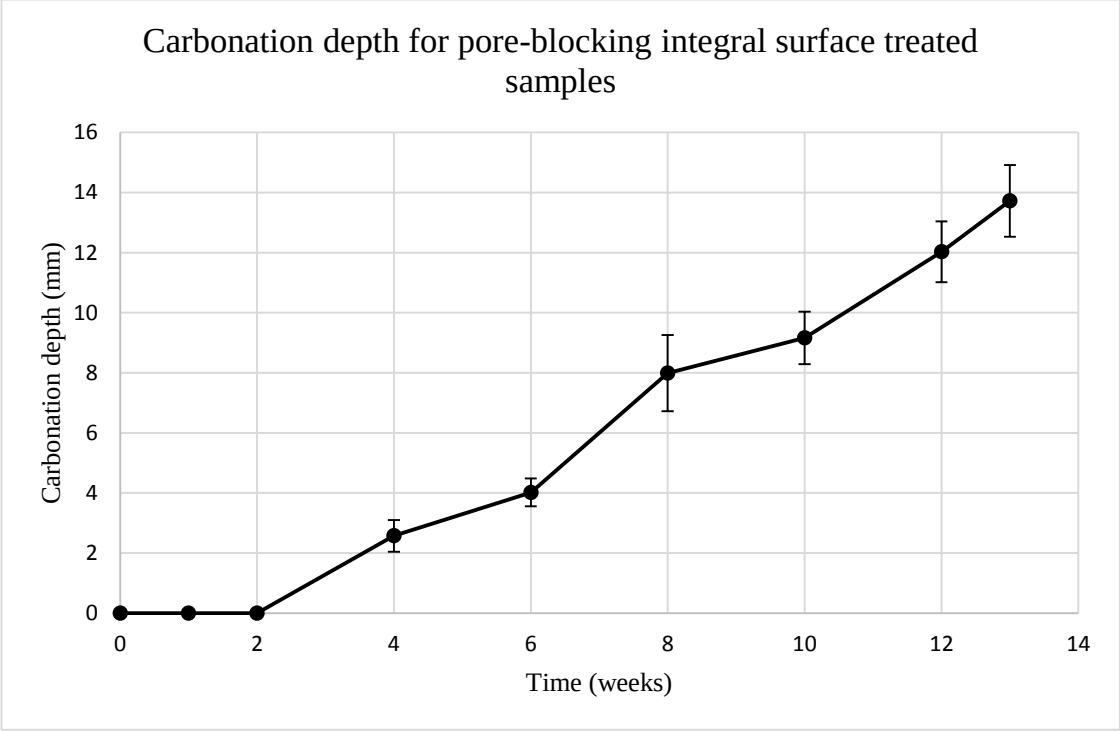

Figure 5-11: Carbonation depth for pore-blocking non-integral surface treated samples with the standard deviation.

Stellenbosch University https://scholar.sun.ac.za

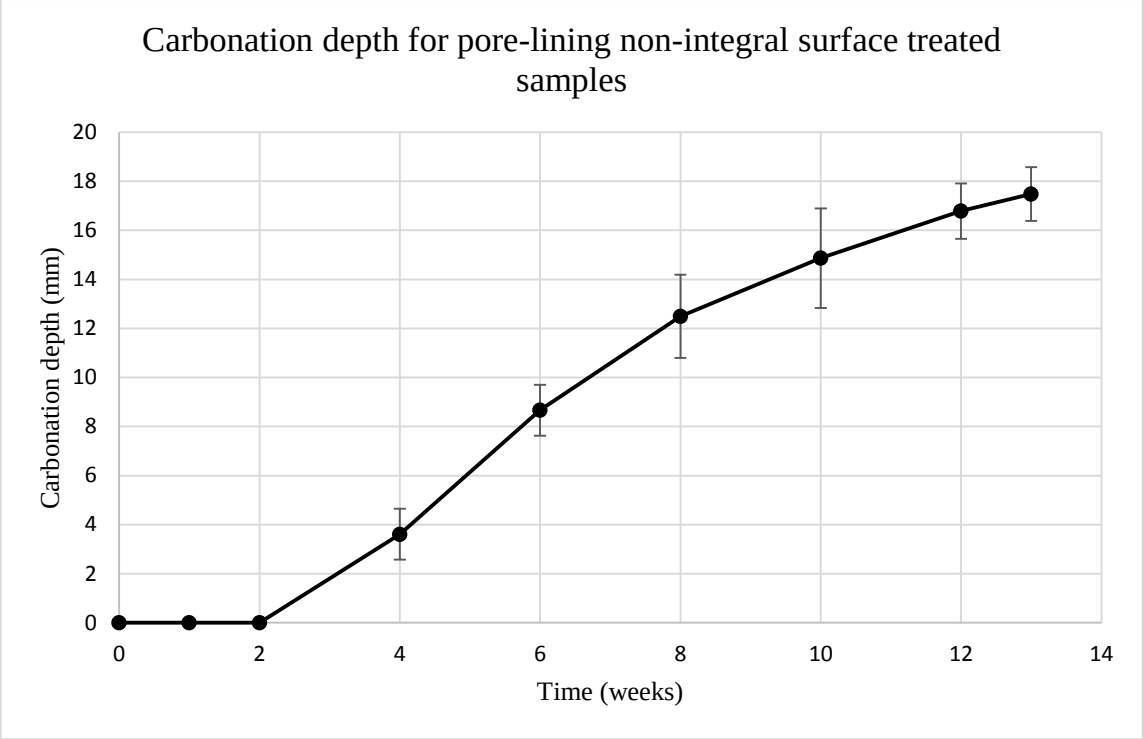

Figure 5-12 Carbonation depth for pore-lining non-integral surface treated samples with the standard deviation.

5.7 Corrosion tests

The corrosion of the steel reinforcement was measured using the HCP test with a $Cu/CuSO_4$ electrode. The testing times were similar to those of the carbonation depth tests. Three specimens for the each of the three types of reinforced LWFC beams were examined individually. The average HCP readings for the control and the two types of surface treatment are shown in Figure 5-13.

During the initial 2 weeks, the HCP was more negative. This coincides with the period when the RH in the carbonation chamber was not yet fully under control and was in the range of 90 % as previously mentioned in section 5.6 on carbonation test. This was due to some salts not absorbing all the excess moisture. According to ASTM C876(2009), if the HCP readings are less than -350 mV, then there is a high probability of active corrosion. However, according to Gu and Beaudoin(1998), a reduction in the concentration of O_2 at the steel reinforcement surface results in more negative HCP readings.

The high RH resulted in low O_2 diffusion to the surface of the steel reinforcement resulting in a shift of the HCP to more negative readings. The integral surface treated reinforced LWFC beams had the most negative readings as they were the least porous. Non-integral surface treatment resulted in intermediary negative HCP values while the untreated control specimens had the least negative readings.

Stellenbosch University https://scholar.sun.ac.za

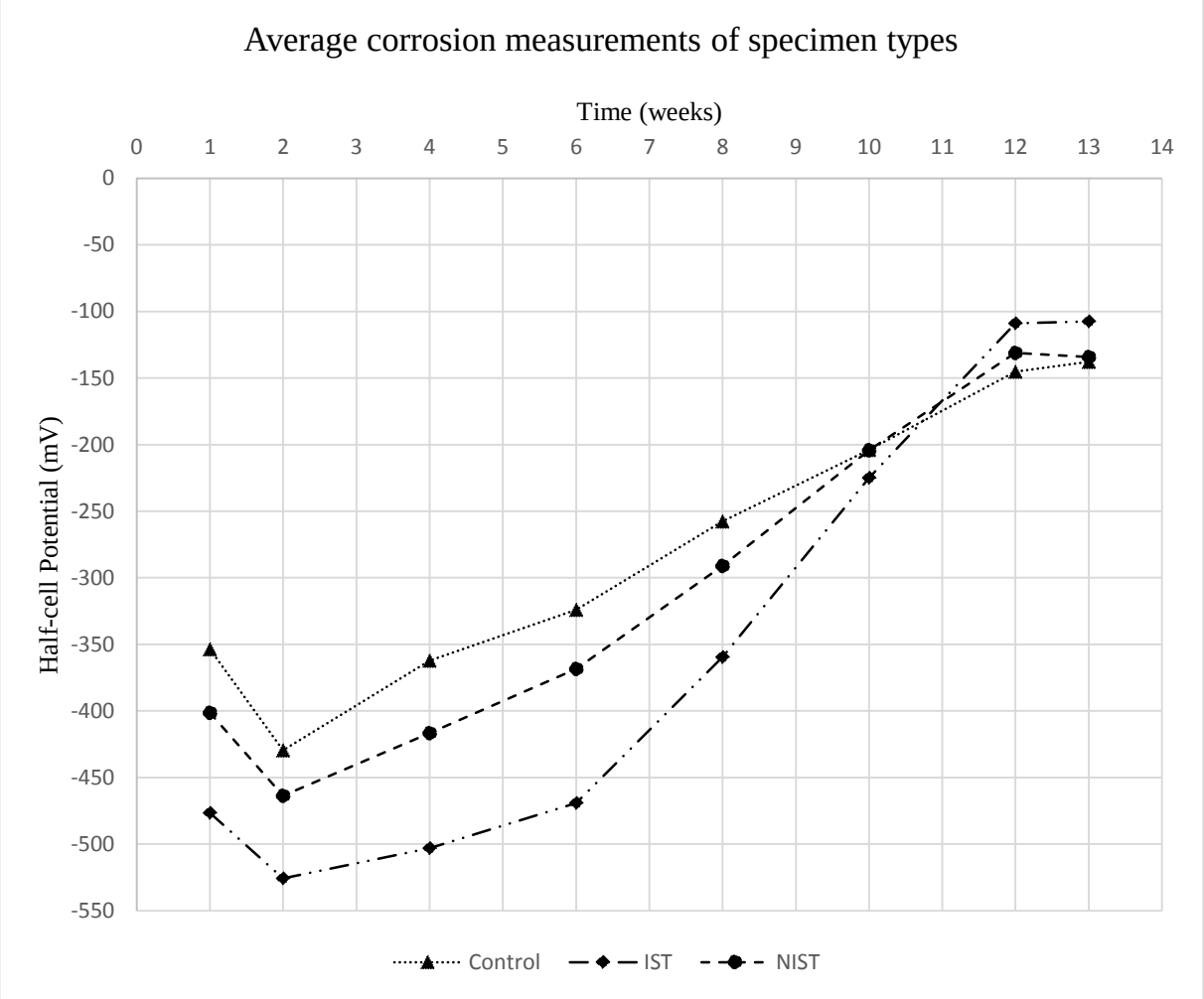

Figure 5-13: The corrosion measurements on reinforced LWFC specimens.

When the RH was stabilised at 60 % and O_2 started diffusing into the concrete matrix to the steel reinforcement surface, the HCP readings for all of the concrete specimens became less negative. As the readings became less negative, they also converged. This phenomenon is clearer in the plots of the individual beams in Appendix C. Even though carbonation rate was high during the period before the final convergence, it was not enough to shift the HCP towards more negative values in accordance with the research by Gu and Beaudoin (1998). The reduced porosity of carbonated concrete would have lowered the diffusion of O_2 thereby making the HCP more positive.

After the convergence of the HCP values, the rate of increase of HCP values had levelled off and it seemed that the effects of carbonation were becoming more prominent. In the last two weeks, the HCP readings were starting to dip towards the more negative side. The effects of the surface treatment were now becoming more visible during corrosion measuring.

In the last two weeks, the integral surface treated beam samples had the least negative HCP readings while the non-integral surface treated beam samples had readings which were marginally higher than the control specimens.

Stellenbosch University https://scholar.sun.ac.za

Given that integral surface treated samples had the least carbonation depth, it would be expected that the HCP readings observed be the least negative. In this case, since they observed readings were greater than -200 mV, it meant that the probability of n corrosion was greater than 90% in accordance with ASTM C876 (2009). Similarly, for non-integral surface treated specimens, while the HCP readings were lower than that of integral surface treated specimens, they were still higher than -200mV threshold for corrosion activity. However, non-integral surface treated samples were more vulnerable than integral surface treated samples. Lastly, control samples had the least HCP readings meaning that they were the most vulnerable to future corrosion.

5.8 Conclusion

The target wet density of the specimens used in this study is 1400 kg/m^3 with an acceptable deviation of ±25 kg/m^3. The penetration depths measured for the pore-lining non-integral surface treatment applied were 50% less than the expected values. Pore sizes and distributions in both types of surface treatment were in tandem with expected trends found in literature. Carbonation resistance in surface treated concrete was higher compared to the untreated control samples.

The conclusions of this study and the recommendations for future research are contained in the next chapter.

Stellenbosch University https://scholar.sun.ac.za

CHAPTER 6 CARBONATION MODELLING FOR SERVICE LIFE

In any scientific research study, available literature is condensed into a theoretical model which becomes a valuable tool to use in interpreting outcomes from practical experiments. In this chapter, carbonation models developed for normal concrete were adapted for use in lightweight foamed concrete (LWFC). Test results from laboratory experiments were compared with data from the adapted models. The disparities between the laboratory results and the adapted models were highlighted and the causes postulated.

6.1 Service Life Modelling versus laboratory results

Carbonation models have been used to predict the carbonation process in concrete. While there are many carbonation models, this research looked at three different models which were discussed in Section 2.7. Of these models, the Parrott model had parameters which were easily available .As a result, the Parrott model, was used for the comparison of experimental results and carbonation models.

.A rough estimate was deduced that the 1-2 weeks of accelerated carbonation at 4-5% of CO_2 by volume was equivalent to one year of natural carbonation. This was also corroborated in research by Varjonen (n.d.). Making the assumption that all C-H is used for carbonation and that one year of natural carbonation is equivalent to 1 week of accelerated carbonation, an adjusted Parrott model was compared to results from acceleration carbonation.

Another reason was that some of the parameters could be adapted for the mix design used in this research and the results obtained are illustrated in Figure 6-1. Despite being adapted to suit the mix design, the prediction of the Parrott model was incomparable to the experimental results. This is similar to the findings in a research by Sanjuan et al. (2003) wherein natural carbonation prediction models produced outcomes that were fairly accurate for natural carbonation but not comparable to accelerated carbonation. One of the reasons for the difference between the natural carbonation and accelerated carbonation results was that there was no consistent relationship between accelerated carbonation and natural carbonation.

Another source of disparity between the prediction models was the effect of surface treatment agents (STA). The non-integral STA, which was a hydrophobic admixture ensured that ingress of liquid water was inhibited or reduced. The effect of this would be on carbonation models that took into account wet and drying cycles as water repelling effect eliminates or minimises the effect of the wet cycles.

Stellenbosch University https://scholar.sun.ac.za

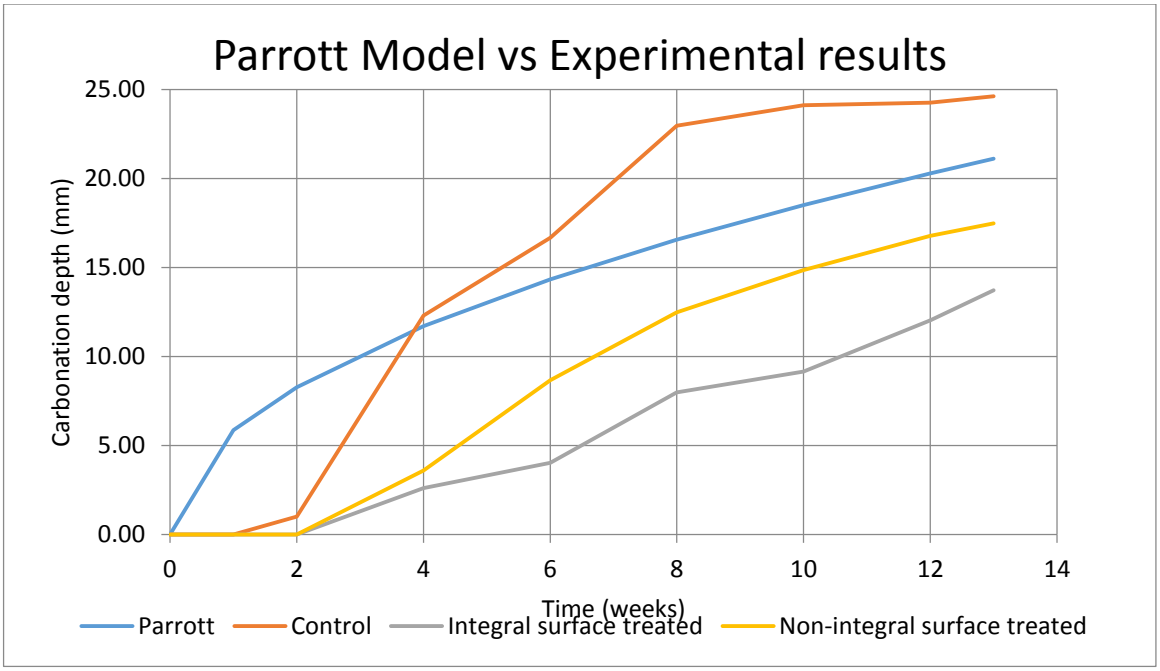

Figure 6-1: Comparison of Parrott model to the experimental results.

Also, the movement of moisture in and out of the concrete would be affected as the hydrophobic film might assume a membrane effect whereby capillary water would be trapped inside the concrete thereby reducing the egress of water vapour. In terms of pore-blockers, the porosity of the concrete would be reduced thereby affecting the diffusion coefficient of the CO_2. Furthermore, the change in porosity due to carbonation of the outer layer of the concrete would have effects on the air permeability of the concrete.

The carbonation rates were affected by the STA as can be seen in Figure 6-2. The control specimens exhibited rapid carbonation rates in the initial phases of carbonation. As the carbonated layer grew, the carbonation coefficients decreased. This observation justifies the moving boundary theory where the increase in the carbonation layer reduces the diffusion rate of the CO_2. This is caused by the densification due to the precipitation of $CaCO_3$.

The hydrophobic non-integral treatment had much slower rates of carbonation compared to the untreated concrete. This observation can be attributed to the reduced RH in the pore system of the specimens thereby reducing the dissolution of CO_2 into the pore solution. This observation is contradictory to findings of Lagerblad (2005), which state that the hydrophobic surface treatment resulted in lower RH in the pore system hence increasing the diffusion of CO_2 into the pores hence increasing the rate of the carbonation process. The reason for the contradiction may be that the RH of the carbonation was controlled to the optimum range of carbonation and any shift of the pore RH resulted in lower dissolution rates of the CO_2.

Stellenbosch University https://scholar.sun.ac.za

The pore-blocking integral treated concrete had the slowest rates of carbonation. As can be seen in Figure 6-2, the correlation equation had a logarithmic while for the control and non-integral treatments logarithmic correlation equations were observed. Also, while both the control and non-integral carbonation rates levelled off and declined towards the end, the integral treated concrete samples had carbonation rates still increasing. This observation can be attributed to effect of the low porosity which impacted the diffusion rates of the CO_2. The moving boundary effect and precipitation of $CaCO_3$ could have further reduced the carbonation rates.

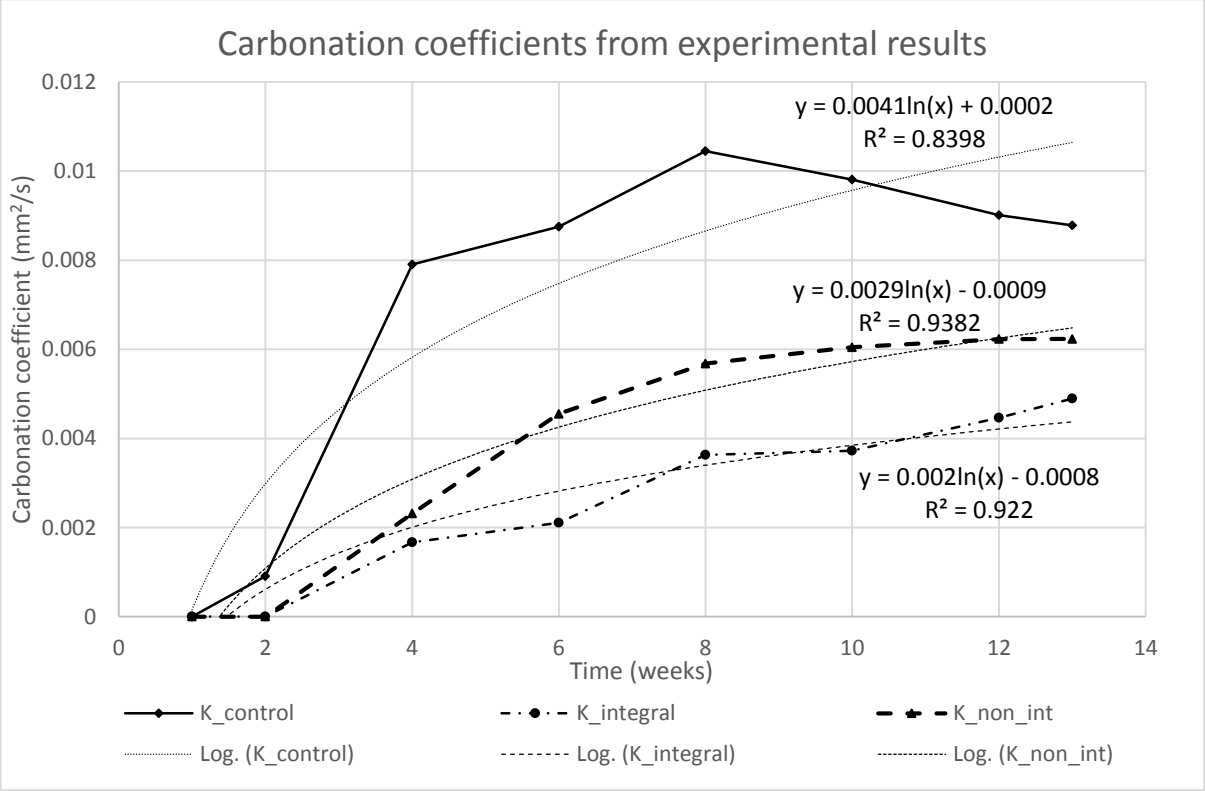

Figure 6-2: Rate of change of carbonation rates

From Figure 6-2, the control specimens showed that the carbonation rate starts to decline after a certain period. Given that the control specimens were the most vulnerable given the lack of protection, the minimum cover depths can be prescribed from their carbonation depth. This was however not possible to ascertain from the data obtained due to the long term nature of the carbonation process.

Stellenbosch University https://scholar.sun.ac.za

CHAPTER 7 CONCLUSIONS AND RECOMMENDATIONS

The purpose of this study was to answer to the durability concerns of reinforced lightweight foam concrete (LWFC), particularly carbonation induced corrosion. In answering to the durability concerns, surface treatment products currently on the market were applied in order to check their effectiveness in retarding carbonation and carbonation induced corrosion in foamed concrete. This ground-breaking study added valuable insight in durability of LWFC, thereby increasing body of knowledge of LWFC.

7.1 Conclusions

Given how properties of LWFC depend on density, a tight acceptance criterion was adopted and attained where the acceptable error tolerance was ±25 kg/m^3. For the integral surface treated concrete samples, surface treatment was added during the mixing. Once accepted and cured, the pore-liner was applied to certain specimens.

The following observations were made:

- The pore-blocking integral surface treatment, an integral STA, did not lead to physical foam destruction.
- The incorporation of integral surface treatment resulted in compressive strength in the order of 30MPa for LWFC of target wet density of 1400 kg/m^3.
- The application of the integral STA resulted in higher 28 day strength compared to control specimens by 30 %.

The penetration depth of the non-integral pore-lining surface treatment was applied after 28 days of curing by way of painting. The penetration depth and compressive strength were measured 7 days after application. The following conclusions can be made:

- The average penetration depth realised was 50 % less than what the manufacturer specified indicating that application had to be calibrated differently for LWFC.
- No gain in compressive strength due to the application of the pore-liner was realised.

An investigation into the effect of surface treatment on the voids was done. This was achieved by using x-ray CT scans to determine the porosity, size, shape and distribution of voids in surface treated LWFC. The following deductions were made:

- Porosity reduced by 20 % in integral surface treated concrete.
- There was little difference in the void shapes in both types of surface treated concrete.
- Integral surface treatment reduced the average void sizes by almost 8%.
- There was greater incidence of void coalescent in non-integral treated concrete.

Stellenbosch University https://scholar.sun.ac.za

The carbonation and corrosion tests were done periodically during the 13 weeks of carbonation exposure. During this period, compressive strength tests were also done. From these tests, the influence of the surface treatments were compared to the untreated concrete samples. The following deductions were made from this task:

- Pore-blockers were the most effective against carbonation ingress by reducing it by 44 %.
- Pore-liners reduced the ingress of carbon dioxide by 29 %.
- The pore-blockers increased the corrosion resistance by 22 % while for the pore-liners it was 4 %.
- The compressive strength gain from use of pore-blockers was between 30-35 % for the duration of the carbonation period
- There was little difference in compressive strength between the control samples and the pore-liner treated concrete.

7.2 Recommendations

The use of surface treatment agents currently available on the market yielded positive results in limiting ingress of CO_2 into LWFC. These results do show that the durability concerns of LWFC can be allayed. The use of pore-liners however, did not yield expected results and this can be attributed to the penetration depth achieved in this research. Based on this work, these recommendations have been made for future research:

- This research be extended include LWFC of other densities and various levels of cement replacement.
- Tests to determine the low penetration of pore-liners in LWFC.
- Further research into the microstructure of LWFC.
- Long term tests on accelerated and natural carbonation to determine the time scaling relationship in LWFC.
- Further research into adaptation of carbonation models to suit LWFC.
- Long term carbonation tests to determine the effect on corrosion and use of definitive corrosion measuring tests.
- Long term tests to develop models for determining minimum allowable concrete cover depths in foamed concrete.

Stellenbosch University https://scholar.sun.ac.za

REFERENCES

Al-Neshawy, F. & Sistonen, E.,2015 Durability of concrete.

Anon, 1988. CPC-18 Measurement of hardened concrete carbonation depth. *Materials and Structures*, 21(6), pp.453–455. Available at: http://dx.doi.org/10.1007/BF02472327.

Anon, 2016a. CT scanner facility at Stellenbosch University. Available at: http://blogs.sun.ac.za/ctscanner/introduction/ [Accessed November 8, 2016].

Anon, 2016b. myVGL.

Assouli, B., Ballivy, G. & Rivard, P., 2008a. Influence of environmental parameters on application of standard ASTM C876-91 : half cell potential measurements. , 43(1), pp.93–97.

Astm C 876, 2009a. *Standard Test Method for Half-Cell Potentials of Uncoated Reinforcing Steel in Concrete*, United States of Americ. Available at: www.astm.org.

Babaei, K., 1986. *Evaluation of Half-cell Corrosion Detection Test for Concrete Bridge Decks*, Seattle.

Bindiganavile, V., 2008b. Foamed concrete. , pp.231–255.

Bofeldt, M. & Nyman, B., 2002a. Penetration depth of hydrophobic impregnating agents for concrete. In *International conference on surface technology and water repellant agents*. pp. 133–142.

Borges, P.H.R. et al., 2009b. Cement and Concrete Research Carbonation of CH and C – S – H in composite cement pastes containing high amounts of BFS. , 40, pp.284–292.

Brady, K.C., Jones, M.R. & Watts, G.R., 2001a. Specification for Foamed Concrete. , p.78.

British Standard, 2004a. BS EN1504-2 .pdf.

Broomfield, J.P., 2013a. *Corrosion of steel in concrete* 2nd ed.,

Cement and Concrete Institute, 2009c. Cementitious Materials for Concrete : Standards , selection and properties. *Concrete*, pp.1–6.

Chen, B. & Liu, J., 2008c. Experimental application of mineral admixtures in lightweight concrete with high strength and workability. *Construction and Building Materials*, 22(6), pp.1108–1113.

Chen, J.J., Thomas, J.J. & Jennings, H.M., 2006a. Decalcification shrinkage of cement paste. *Cement and Concrete Research*, 36(5), pp.801–809. Available at: http://linkinghub.elsevier.com/retrieve/pii/S0008884605002711 [Accessed January 8, 2015].

Chinchón-Payá, S., Andrade, C. & Chinchón, S., 2016c. Indicator of carbonation front in concrete as substitute to phenolphthalein. *Cement and Concrete Research*, 82,

Stellenbosch University https://scholar.sun.ac.za

pp.87–90. Available at: http://dx.doi.org/10.1016/j.cemconres.2015.12.010.

Christodoulou, C. et al., 2013b. Long-term performance of surface impregnation of reinforced concrete structures with silane. *Construction and Building Materials*, 48, pp.708–716. Available at: http://www.sciencedirect.com/science/article/pii/S0950061813006521 [Accessed June 1, 2015].

Chryso, 2013c. CHRYSO ® Fuge B Pore blocking Water Proofer Description CHRYSO ® Fuge B Pore blocking Water Proofer. , pp.1–2. Available at: www.chryso.com.

CO2.Earth, 2016d. Earth's CO2 Home Page. Available at: https://www.co2.earth/ [Accessed June 1, 2016].

Elsener, B. et al., 2003a. Half-cell potential measurements- Potential mapping on reinforced concrete structures. *Materials and Structures*, 36(September), pp.461–471.

Freitag, S.A. & Bruce, S.M., 2010a. *The influence of surface treatments on the service lives of concrete bridges*, Wellington.

Giessler, S., Standke, B. & Büchler, M., 2005a. A new silane system for corrosion reduction of steel reinforced concrete. *Hydrophobe IV: fourth international conference on water repellent treatment of building materials*, 26, pp.17–26.

Glass, G.K., 1995. AN ASSESSMENT OF THE COULOSTATIC METHOD APPLIED TO THE CORROSION OF STEEL IN CONCRETE. , 37(4), pp.597–605.

Gu, P. & Beaudoin, J.J., 1998a. Obtaining Effective Half-Cell Potential Measurements in Reinforced Concrete Structures. *Construction Technology Update No.18*, pp.1–4.

Hager, R., 1998b. The Revolution in Concrete Protection Impregnation with Cream. In *Proceedings of Hydrophobe II*. Zurich: Aedificatio publishers, pp. 205–216. Available at: http://www.hydrophobe.org/pdf/zurich/II_19.PDF.

Hassanein, a. M., Glass, G.K. & Buenfeld, N.R., 1998c. The use of small electrochemical perturbations to assess the corrosion of steel in concrete. *NDT & E International*, 31(4), pp.265–272.

Hilal, A.A., Thom, N.H. & Dawson, A.R., 2015a. On entrained pore size distribution of foamed concrete. *Construction and Building Materials*, 75, pp.227–233. Available at: http://www.sciencedirect.com/science/article/pii/S0950061814011866 [Accessed February 29, 2016].

Hilal, A.A., Thom, N.H. & Dawson, A.R., 2015b. On void structure and strength of foamed concrete made without/with additives. *Construction and Building Materials*, 85.

Hilal, A. a., Thom, N.H. & R. Dawson, A., 2015c. The Use of Additives to Enhance Properties of Pre- Formed Foamed Concrete. *International Journal of Engineering*

Stellenbosch University https://scholar.sun.ac.za

and Technology, 7(4), pp.286–293. Available at: http://www.ijetch.org/index.php?m=content&c=index&a=show&catid=63&id=928.

Ho, D.S. & Ritchie, D., 1992. Howes and Ritchie. In *Proceedings Rehabilitation of Concrete Structures*. pp. 403–407.

Houst, Y.F., 1997a. Carbonation Shrinkage of Hydrated Cement Paste. *Laboratory for Powder Technology, Federal Institute of Technology, Lausanne, Switzerland (EPFL)*, p.12.

Ibrahim, M. et al., 1999a. Use of surface treatment materials to improve concrete durability. *Journal of Engineering Mechanics*, 462(February 1999), pp.36–40.

Janz, M., Byfors, K. & Johansson, L., 2001b. Surface treatments. *Metal Powder Report*, 56(4), pp.36–37.

Jones, M.R. & McCarthy, A., 2005b. Preliminary views on the potential of foamed concrete as a structural material. *Magazine of Concrete Research*, 57(1), pp.21–31.

Kari, O.P., Puttonen, J. & Skantz, E., 2014a. Reactive transport modelling of long-term carbonation. *Cement and Concrete Composites*, 52, pp.42–53. Available at: http://www.sciencedirect.com/science/article/pii/S0958946514000808 [Accessed May 17, 2015].

Kearsely, E.P. & H F Mostert, 2005c. Designing Mix Composition of Foamed Concrete with High Fly Ash Contents. *Use of Foamed Concrete in Construction*, pp.29–36.

Kearsley, E.., 1999b. *The effect of high volumes of ungraded fly ash on the properties of foamed concrete*.

Kearsley, E.. & Wainwright, P.., 2002b. The effect of porosity on the strength of foamed concrete. *Cement and Concrete Research*, 32(2), pp.233–239. Available at: http://www.sciencedirect.com/science/article/pii/S0008884601006652 [Accessed May 28, 2015].

Kearsley, E.P. & Wainwright, P.J., 2001c. Porosity and permeability of foamed concrete. *Cement and Concrete Research*, 31(5), pp.805–812.

Lagerblad, B., 2005d. *Carbon dioxide uptake during concrete life cycle – State of the art*,

Lo, Y. & Lee, H.M., 2002c. Curing effects on carbonation of concrete using a phenolphthalein indicator and Fourier-transform infrared spectroscopy. *Building and Environment*, 37, pp.507–514.

Markeset, I.G. & Myrdal, R., 2008d. Modelling of reinforcement corrosion in concrete - State of the art.

Mindess, S., 2008e. *Developments in the formulation and reinforcement of concrete*,

Moreno, M. et al., 2004b. Corrosion of reinforcing steel in simulated concrete pore solutions. *Corrosion Science*, 46(11), pp.2681–2699. Available at: http://linkinghub.elsevier.com/retrieve/pii/S0010938X04000770 [Accessed January

Stellenbosch University https://scholar.sun.ac.za

30, 2015].

Nambiar, E.K.K.K. & Ramamurthy, K., 2006b. Air-void characterisation of foam concrete. *Cement and Concrete Research*, 37(9), pp.221–230. Available at: http://www.sciencedirect.com/science/article/pii/S0008884607001263 [Accessed December 10, 2014].

National Planning Commision, 2012a. *National Development Plan 2030 Our future - make it work*,

Otieno, M.B., 2008f. *Corrosion propagation in cracked and uncracked concrete*. University of Cape Town.

Panesar, D.K., 2013d. Cellular concrete properties and the effect of synthetic and protein foaming agents. *Construction and Building Materials*, 44, pp.575–584. Available at: http://dx.doi.org/10.1016/j.conbuildmat.2013.03.024.

Papadakis, V.G., 2000a. Effect of supplementary cementing materials on concrete resistance against carbonation and chloride ingress. *Cement and Concrete Research*, 30(2), pp.291–299. Available at: http://linkinghub.elsevier.com/retrieve/pii/S0008884699002495.

Parrott, L.., 1994. Design for avoiding damage due to carbonation-induced corrosion. In *International Congress on durability of concrete*. pp. 283–298.

Paul, S.C., 2015d. *The Role of Cracks and Chlorides in Corrosion of Reinforced Strain Hardening Cement-Based Composite (R / SHCC)*.

du Plessis, A. et al., 2014b. Simple and fast porosity analysis of concrete using X-ray computed tomography. *Materials and Structures*, pp.1–10. Available at: http://link.springer.com/10.1617/s11527-014-0519-9.

du Plessis, A., le Roux, S.G. & Guelpa, A., 2016e. The CT Scanner Facility at Stellenbosch University: An open access X-ray computed tomography laboratory. *Nuclear Instruments and Methods in Physics Research Section B: Beam Interactions with Materials and Atoms*, 384, pp.42–49. Available at: http://dx.doi.org/10.1016/j.nimb.2016.08.005.

Polder, R.B. & Peelen, W.H.A., 2002d. Characterisation of chloride transport and reinforcement corrosion in concrete under cyclic wetting and drying by electrical resistivity. , 24, pp.427–435.

Qian, S.. & Chagnon, N., 2001d. Evaluation of corrosion of reinforcement in repaired concrete. In *International Conference and Exhibition, Structural Faults and Repair*. pp. 1–12.

Qian, S. & Cusson, D., 2004c. Electrochemical evaluation of the performance of corrosion-inhibiting systems in concrete bridges. , 26, pp.217–233.

Ramamurthy, K., Kunhanandan Nambiar, E.K. & Indu Siva Ranjani, G., 2009d. A classification of studies on properties of foam concrete. *Cement and Concrete Composites*, 31(6), pp.388–396. Available at: http://linkinghub.elsevier.com/retrieve/pii/S0958946509000638 [Accessed

Stellenbosch University https://scholar.sun.ac.za

December 24, 2014].

Richardson, M.G., 2004d. *Fundamentals of durable reinforced concrete*,

La Rosa Thompson, J.. et al., 1997b. Characterization of silicate sealers on concrete. *Cement and Concrete Research*, 27(10), pp.1561–1567. Available at: http://www.sciencedirect.com/science/article/pii/S0008884697001671 [Accessed August 19, 2015].

Roy, S.., Poh, K.B. & Northwood, D.O., 1999c. Durability of concrete-accelerated carbonation and weathering studies. *Building and Environment*, 34, pp.597–606.

Roy, S.K., Poh, K.B. & Northwood, D. o., 1999d. Durability of concrete—accelerated carbonation and weathering studies. *Building and Environment*.

SABS Standards Division, 2013e. *SANS 50197-1 : 2013 SOUTH AFRICAN NATIONAL STANDARD Cement Part 1 : Composition , specifications and conformity criteria for common cements*,

SABS Standards Division, 2014c. *SANS 50450-1 : 2014 SOUTH AFRICAN NATIONAL STANDARD Fly ash for concrete Part 1 : Definition , specifications and conformity criteria*, South Africa.

SABS Standards Division, 2006c. SANS 5860 : 2006 SOUTH AFRICAN NATIONAL STANDARD Concrete tests — Dimensions, tolerances and uses of cast test specimens.

SABS Standards Division, 2006d. *SANS 5863 : 2006 SOUTH AFRICAN NATIONAL STANDARD Concrete tests — Compressive strength of hardened concrete*, South Africa.

SABS Standards Division, 2000b. *The structural use of concrete*, South Africa.

SADOWSKI, Ł., 2010b. New non-destructive method for linear polarisation resistance corrosion rate measurement. *Archives of Civil and Mechanical Engineering*, 10(2), pp.109–116. Available at: http://www.sciencedirect.com/science/article/pii/S1644966512600533 [Accessed November 9, 2015].

Saetta, A. V, Schrefler, B.A. & Vitaliani, R. V, 1993. The carbonation of concrete and the mechanism of moisture,heat and carbon dioxide flow through porous materials. *Cement and Concrete Composites*, 23, pp.761–772.

Sandin, K., *Surface treatment agents with water repellant agents*, Available at: http://hydrophobe.org/pdf/delft/I_18.pdf.

Sanjuan, M.A., Andrade, Ã.C. & Cheyrezy, M., 2003b. Concrete carbonation tests in natural and accelerated conditions. *Advances in Cement Research*, 15(4), pp.171–180.

Sanjuán, M.A. & del Olmo, C., 2001e. Carbonation resistance of one industrial mortar used as a concrete coating. *Building and Environment*, 36(8), pp.949–953. Available at: http://www.sciencedirect.com/science/article/pii/S0360132300000457

Stellenbosch University https://scholar.sun.ac.za

[Accessed June 4, 2015].

Sikagard ® -706 Thixo, 2012b. Product Data Sheet. , (August 2007), pp.2–4.

Song, H. & Saraswathy, V., 2007. Corrosion Monitoring of Reinforced Concrete Structures - A Review. , 2, pp.1–28.

Song, Z. et al., 2016f. Experimental exploration of the waterproofing mechanism of inorganic sodium silicate-based concrete sealers. *Construction and Building Materials*, 104, pp.276–283. Available at: http://dx.doi.org/10.1016/j.conbuildmat.2015.12.069.

States, U., 2010c. Standard Specification for Flow Table for Use in Tests of Hydraulic Cement 1. *Annual Book of ASTM Standards*, (C), pp.4–9.

Swenson, E.G. & Sereda, P.J., 1968. Mechanism of the carbonatation shrinkage of lime and hydrated cement. *Journal of Applied Chemistry*, 18(4), pp.111–117.

Varjonen, S., Accelerated Carbonated Concrete as Corrosion Environment. , pp.1–17.

De Villiers, J., 2015e. *Bond behaviour of deformed steel in lightweight foamed concrete*. Stellenbosch University.

Visagie, M., 2000c. *The effect of microstructure on the properties of foamed concrete*. University of Pretoria.

Visagie, M. & Kearsley, E.P., 2002e. Pproperties of foamed concrete as influenced by air-void parameters. *Concrete/Beton*.

Wee, T. et al., 2006e. Air-Void System of Foamed Concrete and its Effect on Mechanical Properties. *ACI Materials Journal*, (103), pp.45–53.

Wei, S. et al., 2013f. Characterization and simulation of microstructure and thermal properties of foamed concrete. *Construction and Building Materials*, 47(November), pp.1278–1291. Available at: http://dx.doi.org/10.1016/j.conbuildmat.2013.06.027.

Zulkarnain, F. & Ramli, M., 2011. Durability of Performance Foamed Concrete Mix Design with Silica Fume for Housing Development. , 5, pp.518–527.

Stellenbosch University https://scholar.sun.ac.za

APPENDICES

Stellenbosch University https://scholar.sun.ac.za

1. APPENDIX A: SAMPLE DENSITIES

Control mix		
cubes (density-kg/m3)		
Wet	***Demould***	**Difference**
1393	1368	25
1401	1349	52
1420	1369	51
1385	1329	56
1383	1359	24
1381	1343	38
1384	1329	55
1388	1335	53
1396	1345	51
1383	1321	62
1381	1331	50
1395	1329	66
1386	1324	62
1420	1335	85
1384	1310	74
1382	1329	53
1417	1323	94
1386	1334	52
1403	1325	78
1412	1369	43
1381	1358	23
1412	1363	49
1393	1356	37
1395	1306	89
1389	1317	72
1389	1324	65
1389	1308	81
1381	1301	80
1398	1344	54
1419	1325	94
1397	1301	96
1381	1332	49

Stellenbosch University https://scholar.sun.ac.za

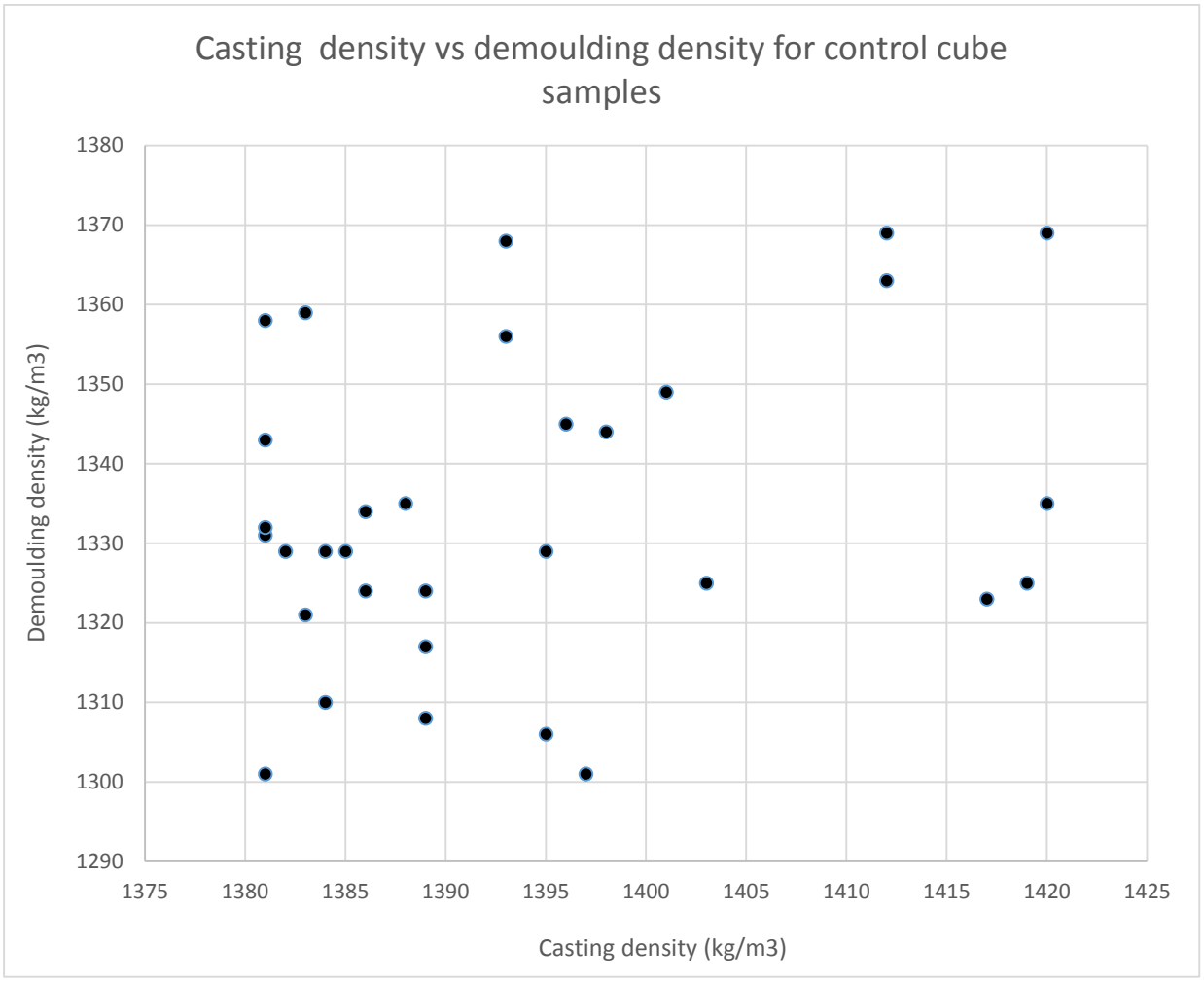

Stellenbosch University https://scholar.sun.ac.za

Non-integral surface treated samples		
cubes (mass-kg)		
Wet	**Demould**	**Difference**
1397	1339	58
1389	1352	37
1384	1354	30
1389	1358	31
1417	1389	28
1403	1379	24
1380	1349	31
1387	1361	26
1383	1360	23
1388	1368	20
1388	1371	17
1380	1374	6
1388	1355	33
1392	1366	26
1397	1368	29
1387	1362	25
1397	1366	31
1420	1391	29
1406	1382	24
1380	1354	26
1382	1356	26
1388	1370	18
1394	1356	38
1393	1365	28
1381	1364	17
1386	1378	8
1394	1356	38
1382	1376	6
1387	1368	19
1392	1371	21
1395	1361	34
1380	1356	24
1381	1351	30
1396	1349	47
1382	1349	33
1388	1351	37
1383	1338	45
1395	1366	29
1420	1391	29
1407	1376	31

Stellenbosch University https://scholar.sun.ac.za

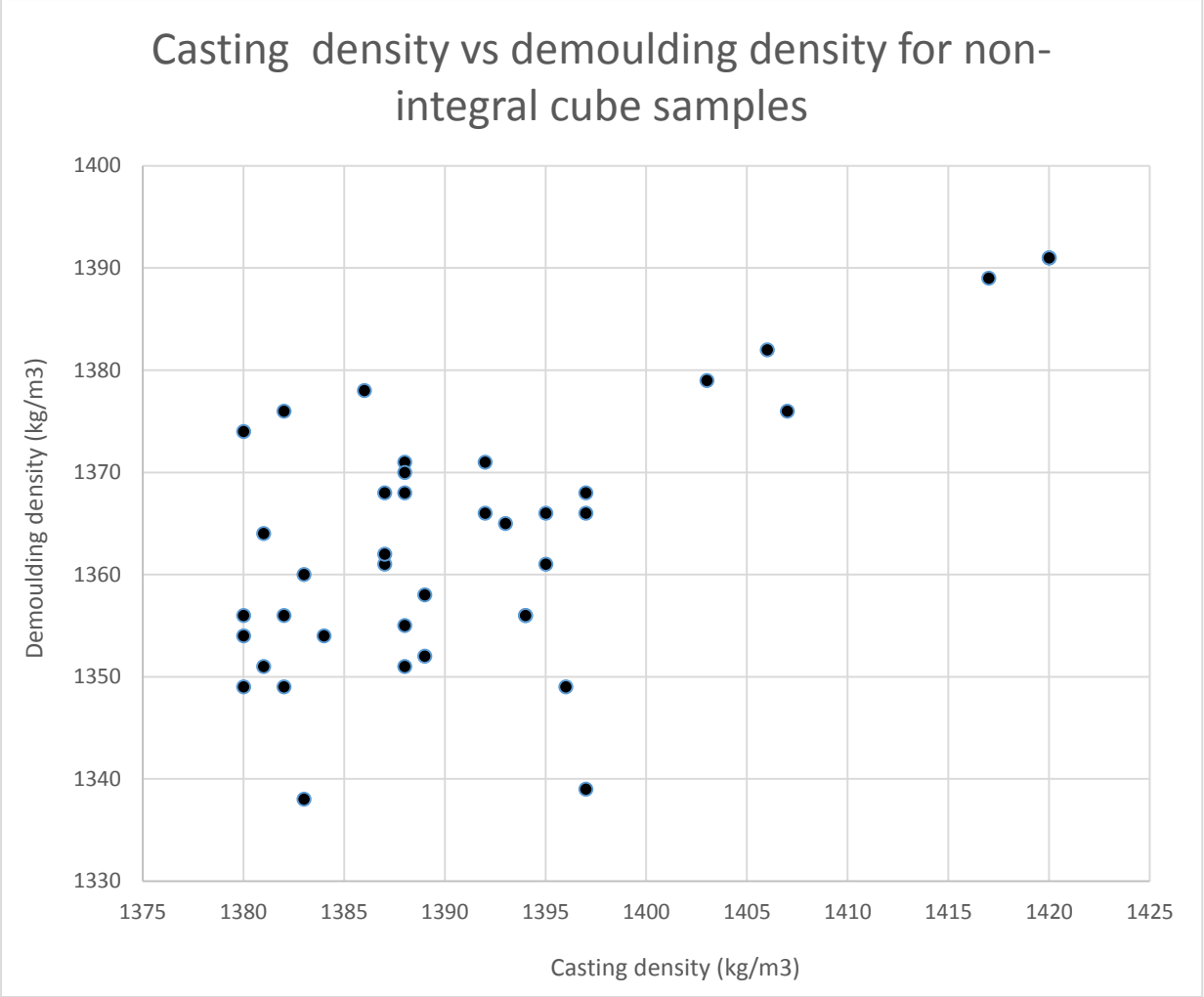

Stellenbosch University https://scholar.sun.ac.za

Integral surface treated samples		
Cube density (kg/m3)		
Wet	**Demould**	**Difference**
1420	1385	35
1420	1381	39
1422	1388	34
1421	1373	48
1419	1376	43
1390	1351	39
1419	1379	40
1418	1357	61
1422	1399	23
1417	1371	46
1419	1384	35
1416	1378	38
1423	1352	71
1418	1379	39
1416	1359	57
1417	1382	35
1394	1315	79
1399	1364	35
1409	1380	29
1410	1367	43
1422	1379	43
1419	1381	38
1408	1370	38
1412	1382	30
1387	1311	76
1424	1397	27
1403	1367	36
1422	1400	22
1421	1375	46
1421	1388	33
1418	1385	33
1419	1393	26
1399	1325	74
1420	1342	78
1421	1390	31
1406	1358	48
1415	1382	33
1410	1387	23
1422	1381	41
1412	1378	34

Stellenbosch University https://scholar.sun.ac.za

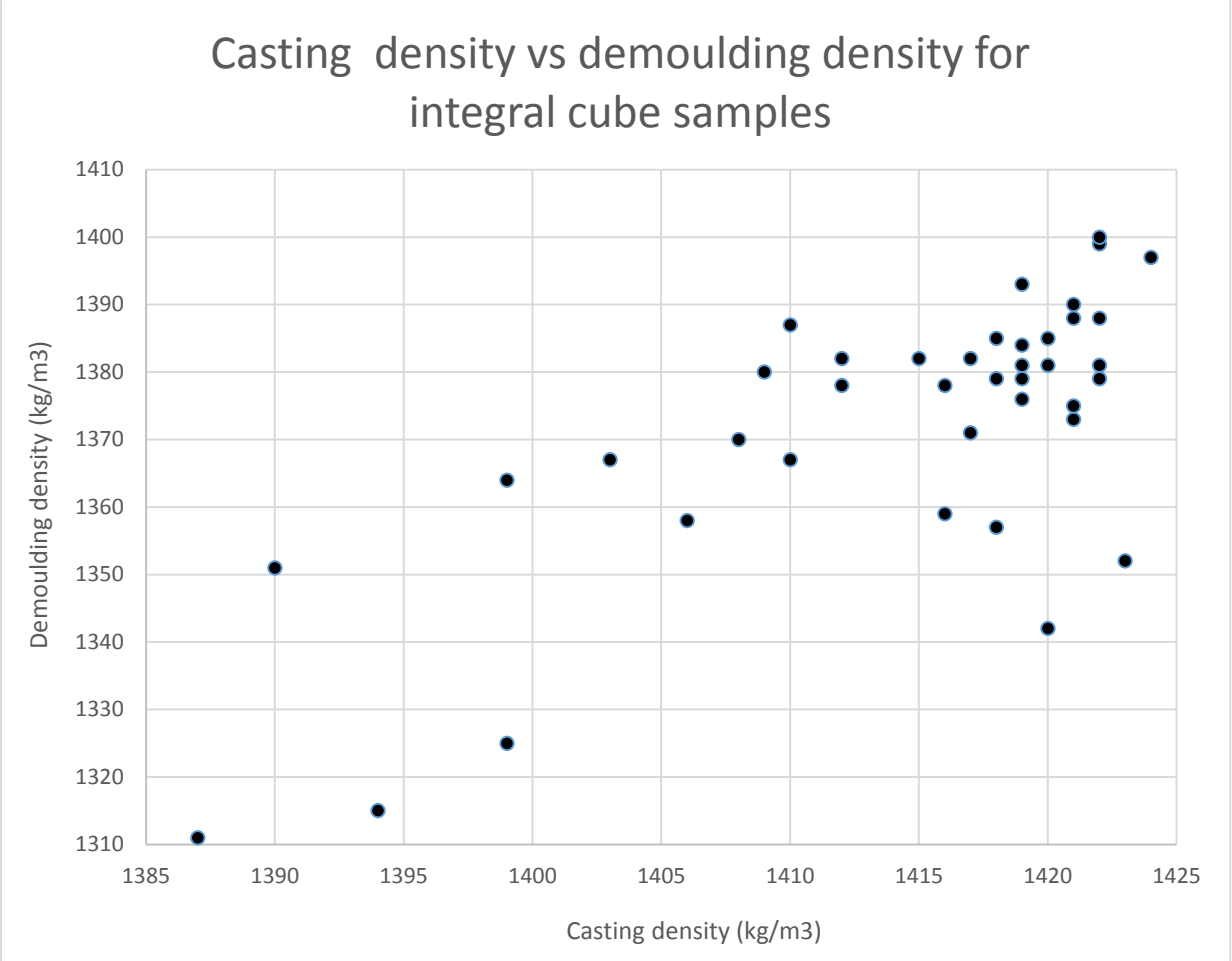

Stellenbosch University https://scholar.sun.ac.za

Control and non-integral surface treated samples		
Beam density (kg/m3)		
Wet	**Demould**	**Difference**
1380	1437	-57
1383	1440	-57
1386	1442	-57
1357	1436	-78
1382	1440	-58
1417	1479	-62
1395	1455	-59
1392	1451	-59

Integral surface treated samples		
Beam density (kg/m3)		
Wet	**Demould**	**difference**
1417	1480	-63
1397	1462	-65
1359	1343	16
1389	1375	14

Stellenbosch University https://scholar.sun.ac.za

2 APPENDIX B PENETRATION DEPTH

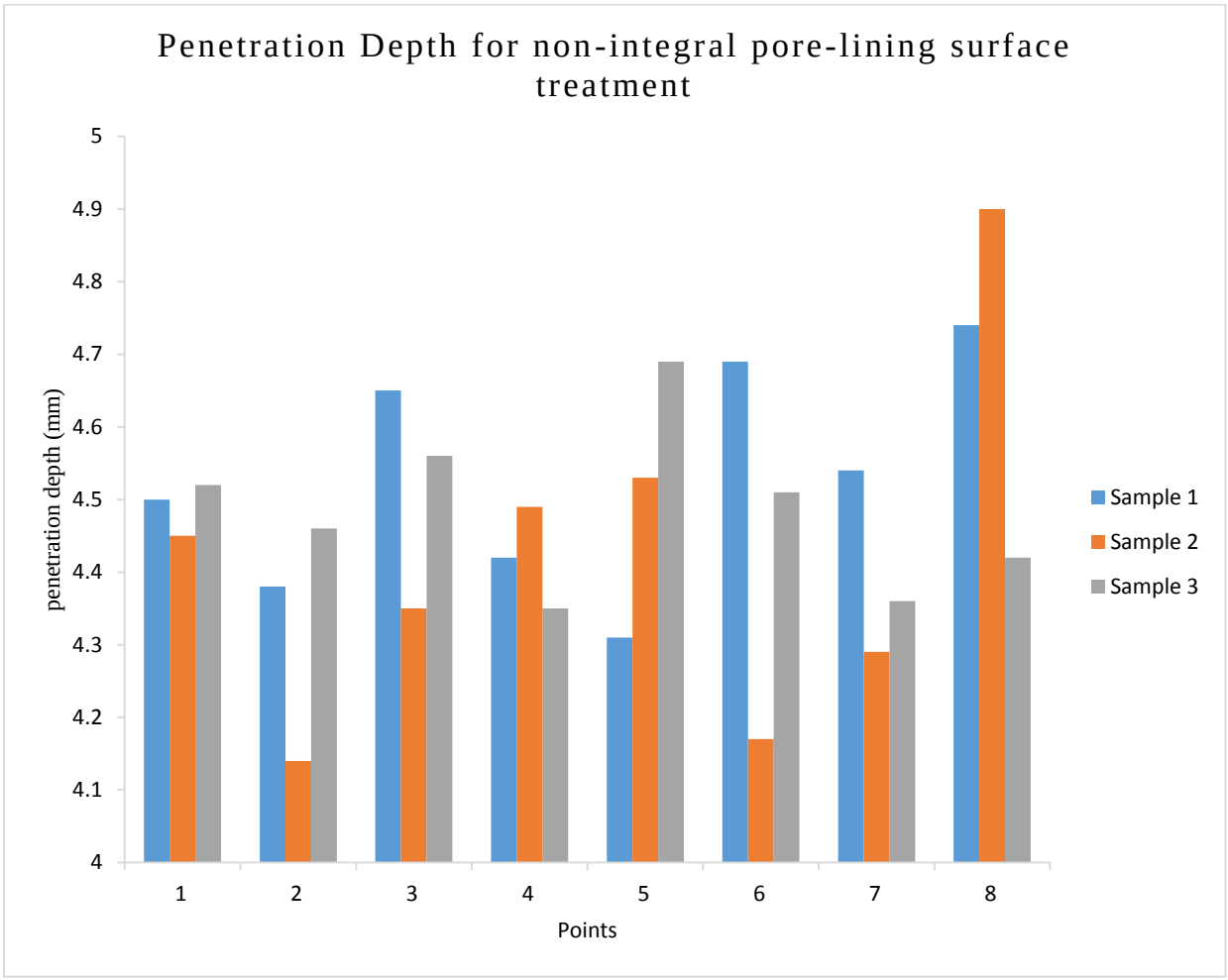

Stellenbosch University https://scholar.sun.ac.za

3 APPENDIX C: CORROSION POTENTIALS

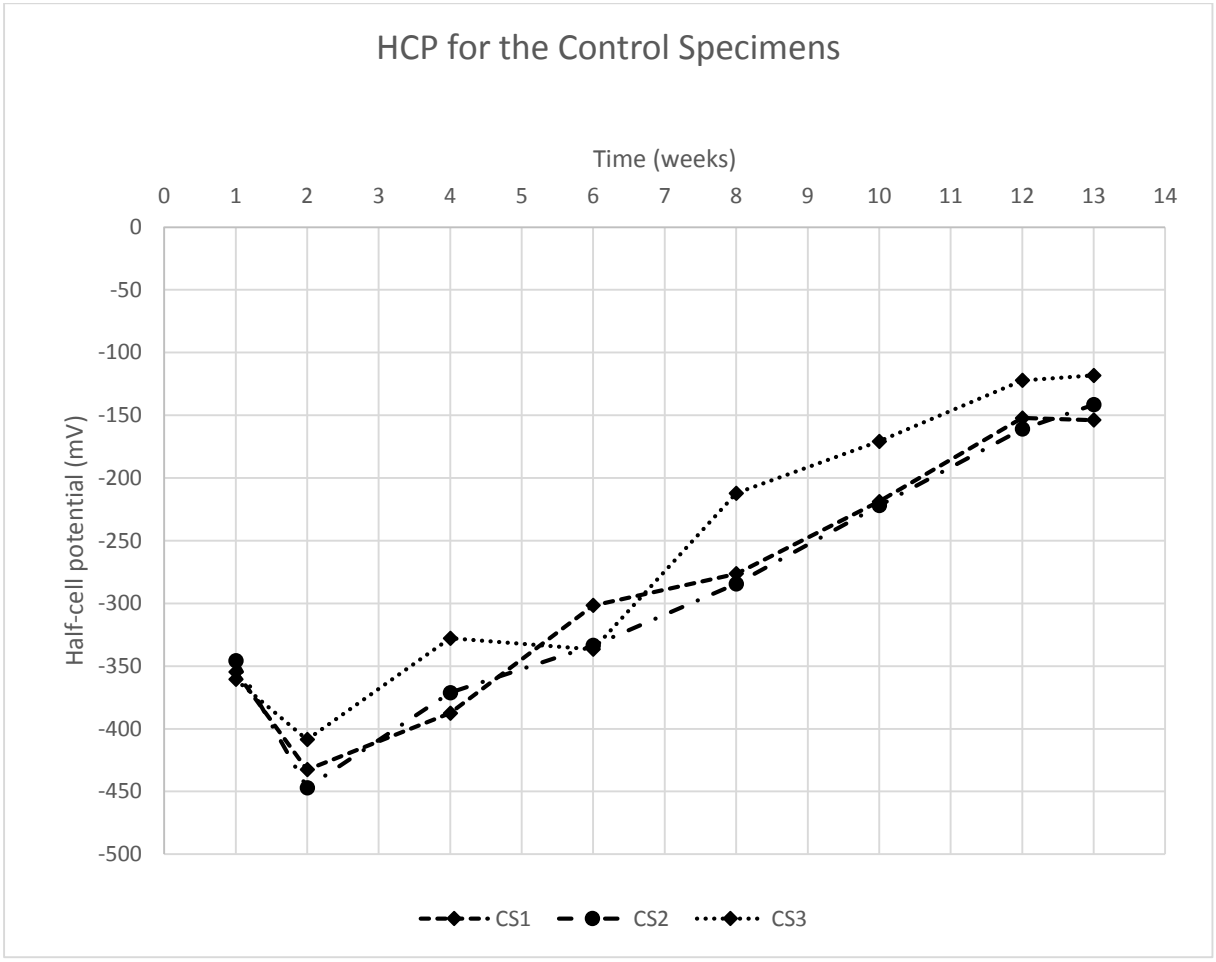

Stellenbosch University https://scholar.sun.ac.za

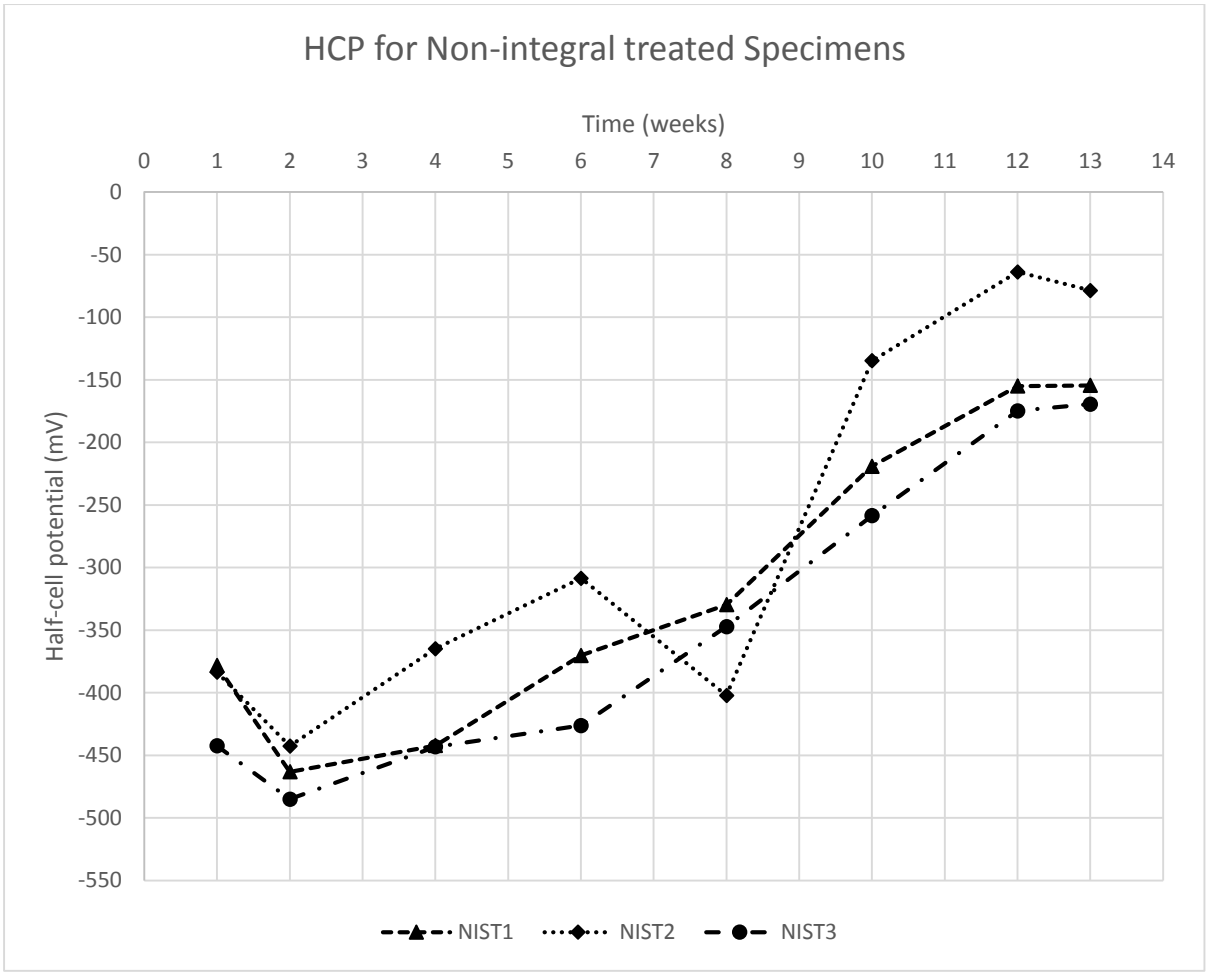

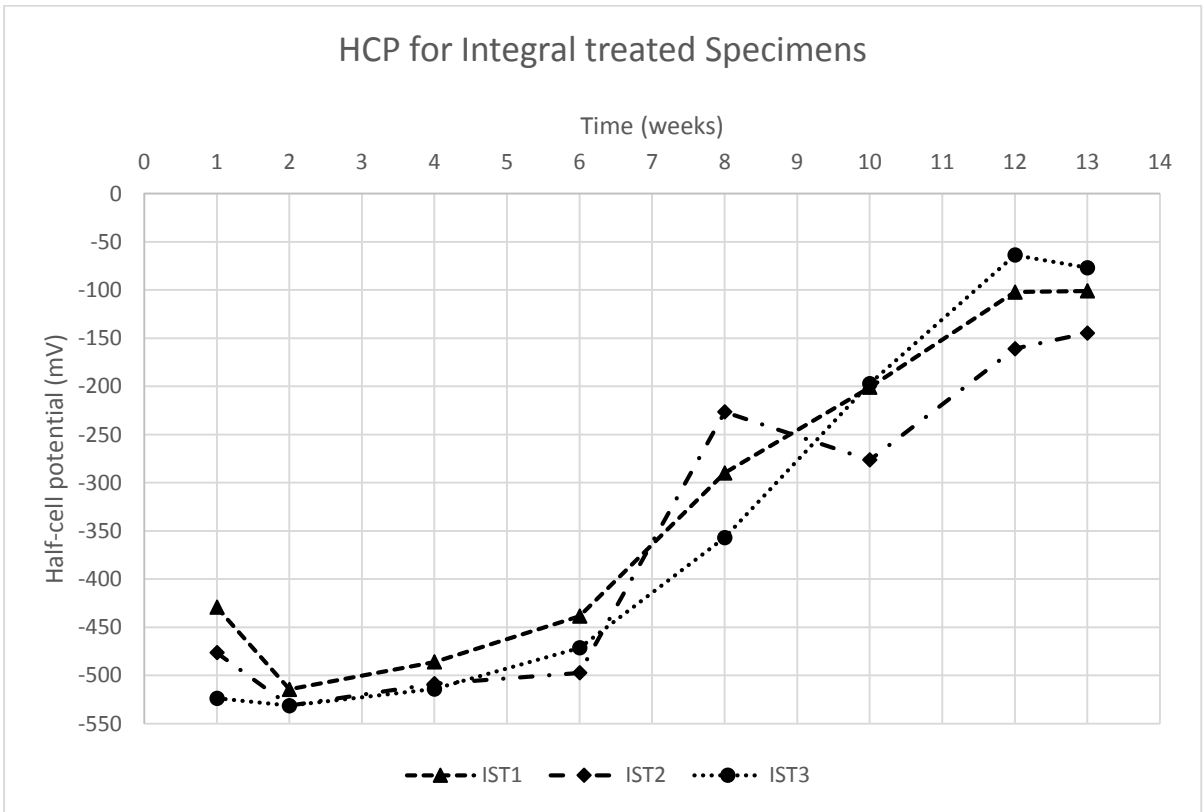

Stellenbosch University https://scholar.sun.ac.za